Politecnico di Milano

School of Industrial and Information Engineering

MSc in Mechanical Engineering

EFFECT OF THE INTERNAL REVERT RECYCLE ON THE NICKEL-BASED ALLOY (CW6MC)

Supervisors:

Silvia Barella

Andrea Gruttadauria

Author:

Mohammad Alimohammadi

Academic Year 2020-2021

Acknowledgment

First and foremost I am extremely grateful to my supervisors, Prof. Barella and Dr. Gruttadauria for their invaluable advice, continuous support, and patience during my thesis. My gratitude extends to the Faculty of Industrial and Information Engineering for the funding opportunity to undertake my studies at the Department of Mechanical Engineering, University of Politecnico di Milano. Additionally, I would like to express gratitude to Dr. Rovatti for her treasured support which was influential in shaping my experiment methods and critiquing my results. My appreciation also goes out to my family and friends for their encouragement and support all through my studies.

Contents

Acknowledgment.....I

List Of Figures: VI

List of Graphs..... XI

List Of Tables XIII

Abstract XIV

Sommario..... XV

1. INTRODUCTION AND AIM OF THE WORK..... 1

2. NICKEL-BASED ALLOYS 3

2.1 APPLICATION OF NICKEL-BASED ALLOYS 5

2.2 CAST NICKEL-BASED ALLOYS 7

2.2.1 Cast Nickel..... 7

2.2.2 Nickel-Copper Alloys..... 8

2.2.3 Nickel-Chromium-Iron Alloys..... 9

2.2.4 Nickel -Molybdenum 9

2.3 CW6MC NICKEL-BASED ALLOY..... 10

2.4 CW6MC AND ALLOY 625..... 12

2.5 MICROSTRUCTURAL CONSTITUENTS 14

2.6 SOLID SOLUTION STRENGTHENING 21

2.7 CONSTITUENTS FROM SOLIDIFICATION 21

2.8 APPLICATIONS 23

3. REVERT 27

4. CASTING IN NICKEL-BASED ALLOY 34

4.1 SAND CASTING 36

4.2 METHODS OF MOULD PREPARATION 37

4.3 CASTING DEFECTS 39

4.4 DEFECT DISTRIBUTION 40

4.5 MAIN CASTING DEFECTS 41

4.5.1 Inclusions 42

4.5.2 Shrinkages and Microshrinkages 43

4.5.3 Surface Crack 47

4.5.4 Recrytallization 47

4.5.5 Fusion 48

4.5.6 Hot Crack 50

4.6 POROSITY PREDICTION IN THE CASTING OF Ni-BASED ALLOYS..... 50

5. MATERIAL AND EXPERIMENTAL METHODS 5.1 MATERIALS.... 54

5.2 SAMPLES PREPARATION..... 57

5.2.1 Cutting..... 57

5.2.3 Polishing..... 58

5.2.4 Chemical Etching..... 60

5.3 CHARACTERIZATION OF SAMPLES..... 61

5.3.2 Optical Microscope..... 62

5.3.1 Optical Emission Spectrometer (OES)..... 64

5.3.3 Scanning Electron Microscope (SEM)..... 64

5.4 HARDNESS..... 66

6. RESULTS AND DISCUSSION..... 67

6.1 MACROSTRUCTURE..... 67

6.1.1 Columnar Structure..... 69

6.1.2 Equiaxed Structure..... 72

6.2 CHEMICAL COMPOSITION..... 74

6.3 DEFECTS ANALYSIS..... 81

6.4 SOLIDIFICATION STRUCTURE 86

6.5 PHASE ANALYSIS 89

6.5.1 General Structure and Composition 89

6.5.2 Laves and Eutectic-like Phases 90

6.5.3 Eutectic-like Structure in As-cast Samples 92

6.5.4 Eutectic-like structure after heat treatment 94

6.5.5 Carbides Structure 95

6.5.6 Carbide Phase in As-cast Samples 97

6.5.7 Carbide Phase After Heat Treatment 99

6.5.8 Oxides Phase 102

6.5.9 Oxide Phase As-cast Samples 104

6.5.10 Oxides Phase After Heat Treatment 106

6.6. Hardness Test 107

7. CONCLUSION 109

Bibliography 112

List Of Figures:

Figure 1. As cast microstructure of CW6MC..... 15

Figure 2. Laves phases morphology: a. lamellar, b. dispersed islands shape [9]. 17

Figure 3. Columnar dendrites and equiaxed dendrites in the sample taken from an as-cast steel billet (left) and a schematic picture of an ideal columnar dendrite. 1, the spacing of the primary arms; 2, the spacing of the secondary arms; 3, the spacing of the tertiary arms.Courtesy to Federal University of Rio Grande do Sul, Brasil/Vinicius Karlinski de Barcellos and Carlos Raimundo Frick Ferreira[22]. 23

Figure 4. Two different kinds of components (valve and tube) with CW6MC alloy 24

Figure 5. Examples of alloy behavior in acidic solutions. Isocorrosion diagram of alloy 625 in A. hydrochloric acid, B. sulfuric acid [19] 25

Figure 6. Corrosion rate versus temperature behavior of alloy 625 and other alloys in wet-process phosphoric acid (A. 42% - B. 54%) [25]..... 26

Figure 7. Effect of revert addition on mechanical properties of M951 nickel-based superalloy [30] 31

Figure 8. Fractographs after rupture at room temperature. (a) 25% recycled alloy (b) 100% recycled alloy[30]..... 33

Figure 9. scheme of sand casting 36

Figure 10. Making a simple mold by hand [34] 39

Figure 11. Distribution of 3 types of defects 40

Figure 12. Effect of the crack area on UTS of casting[35] 41

Figure 13. Inclusion at the surface of a blade root [36] 43

Figure 14. Shrinkage formation principle [36] 44

Figure 15. open and close shrinkage defects [37] 45

Figure 16. Dendritic growth resulting in micro shrinkage [37] 45

Figure 17. Example of micro shrinkage [37] 46

Figure 18. Example of a 3mm surface crack [37] 47

Figure 19. Example of a fusion [37] 49

Figure 20. Example of a hot crack in the surface of the sample 50

Figure 21. Porosity prediction by the ProCAST model and optical microscopy images of porosity. Porosity prediction by the ProCAST model (left) and optical microscopy images of porosity for the defined areas (right). The location of the analyzed section in the NGV is marked by red circle [40]. 53

Figure 22. Dimensions of as-cast samples 54

Figure 23. Focused and analyzed parts of the samples 56

Figure 24. Schematic of machine Mod C250S 58

Figure 25. Schematic of polishing mashing..... 60

Figure 26. A picture to Porosity and oxides analysis 63

Figure 27. Columnar dendritic and Equiaxed central region zones in sample 0%..... 68

Figure 28. Four samples macrostructure; (a) Sample 0%; (b) Sample 30%; (c) Sample 70%; (d) Sample 100%;..... 69

Figure 29. columnar grain structure of four samples; (a) Sample 0%; (b) Sample 30%; (c) Sample 70%; (d) Sample 100%..... 70

Figure 30. Equiaxed grain structure of four samples; (a) Sample 0%; (b) Sample 30%; (c) Sample 70%; (d) Sample 100%;..... 72

Figure 31. 500X magnification of analyzed oxides and porosity..... 82

Figure 32. 25X magnification of primary and secondary dendritic arms in samples (a) Sample 0%; (b) Sample 30%; (c) Sample 70%; (d) Sample 100%;..... 87

Figure 33. (a) Scanning electron microscopy micrograph obtained in scanning electron operation mode showing the γ matrix and the secondary phases, (b) sum of composition elements for the phases; The elemental chemical maps obtained by energy-dispersive X-ray spectroscopy: (c) Ni; (d) Cr;(e) Nb; (f) Mo; (g) Mn; (h) Si; 90

Figure 34. MnS phases in 2500X magnification in sample 1 (0% scrap) microstructure. 91

Figure 35. Porosity and black particles of MnS at 3000X magnification of eutectic-like structure in sample 2 (with 30% scrap)..... 93

Figure 36. Microstructure of eutectic-like structures at 10000X magnification of CW6MC in sample 3 (with 70% scrap)..... 93

Figure 37. 3500X magnification of eutectic-like structure in (a) as-cast and(b) heat treatment samples..... 95

Figure 38. NbC phases in 2500X magnification in sample 1 (0% scrap) microstructure. 96

Figure 39. 150X magnification of alloy microstructure. Carbides of white color are visible in Chinese script and globular morphology. (a) Sample 0%; (b) Sample 30%; (c) Sample 70%; (d) Sample 100%;..... 97

Figure 40. Magnification 1000X of carbides trail in samples 70% and 100%..... 99

Figure 41. 150X magnification of alloy microstructure after heat treatment. Carbides of white color are visible in Chinese script and globular morphology (a) Sample 0%; (b) Sample 30%; (c) Sample 70%; (d) Sample 100%; 100

Figure 42. 3500X magnification of Carbide phase structure in (a) as-cast and(b) heat treatment samples..... 101

Figure 43. Oxide phases in 2000X magnification in sample 3 (70% scrap) microstructure. 103

Figure 44. 150X magnification of alloy microstructure. Oxide phase are visible in black color. (a) Sample 0%; (b) Sample 30%; (c) Sample 70%; (d) Sample 100%; 105

List of Graphs

Graph 1. columnar grains' length in samples 71

Graph 2. Columnar grains' Width in samples..... 71

Graph 3. Equiaxed grains' diameter in samples 73

Graph 4. The weight percentage of carbon in samples 75

Graph 5. The weight percentage of Nitrogen in samples..... 76

Graph 6. The weight percentage of Silicon in samples 77

Graph 7. The weight percentage of Manganese in samples..... 78

Graph 8. The weight percentage of Iron in samples 79

Graph 9. The weight percentage of Nickel in samples..... 79

Graph 10. Defects' area percentage in different samples..... 84

Graph 11. Distribution of defects area on sample 1 in 16 experiment 84

Graph 12. Distribution of defects area on sample 2 in 16 experiment 85

Graph 13. Distribution of defects area on samples 3 in 16 experiment.... 86

Graph 14. Distribution of defects area on sample 1 in 16 experiment 86

Graph 15. Spectrum of the area of eutectic-like phase from the X-ray data collected during X-ray Smart Map acquisition. 91

Graph 16. Spectrum of the area of carbide phase from the X-ray data collected during X-ray Smart Map acquisition 96

Graph 17. Area percentage of carbide phase in samples 98

Graph 18. Spectrum of the area of oxide phase from the X-ray data collected during X-ray Smart Map acquisition..... 103

Graph 19. Area percentage of oxide phase in samples..... 105

Graph 20. Brinnel hardness values in samples 107

List Of Tables

Table 1. Chemical Composition of cast Nickel alloys 8

Table 2. The Minimum and Maximum composition requirements of CW6MC alloys [9]..... 11

Table 3. Chemical composition of CW6MC versus Inconel 625. All the reported values are related to the properly heat-treated product: solution-annealed Inconel 625 and solution-annealed CW6MC [16]. 13

Table 4. Mechanical properties of CW6MC versus Inconel 625. All the reported values are related to solution-annealed Inconel 625 and solution-annealed CW6MC [7]. 13

Table 5. Effect of Cr, Mo, Fe, Nb, Al, Ti in CW6MC alloys 16

Table 6. Main elements and their effect on CW6MC metallurgy [5], [9] 20

Table 7. A typical set of physical properties for Ni-based superalloys [26]..... 29

Table 8 Chemical composition of standard CW6MC [12]..... 55

Table 9. Samples nomenclature..... 55

Table 10. Weight percentage of some elements in samples 81

Abstract

CW6MC is a nickel-based alloy designed to withstand acidic environments for Oil & Gas industry, including mainly cast valves and pipes. In the current work, the revert addition effect on alloy properties was analyzed. Revert is to be intended as runners, feeders, and waste that are discarded by foundries. Trying to reuse them, re-melting scrap in further castings could be an innovative way to recycle a high-value material.

In the present thesis work, four specimens with different compositions were studied, containing respectively 0%, 30%, 70%, and 100% of revert. Macrostructure and microstructure properties, chemical composition, defects, and hardness of the four samples were analyzed to understand and the effect of changes induced by scrap content on material properties.

Keywords: CW6MC, scrap, revert, sand casting, microstructure, macrostructure, secondary phase, hardness.

Sommario

CW6MC è una lega a base di nichel progettata per resistere agli ambienti acidi per l'industria Oil & Gas, comprese principalmente valvole e tubi in ghisa. Nel lavoro corrente, è stato analizzato l'effetto dell'addizione inversa sulle proprietà della lega. Revert è da intendersi come corridori, alimentatori e rifiuti che vengono scartati dalle fonderie. Cercare di riutilizzarli, rifondere gli scarti in ulteriori fusioni potrebbe essere un modo innovativo per riciclare un materiale di alto valore.

Nel presente lavoro di tesi, sono stati studiati quattro campioni con diverse composizioni, contenenti rispettivamente 0%, 30%, 70% e 100% di inversione. Le proprietà della macrostruttura e della microstruttura, la composizione chimica, i difetti e la durezza dei quattro campioni sono stati analizzati per comprendere l'effetto dei cambiamenti indotti dal contenuto di scarto sulle proprietà del materiale.

Parole chiave: CW6MC, rottame, ripristino, colata in sabbia, microstruttura, macrostruttura, fase secondaria, durezza

1. INTRODUCTION AND AIM OF THE WORK

CW6MC is a cast corrosion-resistant nickel-based alloy that specially provides excellent resistance to seawater and chloride stress corrosion cracking. It also has high fatigue and creeps strength. Service environment examples include oxidizing atmospheres, sulfur, and handling organic and inorganic compounds over a wide temperature range. It is frequently used in severe service conditions that involve combinations of acids at elevated temperatures. The relatively high molybdenum level improves resistance to non-oxidizing acids and increases high-temperature strength.

Revert addition effect on CW6MC was studied in this work. Revert is to be intended as runners, feeders, and other metallic parts that are rejected from foundries and are re-inserted in the melt to generate new casting products. For several years, reducing the cost and environmental impact is the main challenge during recycling material in the metalogical process. In the present work, four samples (provided by Fondinox S.p.A.) with different scrap content were analyzed.

- Sample 1 = 0%

- Sample 2 = 30%

- Sample 3 = 70%

- Sample 4 = 100%

The main analysis in this work was done on samples to clearly understand:

- The solidification microstructure

- Chemical effect on alloy properties

- Metallurgical properties in a heat-treated alloy case

- The investigation of samples' chemical composition

-The main elements that affect the chemical composition

Moreover, a casting defects study was performed with particular attention to the inclusion of oxides, shrinkage porosity, gas porosity, and hot cracking. Considering the hot cracking phenomenon, it is not directly influenced by revert content, but by chemical composition, grain size, and dendritic structure. Hot crack is a typical casting defect found in CW6MC and is the main problem of foundries. Thus, hypotheses about defect reduction were proposed. Finally, the responsible factors for hot cracks' appearance were investigated.

2. NICKEL-BASED ALLOYS

Nickel-based alloys are generally known as difficult to machine materials because of their toughness, high heat resistance and high operating temperatures, hardness, strength to weight ratio, and chemical property to react with tool materials, low thermal conductivity and creep resistance. Although these whole properties are necessary to design requirements, they cause a greater challenge to manufacturing engineers due to the high temperatures and stresses generated during machining. The tool materials with better hardness like carbides, ceramics, and CBN have been regularly used for machining nickel-based alloys. Betterments in machining productivity can be attained with advanced machining techniques such as rotary machining [1]. As an example, in the aerospace engine, around 50% of materials used, mainly in the gas turbine are Nickel-based alloys [2]. The main strength of the Nickel-based alloys is being heated resistant, having high melting temperatures, retaining their mechanical and chemical properties at high temperatures, high corrosion resistance as well as thermal fatigue, creep, erosion, and thermal shock[3]. These properties are required for the efficient and effective service performance of the domains in which the Nickel-based alloys are used. The Nickel-based alloys can be strengthening and hardening through intermetallic compound precipitation in the FCC matrix[4]. Nickel-based alloys play an important role in gas turbine engines. In addition to their use in marine, aircraft, industrial, and vehicular gas turbines. Nickel-based alloys are now also used in rocket engines, space vehicles, nuclear reactors, submarines, experimental aircraft, petrochemical equipment, steam power plants, and

other high-temperature applications. Nickel-based alloys are known as the most difficult to machine materials to satisfy quality and production requirements. The Nickel-based alloys' work-hardened rapidly. High pressures that accompany machining causes a hardening effect that slows down further machining and may also cause warping in small components [5].

Nickel is obtained from two types of deposits which are sulfide and laterite ores. Nickel demand has been increased mainly because of greater consumption in Europe, the USA, China, South Korea, and Japan. Trends are very strong in BRIC countries (Brazil, Russia, India, and China). Therefore, growing market demand for these alloys is driving the manufacturing sector to explore options for higher material removal rates (MRRs)[6]. It is considered that Nickel-based alloys have the best high-temperature mechanical properties compared to other materials. The following characteristics are to be made Nickel-based alloys difficult to cut:

a) High strength under elevated temperatures
b) High hardness
c) High strength of the material
d) High degree of work hardening
e) Poor thermal conductivity
f) High tendency of BUE (Built-Up Edge) [7].

Single crystal Nickel-based alloys casting compositions have been developed for their excellent high temperature creep strength properties as turbine blades and for the fabrication of other metallic components that

require strength properties during prolonged and repeated use at very high temperatures [8].

Nickel-based alloys are used for heat-resistance and corrosion resistance applications. On one hand, nickel shows a high melting point (1453°C) and boiling point (2730°C). These two properties and the coefficient of thermal expansion, the thermal conductivity, and the recrystallization temperature, allow high-temperature resistance applications. A clear distinction between corrosion-resistant alloy and heat-resistant; one is not always exhibited: some nickel-based alloy, as CW6MC (cast counterpart of Inconel 625) or CY-40 (cast counterpart of Inconel 600), show resistance to temperature and severe environments at the same time. Therefore, companies wrongly tend to define the alloys that show these two requirements together as alloys [2].

2.1 APPLICATION OF NICKEL-BASED ALLOYS

These alloys have been developed for high-temperature service and include iron, cobalt, and nickel-based materials, although at present they are principally nickel-based. These materials are mostly used in aircraft and power generation turbines, rocket engines, and other challenging environments, including chemical processing and nuclear power plants. The aero gas turbine was the impetus for the development of Nickel-based alloys in the early 1940s when conventional materials available at that time were insufficient for the demanding environment of the turbine. Therefore, it can be said that “the development of Nickel-based alloys made

the modern gas turbine possible". A major application of Nickel-based alloys is in jet engines, turbine materials, both disc and blades[9]. The use of alloys can allow the operating temperature to be increased from 650 ℃ to 710 ℃. Besides increasing efficiency and power output, higher temperatures result in reduced emissions because the combustion cycle is more complete. Nickel-based alloys can play an important role in improving energy efficiency in steam turbines used to generate electricity. Nickel-based alloys are increasingly finding applications in the oil and gas industry. In some of these environments, high pressure and temperatures up to 232℃ can be encountered. Processing of oil and natural gas under these typical environmental conditions purely requires special materials. Nickel-based alloys 718, 725, and 925 are commonly used in oil and natural gas production. These alloys contain molybdenum and chrome which help in resisting corrosion. The nickel-based alloy 718 was first developed for use in the gas turbine and aerospace industry but has become the preferred material for the manufacture of wellhead components, auxiliary and downhole tools, and subsurface safety valves [10].

2.2 CAST NICKEL-BASED ALLOYS

Based on corrosion resistance, cast nickel-based alloys mainly are defined into five groups:

- Cast nickel
- Nickel-copper
- Nickel-chromium-iron
- Nickel-chromium-molybdenum
- Nickel-molybdenum

2.2.1 Cast Nickel

It is classified as the grade CZ-100. It is the best alloy to resist concentrated and anhydrous caustic at elevated temperatures. It can be also used where applications require no contamination of nickel from other elements. The maximum amount of carbon must be 0,75% and one of silicon 0,1% (weight percent). Table 1 shows the chemical composition of this alloy based on weight percentage. This high-carbon CZ-100 alloy shows excellent castability. When castings are welded with a wrought system the maximum allowed carbon content is reduced to 0,1% or less, but this decreases the castability of the alloy. Thus, this alloy can be welded, special attention is needed if the sulfur amount is too high due to welding embrittlement. These alloys are mainly applied in plants for the production of caustic soda or other components in contact with it. Even a small amount of oxygen and sulfur can have a detrimental effect on alloy corrosion resistance.

Table 1. Chemical Composition of cast Nickel alloys

Component	Carbon	Manganese	Silicon	Phosphorus	Sulfur	Nickel	Copper	Iron
% in material	*1.00% Max*	*1.50% Max*	*2.00% Max*	*0.03% Max*	*0.02% Max*	*95.00% Min*	*1.25% Max*	*3.00% Max*

2.2.2 Nickel-Copper Alloys

Copper-nickel (CuNi) is an alloy of copper that contains nickel and strengthening elements, such as iron and manganese. These alloys are materials with relevant importance and high interest in naval and marine fields and have been widely used in applications such as ship piping, boat hulls, pump bodies, seawater condensers, or heat exchanger tubes [11]. Their excellent corrosion properties are due to the high proportion of nickel in the composition and the difficulty of copper to be ionized. The corrosion resistance appears because of a protective film of copper oxide (Cu2O) formation. The presence of nickel reduces the number of defects on the protective film, enhancing the efficiency of the resistance layer [12]. These cast alloys are used in chemical processing industries for their corrosion resistance in oxidizing or reducing agents. C grade castings show high resistance in oxidizing environments such as contact with hydrochloric, sulfuric, and nitric acids. They exhibit excellent corrosion resistance in seawater, salts, and organic acids. The C grade offers excellent mechanical properties due to the solution strengthening effect. In applications where is required better weldability, carbon content must be reduced. These alloys

are widely used where higher corrosion resistance and temperature resistance are required CW6MC alloy is considered the corresponding cast alloy of wrought Inconel 625. Figure 1 illustrates the corrosion loss of Ni-Cr-Mo alloys depending on Cr, Mo, and W amount.

2.2.3 Nickel-Chromium-Iron Alloys

Nickel-chromium-iron alloys are used extensively in nuclear power systems for their resistance to general corrosion, localized corrosion, and environmentally assisted cracking. These alloys show outstanding resistance to environmentally assisted cracking in most water-reactor environments, these alloys are prone to welding defects, most notably to ductility dip cracking. Ductility dip cracks are intergranular and can be surface connected, which is often an unacceptable condition in components where fatigue, corrosion fatigue, or other forms of environmentally assisted cracking can occur [13].

2.2.4 Nickel -Molybdenum

Owing to the high corrosion resistance of the Ni-Mo alloys containing about 27wt % Mo, many investigations have been devoted to the electrodeposition of these layers. Ni-Mo alloy coatings were then prepared using direct current or pulse plating. However, the mechanism of molybdenum electro crystallization is still not elucidated. Indeed this metal has never been deposited in a pure state from aqueous solutions whereas its code position with iron-group metals is possible [14]. Several hypotheses have been proposed. The most recent investigation mentioned the possible multistep

reduction of some molybdic species leading to a molybdenum oxide which would be reduced by atomic hydrogen previously adsorbed on the inducing.

Metal N12-MV and N-7M are the main nickel-molybdenum alloys. They must not be cooled too slow due to the consequent reduction in ductility, weldability, and corrosion resistance. Solution treatment and following quenching are needed to make their employment possible. The presence of molybdenum in solid solution allows achieving high tensile strength. The main applications are related to the presence of hydrochloric acid at high temperatures or chemical resistance to sulfuric acid, phosphoric acid, and other chemicals [15].

2.3 CW6MC NICKEL-BASED ALLOY

CW6MC is a member of low carbon high Ni-Cr-Mo alloys that offers the highest corrosion resistance amongst stainless steel and related alloys to oxidizing agents such as chlorine dioxide, especially when it comes to pitting, crevice, and stress corrosion cracking. Cast alloys are covered by the ASTM standards [2]. Most alloys have been developed as cast equivalents of well-known wrought Ni-Cr-Mo alloys. The atomic structure of the Ni-Cr-Mo alloys is face-centered cubic (fcc). In this respect, they are like the austenitic stainless steels and the super austenitic. Due to the high alloying content, they are more susceptible to the formation of deleterious phases during cooling. They are normally supplied in the solution annealed condition. In this study, the CW6MC will be concerned, which is used in a high range of components, specifically its corrosion resistance, high strength, and good machinability and weldability. CW6MC is the cast

counterpart of Inconel 625. Therefore, Inconel 625 is one of the most known superalloys that initially was developed for slightly high-temperature applications but today is mainly used in the wet-corrosion environment [16]. Table 2 shows the minimum and maximum composition requirements of CW6MC alloys.

Table 2. The Minimum and Maximum composition requirements of CW6MC alloys [9].

Elements	C	Mn	P	S	Si	Mo	Fe	Ni	Cr	Nb
Max	0	0	0	0	0	8	0.5	55.4	20	3.2
Min	0.06	1	0.015	0.03	1	10	5	68.9	23	4.5

Other requirements are based on the heat treatments which are necessary before components employment: CW6MC must be heated until 1175 °C minimum and then rapid cooling in water or other medium is needed. The heat treatment allows the solubilization of elements and the consequent alloy strengthening. To meet the better corrosion resistance/mechanical properties agreement, it could be necessary to heat treat the component at higher temperatures concerning the minimum value. Tensile properties are defined in terms of minimum tensile strength, for this alloy tensile strength is 485MPa, the minimum yield strength is 275 MPa and minimum elongation is 25% and the hardness is between 0 – 176 Brinell.

2.4 CW6MC AND ALLOY 625

Both CW6MC and alloy 625 are eligible for corrosion-resistant applications; they both exhibit a good compromise between mechanical properties and corrosion resistance. Therefore, they are suitable materials for applications such as oil and gas components. The main difference between the two alloys is the method of manufacturing: CW6MC is a cast alloy while Inconel 625 is a wrought one. Generally, forging is preferred to casting, because it provides more homogeneous products due to the absence of segregations. The main consequence of this observation is the achievement of better mechanical properties in wrought products, such as the obtainment of the maximum or higher allowed value of hardness. Hence, the better choice of material appears to be wrought Inconel 625. However, the material choice is not only related to mechanical properties: the overall costs of the production must be considered. A wrought product as Inconel 625 needs a further heat-temperature treatment to reduce hardness under the defined maximum value. This process increases the overall cost of production [8]. In standards, casting is listed as an alternative technique to forging, for example, even centrifugal casting of CW6MC can be used to produce metallic gaskets for oil and gas applications. This technique allows to achieve hardness value lower with respect to Inconel 625 and the values proposed by the standard are reached without the need for further heat treatment. Thus, the save of costs is obtained [10].

Considering the standard maximum chemical composition of the two alloys, there are no huge differences. The similar chemical compositions are shown

in Table 3. Slight changes of composition in cast alloy are exploited to improve the castability and soundness of the final product. Regarding mechanical properties showed in Table 4, the elongation and tensile strength of the wrought product are higher than the cast one, while the difference in yield strength is negligible[17].

Table 3. Chemical composition of CW6MC versus Inconel 625. All the reported values are related to the properly heat-treated product: solution-annealed Inconel 625 and solution-annealed CW6MC [16].

	Ni	**Cr**	**Mo**	**Nb**	**Ti**	**Al**	**Fe**	**C**	**Co**	**W**	**Mn**	**Si**
625	Bal.	20-23	8-10	3,15-4,15	0,4	0,4	5,0	0,1	0-1	-	0,5	0,5
CW6MC	Bal.	20-23	8-10	3,15-4,5	-	-	5,0	0,06	-	-	1	1

Table 4. Mechanical properties of CW6MC versus Inconel 625. All the reported values are related to solution-annealed Inconel 625 and solution-annealed CW6MC [7].

	Tensile strength [MPa]	**Yield strength [MPa]**	**Elongation [%]**
625	690	276	30
CW6MC	485	275	25

Depending on thermal treatments, a distinction between two grades of alloy 625 can be done following the standard ASTM B705-17. Grade 1 is related to annealed alloy 625 and Grade 2 consider the solution-annealed alloy. Grade 1 shows a minimum tensile strength requirement of 827 MPa rather than the 690 MPa of Grade 2. The overall quoted values are related to standard ASTM B705-17 that is typical of welded pipes, other standards, and so other requirements, which can be found depending on application [1]. In contrast, CW6MC follows the standard ASTM A494/A494M where is specified that the thermal treatment requirement is only one: solution-annealing. CW6MC components must be brought at 1175°C, hold at this temperature for sufficient time and quench in water or another cooling medium [5].

2.5 MICROSTRUCTURAL CONSTITUENTS

Figure 1 (a and b) shows the as-cast microstructure of CW6MC. The microstructure reveals the presence of austenite matrix and another intermetallic phase which is formed as a result of the segregation of alloying elements like Nb and Mo during the solidification. The final microstructure of the solution annealed CW6MC is a mixture of austenite and a small volume fraction of this Nb-Mo-rich intermetallic phase. It is not possible to realize an intermetallic precipitate-free microstructure for this alloy in both the wrought and cast form. One can only minimize it using strong experience. This requires an understanding of the complex interplay between composition, heat treatment practice as well as solidification parameters.

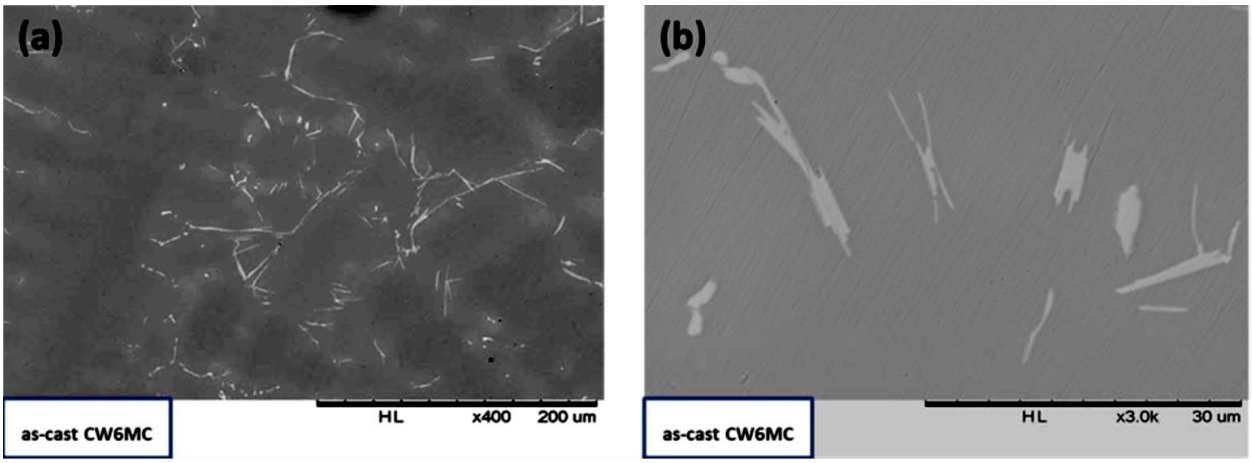

Figure 1. As cast microstructure of CW6MC

The microstructure of cast CW6MC alloys also has oxide inclusions particles of 7-10 µm in size due to the air induction melting process [18]. One approach to testing the quality of heat treatment is to have impact toughness testing specified as a part of the quality control. The impact toughness values are severely impaired due to the presence of a significant fraction of intermetallic phase present, which is normally a result of improper heat treatment procedure [9]. Table 5 shows the effect of some important elements of CW6MC alloys.

Table 5. Effect of Cr, Mo, Fe, Nb, Al, Ti in CW6MC alloys

Element	Chromium and Molybdenum	Iron and Niobium	Aluminum and Titanium
Effect	high corrosion resistance high solid solution strengthening	increase alloy strength with solid solution mechanism	allows achieving good weldability

In comparison to CW6MC, alloy 625 exhibits a higher amount of aluminum and titanium, but due to the addition of aluminum and titanium in the deoxidation process also its cast counterpart could present these two elements as traces. Alloy casting metallurgy is mainly based on the consequent segregation of niobium during the last stage of solidification. Niobium exploits the formation of Laves phases of primary carbides. The formation of various phases is influenced by the carbon/niobium ratio. In the High C/Nb ratio, the formation of γ + NbC can be found. On the other hand, in Low C/Nb ratio, the initial formation of γ + NbC and subsequent Laves phase formation as solidification proceed. Finally, in the intermediate C/Nb ratio, the initial formation of γ + NbC and subsequent Laves phase formation as solidification proceed. Not only this ratio affects the final microstructure but, as in all casting products, also other alloy chemistry variations and the solidification rate can contribute.

Laves phase can form during solidification made by a high amount of iron and silicon in the sample. These alloys have affected the solidification microstructure. Mechanical properties like Charpy V-notch impact energy, reduced with increasing the Laves phases, so the amount of iron and silicon should be controlled in the samples. Besides, molybdenum and niobium have a big role in the samples because they promote Laves phase formation too[4].

The morphology of laves phases can be lamellar or island dispersed type as illustrated in Figure 2. Typical formulas of these phases are Fe_2Ti, Fe_2Nb, Fe_2Mo but $(Fe,Cr,Mn,Si)_2(Mo,Ti,Nb)$ is the general formula to describe them [19].

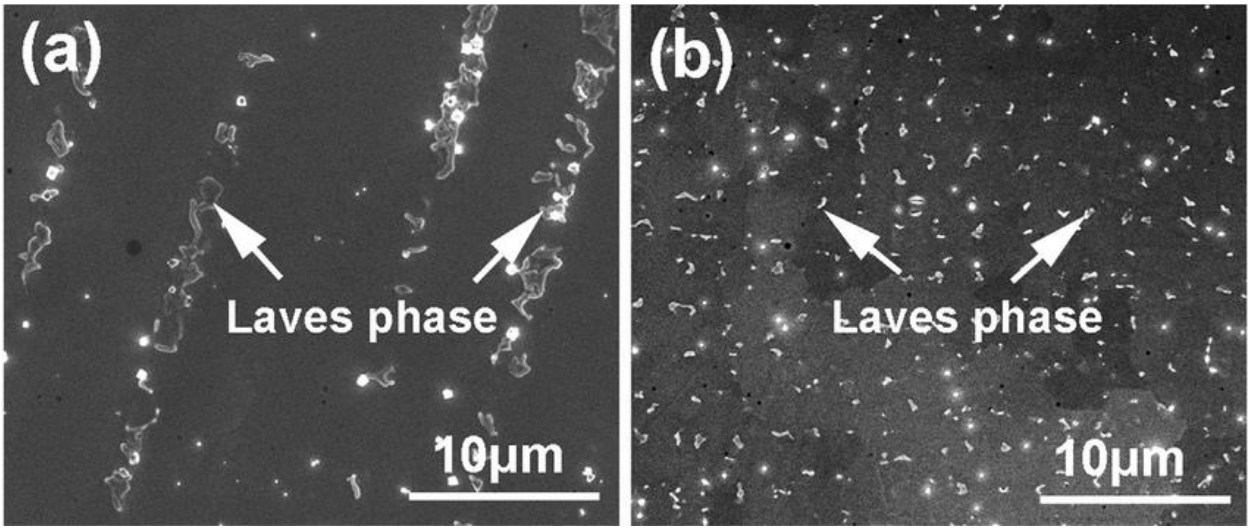

Figure 2. Laves phases morphology: a. lamellar, b. dispersed islands shape [9].

In CW6MC, It is possible to find nitrides formation because of Nitrogen. The most common nitrides in this alloy are TiN and NbN. Nitrides can act as nucleation sites for MC carbides and grains. They are typically

considered detrimental due to their embrittlement effect. Nevertheless, nitrides are generally in low amount, so they are not the only responsible in the loss of tensile properties. It has been also demonstrated that nitrogen induces grain refinement in the nickel-based alloy [20].

The role of carbides in Nickel-based alloys is complex and dynamic. Most investigators believe that carbides do exert a significant and beneficial effect on rupture strength at elevated temperatures. In addition, it is quite clear that carbide morphology can influence ductility, and also that carbides can influence the chemical stability of the matrix through the removal of reacting elements. The three main types of carbides found in the nickel-based alloy are MC, M23C6, and M6C. Cr7C3 can also be present but is rare. The MC carbides are a major source of carbon for the alloy to use later if it interacts chemically. They have an FCC structure and are normally considered amongst the most stable compounds in nature. They are formed either in the liquid state or at high temperatures after solidification. They exist in blocky or script morphologies within the grains and along the grain boundaries. The elements titanium, tantalum, niobium, and hafnium are the main MC-forming elements with the less reactive elements such as molybdenum and tungsten also being involved. The M23C6 carbides are usually predominant in alloys of high chromium content, where they form during lower-temperature (760–980°C) heat treatment and service, both from the degeneration of MC carbides and from soluble carbon residue in the alloy matrix. They have a significant effect on the properties of nickel alloys. When present as discrete particles in grain boundaries, their critical location promotes a significant effect on rupture

strength, apparently through inhibition of grain boundary sliding. However, properties are adversely affected when M23C6 carbides exist in the form of cellular structures or as films in grain boundaries [21].

In CW6MC, Carbides are commonly observed, and they can be intergranular and intragranular. They are primarily (Nb, Mo)C with lower content of nickel and chromium, but the formation of M6C, M23C6 is also possible. Generally, they may provide a beneficial effect on rupture strength but their impact on mechanical and tensile properties is also influenced by their shape and distribution[1]. It is possible to find niobium carbides in a blocky or Chinese script morphology. Due to carbide's great stability, once formed, they cannot be removed by consequent heat treatments. Therefore, if they are concentrated in a not uniform way and they are grouped in bands, loss in ductility in the direction perpendicular to their orientation axis is possible. Despite that, Laves phase's role in decreases ductility is more severe than the carbides effect.

Given the above considerations, carbide formation and Laves particles play the main role in the solidification of CW6MC. The reduction, as far as practicable, of niobium and carbon levels, and the amount of iron, molybdenum, and silicon, is an adequate trick to obtain the desired properties [8]. Table 6 illustrates the effect of the main elements on CW6MC.

Table 6. Main elements and their effect on CW6MC metallurgy *[5], [9]*

Element	Effect
Nickel	Formation of face-centered cubic matrix
Carbon	Carbide formation and moderate solid solution hardening increases hot cracking susceptibility
Chromium	Improves corrosion resistance, moderate solid solution hardening
Molybdenum	High solid solution hardening, improves corrosion resistance, increases density, carbides formation, Laves formation
Niobium	High solid solution hardening, carbide formation, laves formation, increases hot cracking susceptibility
Iron	Decrease corrosion resistance, improve workability, Laves formation
Silicon	Laves phase formation increases hot cracking susceptibility
Nitrogen	Grain refinement effect, gas porosity formation

2.6 SOLID SOLUTION STRENGTHENING

As already discussed, commercial austenitic alloys always contain substantial alloying additions in solid solutions to provide strength, creep resistance, or resistance to surface degradation. Also, the stronger alloys contain elements, that, after suitable heat treatment or thermal-mechanical processing, result in the formation of small coherent particles of an intermetallic compound. Therefore, typical nickel-based alloys like CW6MC are variations of an austenitic nickel-chromium–tungsten (or molybdenum) matrix. In order to obtain useful solid solution strengthening, an alloying element should satisfy the following requirements:
(i) it should have a wide range of solid solubility in the matrix;
(ii) it should have a large difference in atomic size with the matrix;
(iii) it should have a high melting point.

The solid solution elements typically found in the γ phase are likely to include aluminum, chromium, iron, titanium, tungsten, vanadium, cobalt, and molybdenum [2]. The difference in atom diameter from that of nickel varies from +1% for cobalt to +13% for tungsten.

2.7 CONSTITUENTS FROM SOLIDIFICATION

In most commercial nickel-based alloys, the solidification structure after casting is dendritic, containing zones of columnar and equiaxed dendrites. The word dendrite comes from the Greek word “dendron” which means a tree. The dendrite is a tree-like structure and it is growing when the melt

is freezing, and the main growth direction is against the heat flow direction. The dendrite has the primary arm or the main branch and then arms of higher orders as the secondary arms, tertiary arms, etc. Figure 3 shows columnar dendrites and then equiaxed dendrites in the sample taken from an as-cast steel billet. The driving force for growth is the undercooling of the melt. With increasing undercooling, the Gibbs free-energy difference increases between the liquid and solid-state and exceeds the energy barrier so that solidification can take place. One main reason for the energy barrier is the surface energy of the solid. In the case of steel and many other metals, the surface energy is anisotropic and so the growth in certain directions is energetically favored. This is one of the main reasons why the growing morphology is typically dendritic. Typically, this energetically favored direction of the crystal turns against the direction of the heat flow. Other solidification morphologies also exist, as cellular and planar, but they need special compositions and/or cooling conditions and are not typical for steels. With a high enough cooling rate, it is also possible to get amorphous solidification, which means that the solid is noncrystalline and lacks the long-range order characteristic of a crystal. Anyhow, very high cooling rates are required to suppress nucleation in metallic systems, and special RSP (Rapid Solidification Process) processes are needed for that [22].

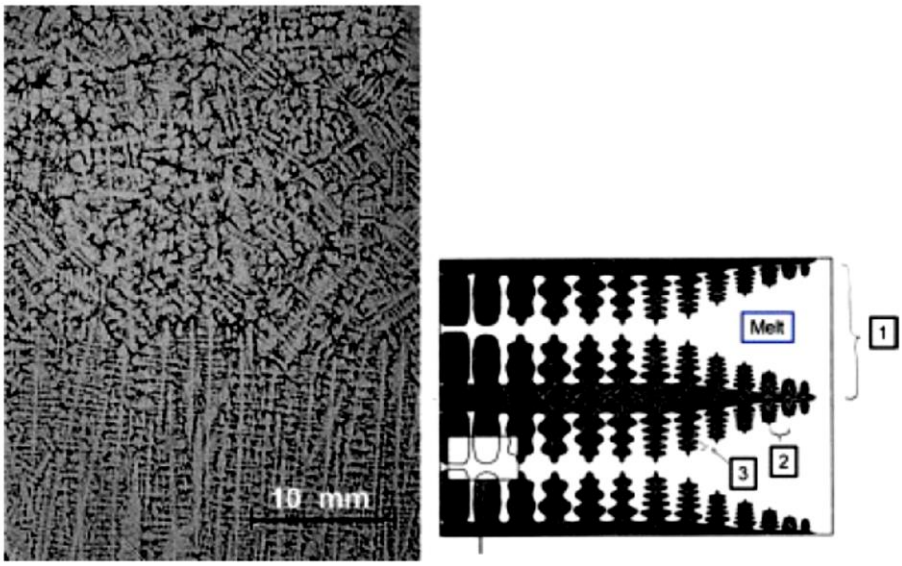

Figure 3. Columnar dendrites and equiaxed dendrites in the sample taken from an as-cast steel billet (left) and a schematic picture of an ideal columnar dendrite. 1, the spacing of the primary arms; 2, the spacing of the secondary arms; 3, the spacing of the tertiary arms.Courtesy to Federal University of Rio Grande do Sul, Brasil/Vinicius Karlinski de Barcellos and Carlos Raimundo Frick Ferreira[22].

2.8 APPLICATIONS

Low carbon high Ni-Cr-Mo alloys offer the highest corrosion resistance amongst stainless steels and related alloys to oxidizing agents such as chlorine dioxide, especially when it comes to pitting, crevice, and stress corrosion cracking. Cast alloys are covered by the ASTM standards [23]. Most alloys have been developed as cast equivalents of well-known wrought Ni-Cr-Mo alloys. However, there are also proprietary grades that have been successfully employed for various applications[19]. These alloys are usually selected only for the most severe service conditions where less costly stainless steels have proven their inadequacy in terms of their engineering functionality[16]. Like other nickel-based alloys, CW6MC is suitable for corrosion-resistant applications because its surface can passivate when the

metal reacts with the environment. The formation of this invisible and thin oxide film is the key to achieve high wet-corrosion resistance. Passive films are generally free of pores, but some aggressive ions present in water may weaken their stability. For example, sulfate ions in seawater can increase the corrosion attack. Pump and valve components in aggressive conditions can be a suitable application of this alloy. Figure 4 illustrates some typical CW6MC components.

Figure 4. Two different kinds of components (valve and tube) with CW6MC alloy

Figure 5 illustrates the corrosion behavior of the CW6MC wrought counterpart in two different acidic solutions.

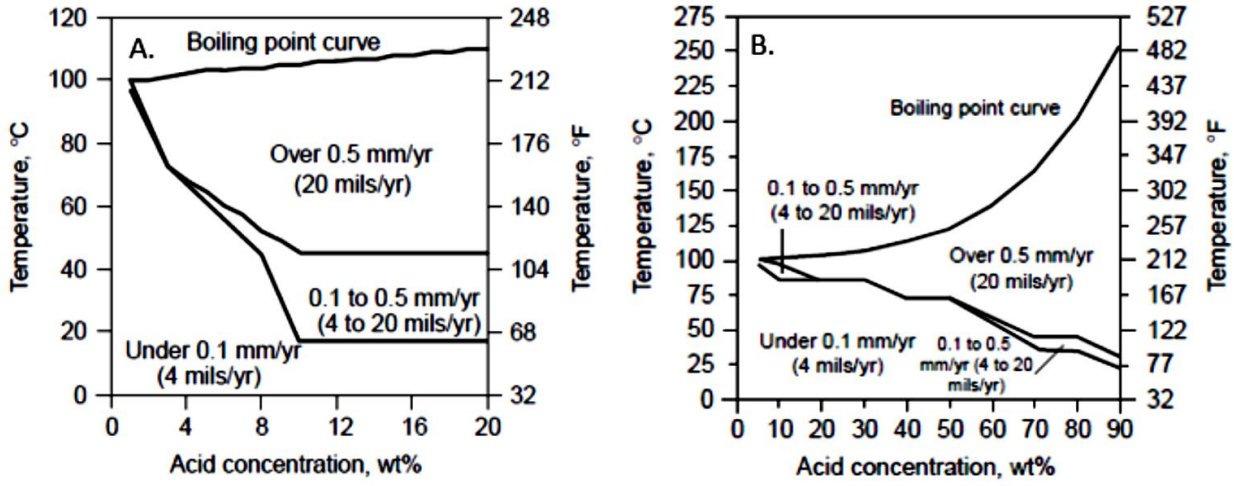

Figure 5. Examples of alloy behavior in acidic solutions. Isocorrosion diagram of alloy 625 in A. hydrochloric acid, B. sulfuric acid [19]

Due to its mechanical strength and resistance to acids, CW6MC was used in the processing of phosphate ores with a high content of impurities because of its corrosion and chemical resistance to phosphate slurries. Phosphoric acid is not one of the most aggressive compounds on metals, anyway, the presence of fluoride, chloride, and silica in phosphate ores can be aggressive. These last compounds enable the formation of acids that show high corrosive power. Nowadays, for this specific application CW6MC has been replaced by alloy 31 that gives better performances due to its higher chromium content, but CW6MC is still used in other severe environments as sour-gas conditions [17].

CW6MC can be also used in components for the production of super phosphoric acids (P_2O_5), such as parts of heat exchangers, equipment for the removal of gaseous fluorine compounds, pumps, and so on. The behavior of the wrought counterpart of CW6MC is shown in Figure 6 [24].

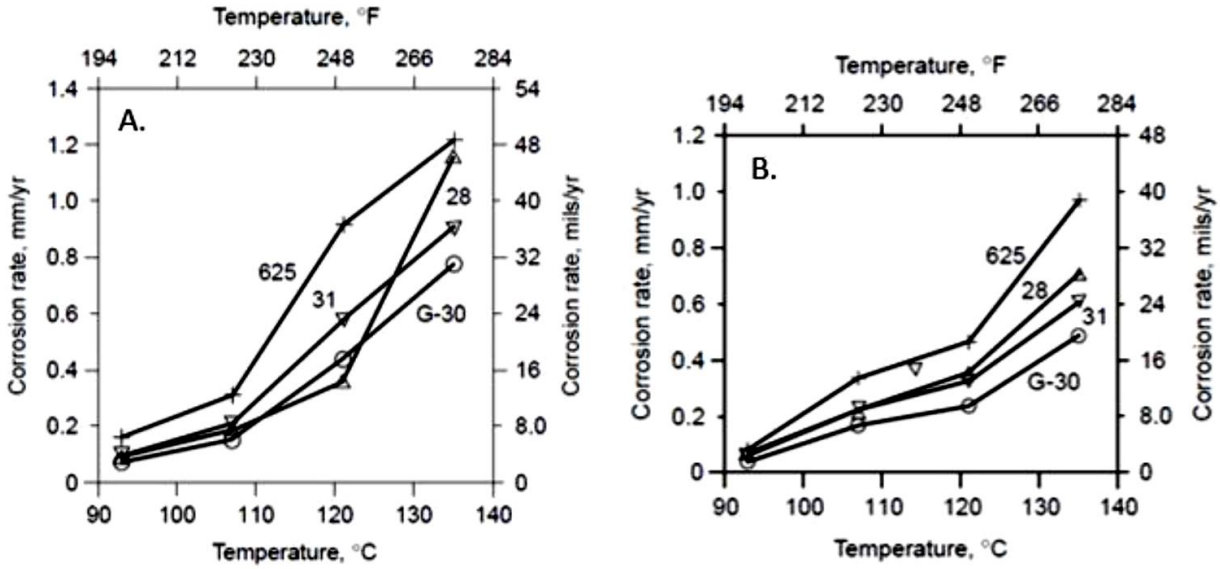

Figure 6. Corrosion rate versus temperature behavior of alloy 625 and other alloys in wet-process phosphoric acid (A. 42% - B. 54%) [25]

3. REVERT

As metals are important recyclable resources, recycling provides the freedom to reuse metals. Recycling can contribute to the sustainability of their use and keep demand under control. The term “recycling” has become common for metals and is widely used for extracting metals from e-waste, sophisticated alloys, and spent catalysts. Still, it remains a challenging task to recycle superalloys efficiently because superalloys are produced in a low quantity than stainless steel [26]. Moreover, the increasing demand for superalloys is a sign that there will be a huge amount of spent/scrap generation in near future. It is an associated problem to understand how it will be possible to make their recycling cost-effective. In contrast, the rare alloying elements in advanced superalloy production are not presently mined but are produced as by-products of primary metals. A shortage of such elements can significantly affect modern technology. Hence, it is the goal to utilize the maximum materials’ efficiency with the lowest possible consumption. Recycling of superalloys will become an increasing need and will help meet the energy requirement and reduce our dependence on resources that are subject to market fluctuations. To sustain the demand of technology humans need to continuously produce metallic materials, especially new technology and demands exploit all the elements in the periodic table. Based on these requirements the stocks of metals are changing in time, in the past centuries, Earth’s crust had a significant amount of available reservoir, but now these stocks are running out. Nowadays, the most significant portion of metals available on planet has just been extracted in the past years and is stuck in our object and

buildings. Therefore, the idea of metals' long-term availability and the recycling idea is discussed [27].

To elucidate the behavior of different alloying elements during the recycling process, it is imperative to have an understanding of the chemistry, microstructure, and properties of different types of superalloys. Each element has specific properties. An ideal product tries to enhance some of these properties with the correct selection of elements to generate an added value material. As industries grow, they are looking for the combination of the perfect elements to guarantee the better performances of the product. This observation explains how the use of various metallic elements evolves in applications. Jet-engines can be considered as a typical application of nickel-based alloys. These alloys have been developed to obtain the desired corrosion resistance and high-temperature resistance. The first material employed to resist such conditions was stainless steel. It has been progressively replaced by nickel-chromium alloys containing aluminum, titanium, and niobium. In 1930 arrived a new cobalt-based alloy, the Vitallium alloy, able to resists severe environments. Subsequently, the addition of other elements in the superalloy composition enabled material properties improvement. The distinction between first, second, third generation of superalloys depending on the presence and amount of rhenium is a typical example [27].

In addition to element exploitation, there is another issue, that is environmental implications. Because during processing, extraction, and production it is fundamental to consider that some metals can be toxic for people or the emission produced during the manufacturing of metallic

components can pollute land, air, and water. So based on all these reasons, materials recycling has to be a central factor in industries [28].

Ni-based alloys constitute a large fraction of the materials constructed for work under tough operating conditions because of their unique combination of physical and mechanical properties. Before going through the role of each element in the cycling process and their changes, the typical properties of Ni-based superalloys should be concerned. A typical set of properties for Ni-based alloys is presented in Table 7[26].

Table 7. A typical set of physical properties for Ni-based superalloys [26]

Properties	**Typical ranges**
Density	7.7–9.0 g/cm3
Melting point	1320–1450 ℃
Elastic modulus	210–160 GPa @25–800 ℃
Thermal expansion	8–18 9 10-6 ℃
Thermal conductivity	11–22 W/m/K@25–800 ℃

Recycling can be considered for foundry products. Regarding cast nickel-based alloys, it is a fact that the final product approximately shows 30% of the original alloy melted weight. The remaining 70% ends up in runner, feeder, metal scrap, and machining waste. Nowadays, foundries are trying to recycle metal scrap to save costs. The idea is to generate "revert alloys", produced re-melting scrap. However, defects as porosity, oxides, and cracks, can increase if a great percentage of recycled material is used in the charge [29]. On the other side, elements also affect the mechanical properties of the final material. For example, some investigations reported that minor elements such as silicon, nitrogen, and oxygen slightly change and affect alloy properties. In any case, these minor elements do not affect the morphology of the dendritic structure, which is mainly changed by solidification parameters. In contrast, the morphology of primary carbides is influenced by revert additions. Carbides are exhibited with a more globular shape in virgin material rather than the recycled alloy. Passing from virgin to revert alloy, mechanical properties worsening is mainly associated with oxygen and nitrogen increase. Figure 7 illustrates the loss of mechanical properties in a nickel-based superalloy increasing revert material. The main responsible for this phenomenon can be considered oxides, nitrides, and porosity that increase their amount [30].

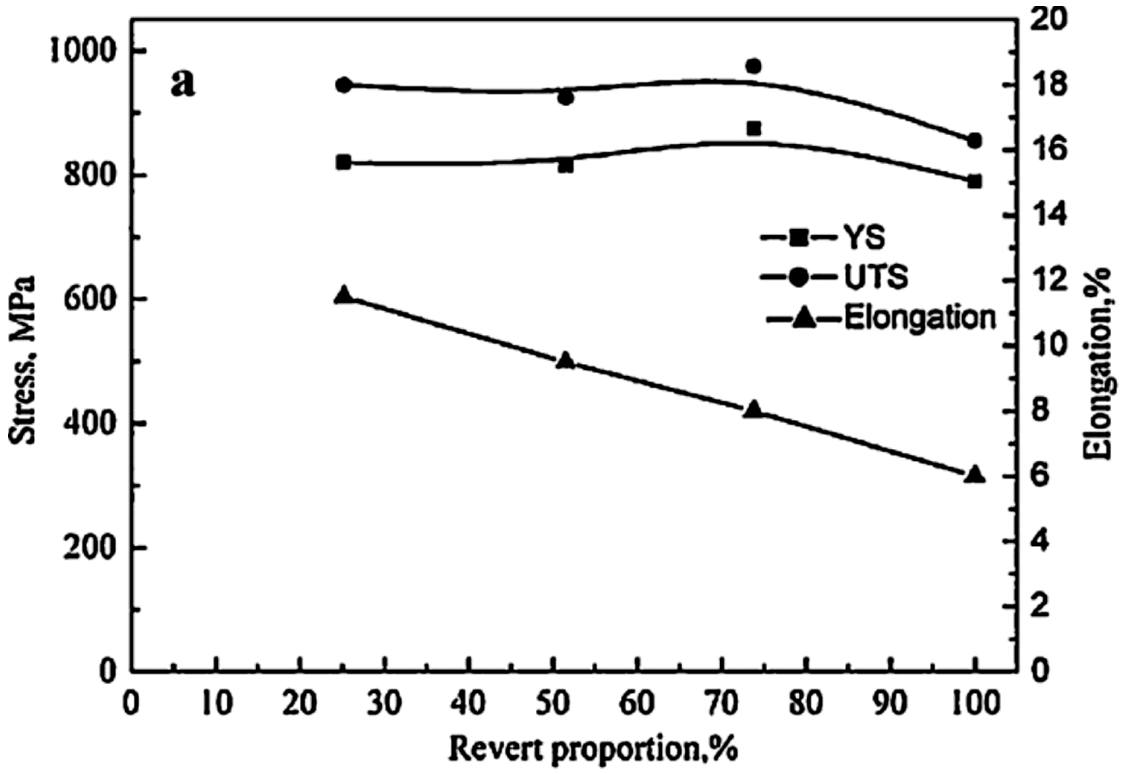

Figure 7. Effect of revert addition on mechanical properties of M951 nickel-based superalloy [30].

In particular, nitrogen and oxygen content increase with the number of remelts. Nitrogen in virgin alloys is able to be released easily and uniformly, while in revert alloys it is released less efficiently. Thus, nitrogen in virgin alloys is not in the same form as the one in revert ones. Probably, in recycled alloy most of the nitrogen is not only in the gas phase but tends to react forming compounds. These constituents cannot be easily dissolved at remelt temperature. In particular, the solubility of nitrogen increases as the chromium content increases. Thus, alloys with high chromium contents can be subjected to this phenomenon. Nitrogen increases with revert also because it is entrapped during the new pouring process, but mainly it comes from the surface of the virgin scrap. In virgin scrap, gases from atmosphere and from hot mould contacts remain in

subsurface regions. Thus, the scrap with high nitrogen content is then re-inserted in the new revert material, and TiN, Ti(CN), or Cr(CN) formation could be possible. Nitrides and oxides in the revert material, tend to stabilize MC carbides or other phases, but this phenomenon brings to alloy embrittlement. Part of nitrogen tends also to form gas porosity: it has been demonstrated that in revert alloys gas porosity is in a higher amount. Microporosity formation is one of the main responsible for revert alloys' mechanical properties reduction [29].

Fracture surface observations are useful to understand the alloy behavior varying revert content. The fracture surface shows that cracks propagate along grain boundaries, thus they follow intergranular paths. However, a high level of porosity and inclusions can create inhomogeneous deformation on the surface because they generate stress concentration between the matrix. Consequently, the fracture mode can be mixed (transgranular and intergranular at the same time). Increasing revert material more porosity can be found on the fracture surface. This is due to the higher content of oxygen and nitrogen and the fracture mode is expected to be mixed. Another fracture surface is illustrated in figure 8 The fractography of 25% and 100% recycled alloys at room temperature are shown in this figure. The intergranular type fracture is the main fracture mode of these alloys in the room. Less faceted-cleavage type is also observed on the fracture surface of the 25% recycled alloy (Figure (8a)). While the cast pores are observed on the fracture surface of the 100% recycled alloy, indicating that the cast pores might accelerate the crack propagation (Figure (8b)) [30].

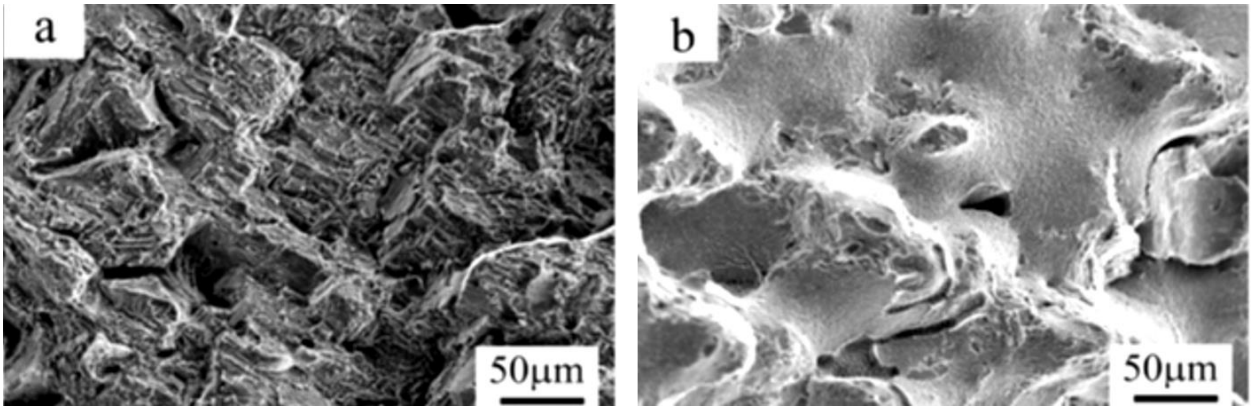

Figure 8. Fractographs after rupture at room temperature. (a) 25% recycled alloy (b) 100% recycled alloy[30].

4. CASTING IN NICKEL-BASED ALLOY

Casting is a manufacturing process that entails the pouring of molten metal into a three-dimensional mold to create a metal part. By using castings, manufacturers can create a wide variety of intricate solid shapes for use in various applications. For example, cast parts are often found in automotive components, aerospace parts, electronics, medical devices, and construction supplies. Although, nowadays there is a lot of new and advanced manufacturing process, like 3D machining, laser, plasma and so on, for some materials as Nickel-base alloys, casting processes are using. Casting is one of the world's oldest manufacturing processes, with traditional forms such as sand and investment casting dating back thousands of years. Thanks to modern technology, however, sophisticated hot forming processes such as die-casting have become commonplace in recent years, providing manufacturers with more options than ever. No need to say, wrought alloys are more homogeneous than cast alloys because they do not present segregations due to the solidification process. Segregation in casting cannot be avoided because its development is a natural phenomenon. Based on the mechanical and chemical composition of materials, all the alloys can not be produced by forging, and in these specific cases, the only way of production is casting. Moreover, in the case of Nickel base alloys, casting can be tailored smartly and easily to obtain the desired properties [31].

Same as other manufacturing processes that are changing and improving, the casting process has undergone radical changes, some affecting the basic sand casting system, and others improving new sophisticated processes. The introduction of the most sophisticated sand and binder, and the higher attention to developing new specific processes, has refined the foundry operations. The consequence is the obtainment of the desired “net-shape” final product [32]. New casting methods offer extreme precision and high dimensional accuracy, making it ideal for small parts that require a certain amount of fine detail. In this regard, it excels at creating thin-walled metal parts with complex shapes and sizes.

Regarding nickel-based alloys, wrought and cast alloys are generally used in combination due to their similar performances. Cast alloy's performances depend on castings' microstructural quality. Thus, the amount of segregation, carbides, and intermetallic phases is fundamental. Due to the less homogeneity, cast alloys exhibit corrosion rates that vary significantly with the casting techniques and passing from one cast to another. This observation explains why the corrosion rates of the corresponding wrought alloys are generally lower compared to the values of the cast products [33].

A comparison between casting and forging shows that, while there are some disadvantages in casting, like less homogeneity, less ductility, and more coarse structure of grains. But by casting, we are allowed to obtain complex shapes and the composition can be easily tailored.

4.1 SAND CASTING

As a method of producing metal shapes, sand casting is very long-standing and currently occupies the most important position in the metal casting industry. Well over 90% of the total foundry production is probably cast into sand molds. The main features which contribute towards this popularity are the ease, the economics and, above all, the flexibility of the process, which may be utilized for the production of practically any quantity of castings from one upwards and ranging in weight from tens of grams to hundreds of tons. Modifications to production methods are relatively easy and the sand casting process is suitable for practically all of the cast metals including plain carbon, alloy, and manganese steels, white and grey irons, nodular iron, nickel, and copper alloys, gun-metals, phosphor, and aluminum bronzes, brasses, aluminum alloys, and magnesium alloys.

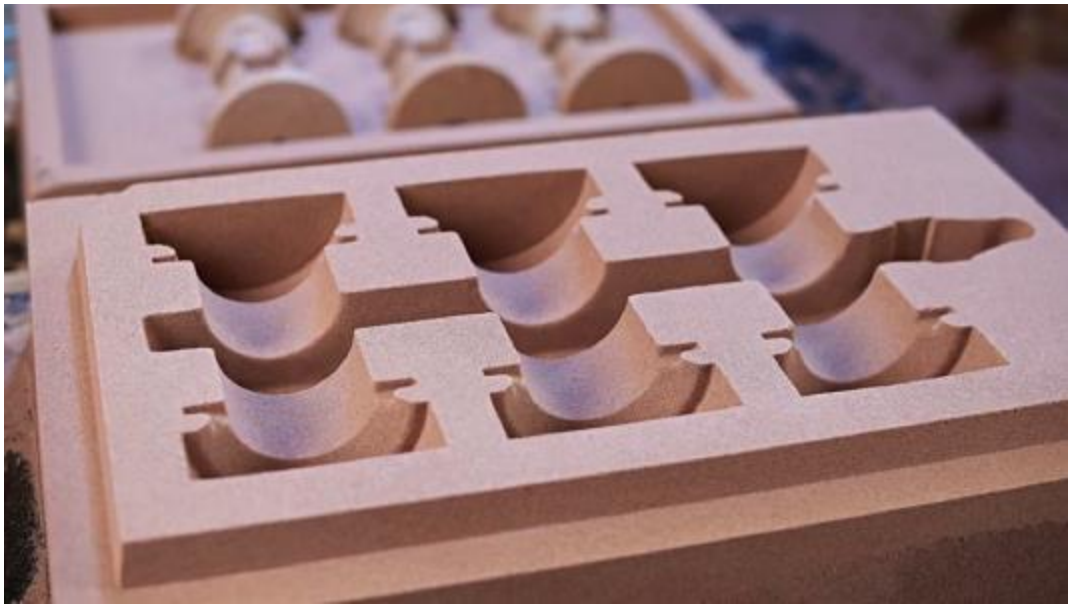

Figure 9. scheme of sand casting

Conventional sand casting is not a precision process and, where high degrees of accuracy are required, machining of the castings is often necessary. However, current developments such as high-pressure molding and chemically cured bonds that produce accurate and rigid molds are making the process competitive in this respect with the higher precision processes such as shell molding or investment casting. Of the various processes, castings made in sand generally have the lowest surface finish quality and other possible limitations are in speed of production and intricacy or thinness of section that may be poured successfully. However, the process is a relatively inexpensive one, especially in raw material costs. While the basic principles of sand casting remain virtually unchanged, developments in techniques have been made, particularly over the last few decades, and these continue at present. Such innovations as new molding materials (sands and binders), new methods of molding and core making including mechanization and automation, involve very considerable amounts of technological skills and have led to improved efficiency in production and better-quality castings. Thus, the current trends are towards improving casting quality still further and towards processes that involve less skilled manual functions [34].

4.2 METHODS OF MOULD PREPARATION

The manufacturer of molds of the required shape and dimensions is a vital part of the production of sand castings and several different techniques are employed. These usually require a pattern, the accuracy, and quality of which governs to a great extent the reproduction of a satisfactory mold and,

eventually, the casting. In jobbing foundries, where only a few castings per pattern are required or their manufacture is infrequent, hand molding may be employed. The basic techniques employed in making a simple mold are shown in figure 10, in this case, the pattern is split into two portions and use as being made of the natural taper. A minimum of two molding boxes is required to permit withdrawal of the pattern after molding. A split pattern is easier to mold, this is because with a solid pattern unless one suitable face happens to be flat, it is necessary to make use of an intermediate box part called an offside. This is simply a lightly rammed-up box into which the pattern is pressed before making up the drag part in the normal manner. In this case, the molder can choose the parting line to suit the job and it need not be in a single plane. For several castings off, the offside may be more permanent such as plaster or dried sand. A match plate pattern may be employed for the production of larger numbers of castings and this involves mounting the two halves of a pattern on opposite faces of wood or metal plate which is drilled to suit the locating pins or the molding box. The drag and cope parts are ramped-up with the match [34].

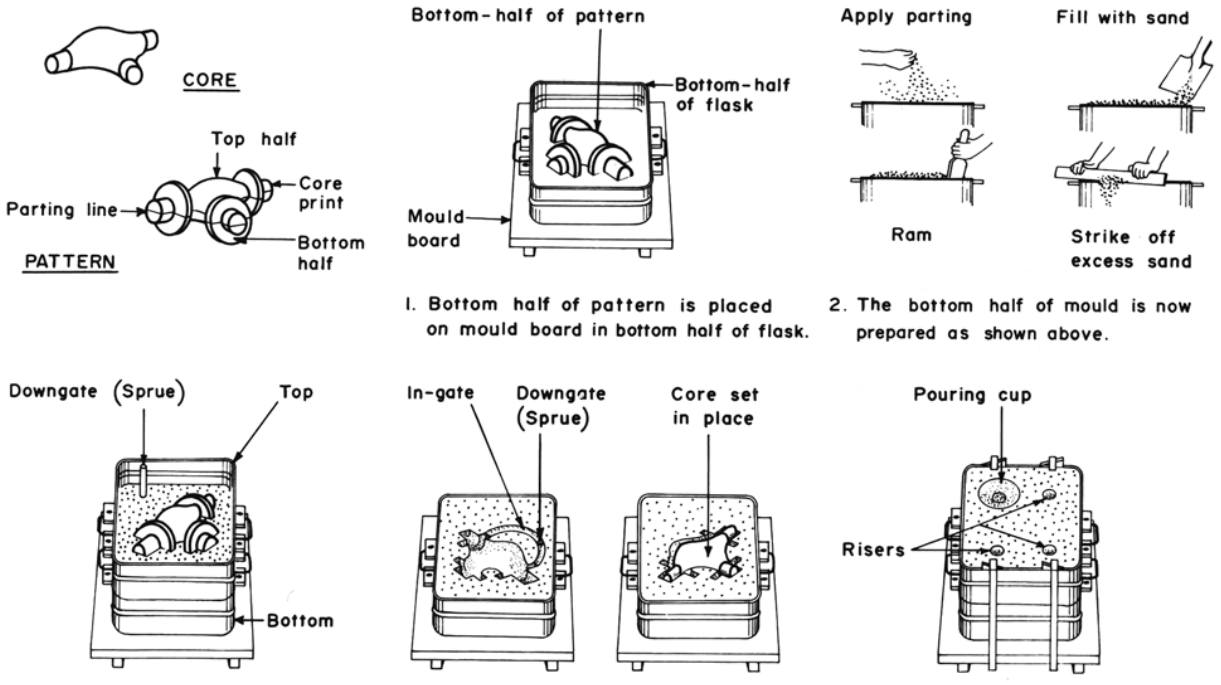

Figure 10. Making a simple mold by hand [34]

4.3 CASTING DEFECTS

The causes of casting defects can be categorized as direct or indirect. For example, one of the sources of gas porosity in Nickel castings is an excessive amount of gases, in particular hydrogen and nitrogen, dissolved in the melt. This, in turn, can be due to poor degassing practice and improper contents of one or more of the following elements in the melt: Al, Ti, Mn, S, Si, or the very rusty scrap used. The quality of the charge materials is therefore an essential parameter, of which the scrap seems to be most unstable. At the end of the whole chain of causes, there is usually a man whose influence on the process is often the least predictable. The selection of parameters, which should be network inputs, is essential. In principle, all the possible

causes, direct and indirect, can be included to assure that nothing important is omitted. However, collecting values of all possible parameters may be costly or even unfeasible in a given foundry. Hence, a careful analysis has to be made for each type of defect to determine the list of network inputs.

When the casting cools and solidifies, bubbles form because the solid form of the metal cannot hold as much gas as the liquid form. These bubbles appear on casting as rounded, circular cavities or holes.

4.4 DEFECT DISTRIBUTION

In order to select the most gainful defect types, an insight into the production scrapping levels was required. To obtain a global perspective, both the internal and external productions were looked into. First, the researchers highlighted that on a global production scale, casting defects are not the most common ones (Figure 11).

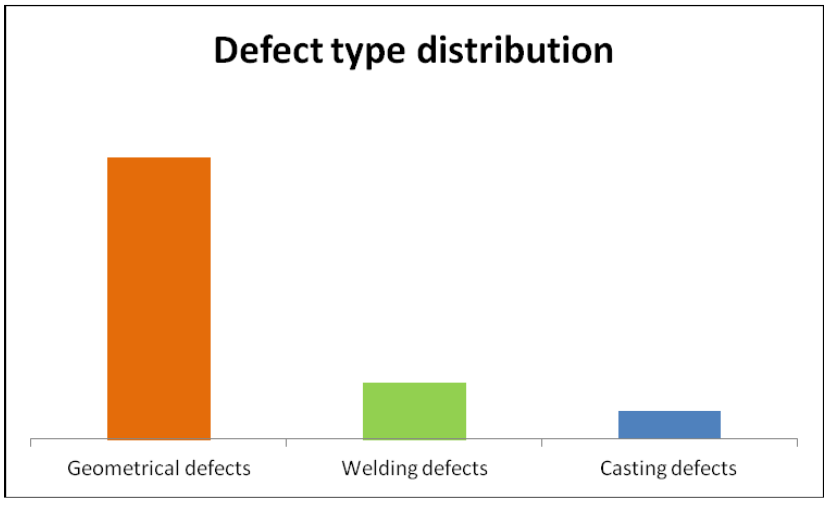

Figure 11. Distribution of 3 types of defects

When a part is defective, it can either be scrapped or submitted to a concession procedure. Concessions can concern a single part or a whole batch, and their purpose is, through defect analysis, calculation, and comparison to previous cases, to establish if the defective aspects can be overlooked, and the parts sent back to production. Therefore, it was possible to obtain an estimation of the defective parts distribution of the external production through the concession reports provided by the suppliers, which had deemed some of their defective parts to be possibly saved.

4.5 MAIN CASTING DEFECTS

Based on Figure 12, cracks are the most dangerous defects in casting because they are planar defects with the main dimension. Not only the size of defects is important, but also their density: small defects can be dangerous if they are accumulated in a specific region of the entire volume.

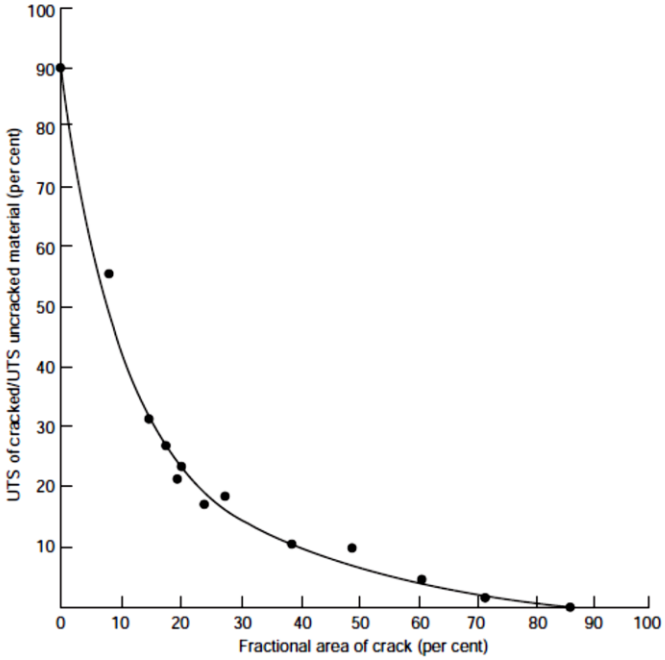

Figure 12. Effect of the crack area on UTS of casting[35]

Cracks are considered casting defects. The distinction between solidification defects and casting ones is fundamental. The first ones are known as shrinkage porosity or shrinkage pipe that can be easily controlled and generally are not extremely harmful, the second ones include the main detrimental defects in casting products. Below, the main casting defects which appear during the processes are discussed[35].

4.5.1 Inclusions

Inclusions are unwanted elements trapped inside the matter during solidification. Their origins can be:

- Impurity of the material (oxides, precipitate, or other external particles)

- Internal surface of the mold (ceramic bits plucked from the mold during pouring)

- Surface of the ceramic core

To avoid impurities when pouring the metal, a filter can be added to the casting shaft. The core and shell proprieties are also being researched: for instance, a significant difference in thermal expansion coefficient between the elements of the assembly can lead to overstresses and thus breakings of small bits of mold. In general, inclusions have poor mechanical properties compared to the poured material. They also have a limited cohesion with the surrounding metal and are therefore weaknesses in the matter and preferential areas for crack initiation.

Figure 13. Inclusion at the surface of a blade root [36]

4.5.2 Shrinkages and Microshrinkages

Shrinkage occurs because metals are less dense as a liquid than a solid. A shrinkage cavity is a depression in a casting that occurs during the solidification process. Shrinkage porosity appears with angular edges, compared to the round surfaces of gas porosity. Cavities might also be paired with dendritic fractures or cracks. Large shrinkage cavities can undermine the integrity of the casting and may cause it to eventually break under stress. Figure 14 shows the Shrinkage formation principle.

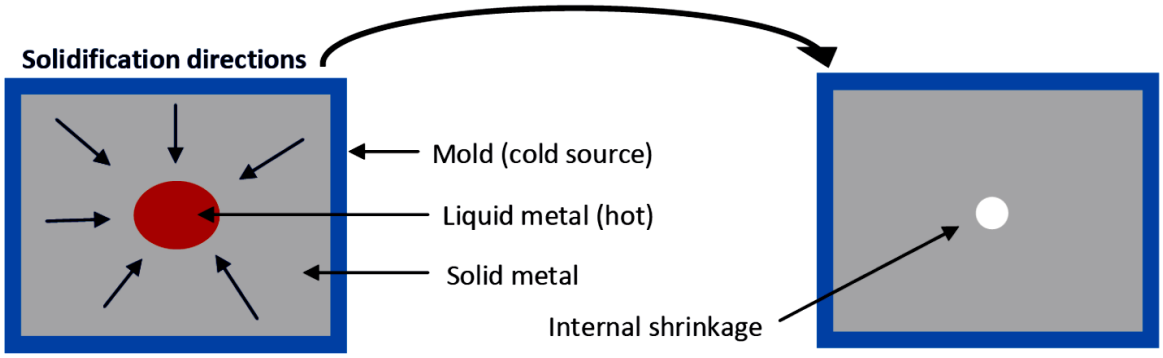

Figure 14. Shrinkage formation principle [36]

It should expect some shrinkage during solidification. Factor a shrinkage allowance into the pattern design before casting. Shrinkage can result in two types of casting defects, open and close shrinkage defects. As shown in figure 15 in open ones, these are open to the atmosphere. Air compensated as the shrinkage cavity forms. Pipes are open shrinkage defects that form at the surface and burrow into the casting. Caved surfaces are shallow, open shrinkage defects that form across the surface of the casting. On the other hand, closed shrinkage defects form within the casting. Macro shrinkage can be viewed with the naked eye, but micro shrinkage cannot. Closed shrinkage defects usually appear at the top of hot spots, or isolated pools of hot liquid. Prevent shrinkage cavities by improving casting structure Alloys always shrink when changing from molten to solid. This is because the density of a casting alloy in the molten state is lower than that in the solid-state.

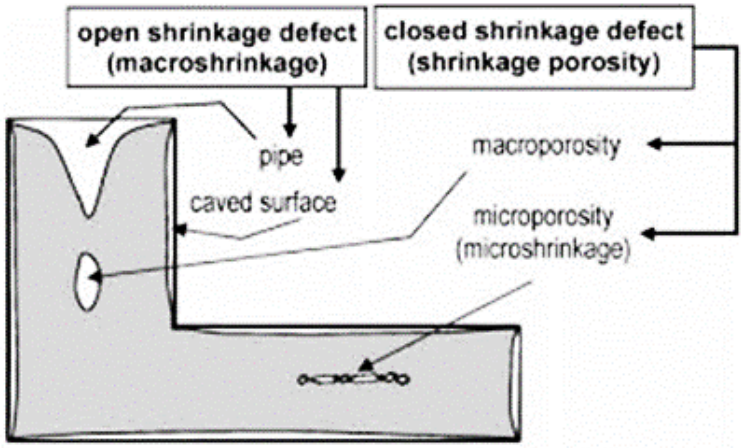

Figure 15. open and close shrinkage defects [37]

A micro-shrinkage has the same principle of formation but at the dendrite scale: a pocket of liquid metal is trapped between the dendrite arms, resulting in dendritic micro shrinkage (see Figure 16).

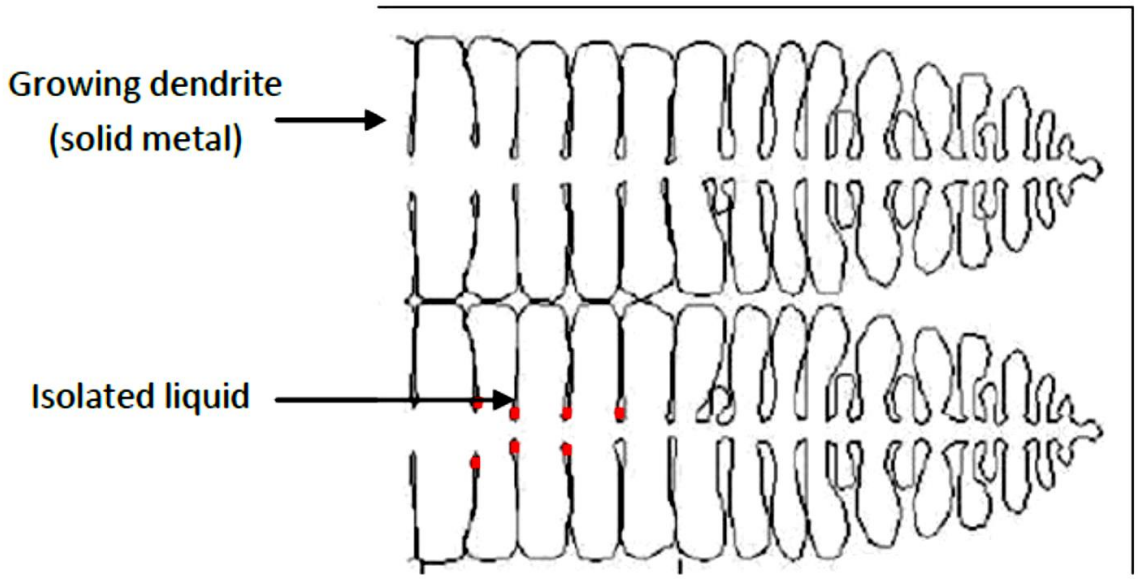

Figure 16. Dendritic growth resulting in micro shrinkage [37]

An example of micro shrinkage is visible in figure 17, such defects have an impact on the mechanical properties of the part: they induce stress concentration and are preferential crack initiation sites.

Figure 17. Example of micro shrinkage [37]

Moreover, the control of the solidification front evolutions is the key to preventing shrinkage defects. Below there are some strategies to improve the overall casting structure, which can prevent shrinkage casting defects.

- Design a running (gate) system with risers that ensure a continuous flow of molten metal
- Increase local heat dissipation by inserting internal chills, cooling ribs, or cooling coils
- - Reduce casting temperature to limit the total volume deficit

4.5.3 Surface Crack

The casting process can lead to residual over-stresses in some part's areas. To release the surplus of internal energy accumulated, a surface crack can appear. These defects can be avoided by geometrical adjustments of the part: indeed, smooth geometrical changes lead to fewer over constraint areas, thus reducing the chance of crack formation. Thermal dilatation equilibrium can also help avoid crack defects [37].

Figure 18. Example of a 3mm surface crack [37]

4.5.4 Recrytallization

If a single crystal endures local plastic deformation before quenching, it accumulates internal energy. This energy can be released during heat treatment and, if sufficient, locally re-orient the crystal and create a grain.

Such grains have very poor mechanical properties because of disorientation and lack of strengthened grain boundary. Plastic deformations at the origin of the grain can be due to shocks while suppressing the shell or thermal dilatation incompatibilities between the ceramic shell and the metal during cooling.

Parasite grain

During the solidification of a single crystal, another grain can germinate from inclusion or a cold point, resulting in a parasite grain with random orientation and with unwanted grain boundaries. The thermal environment has to be controlled to avoid such cases.

Disorientated grain

The primary orientation of a single crystal is of primary importance for the part properties. If during solidification, the selection of the grain orientation is not correct, the primary axis of the grain is too different from the loading axis and thus the mechanical properties degrade.

4.5.5 Fusion

Fusion occurs when sand grains fuse with molten metal. It appears as a thin crust with a brittle, glassy appearance firmly adhered to the casting [36].

Figure 19. Example of a fusion [37]

Two main factors can cause fusion:

- Low refractoriness of clay or sand
- Too high pouring temperature of molten metal

Refractoriness is the ability of the molding material to resist the temperature of the liquid so it doesn't fuse with the metal. Silica sand has the highest refractoriness. Improving the refractoriness of the molding material and/or reducing the pouring temperature of the molten metal will help prevent fusion.

4.5.6 Hot Crack

Cracks appear in the form of irregular crevices in a branched pattern.

Figure 20. Example of a hot crack in the surface of the sample

Some cracks are obvious and easily seen, while others can require magnification. Cracks occur as the casting cools, towards the end of solidification. If the solidifying metal does not have sufficient strength to resist tensile forces during solidification, hot tears will appear. Hot tears are mostly caused by poor mold design. Modifying the mold to improve collapsibility can easily resolve these issues [37].

4.6 POROSITY PREDICTION IN THE CASTING OF Ni-BASED ALLOYS

Knowledge of casting defects and causes is essential to managing casting quality. It should be set, defect tolerances, and quality expectations with the suppliers before production to help them understand your quality standards. The manufacturer must strictly control the quality of each

casting process. Experienced importers rely on quality control inspections to limit casting defects in their products before they leave the factory. To increase the final quality of the products, porosity prediction should be applied to them. Most of the research on porosity prediction has been focused on Al alloys and steels [38] and the work on Ni-based alloys is more limited. Simulation of solidification to predict porosity in investment castings from Ni-based alloys started a long time back; though, very simple geometries were considered in the earlier works. Overfelt et al. [39] developed a computer solidification model for the castings of plates with thicknesses of 2.54, 12.7, and 25.4 mm made from the In-718 Ni-based alloy. The model was used to validate and disprove various phenomenological criteria for predicting porosity. The computer model was shown to be effective in predicting unfed centerline shrinkage in the 25.4-mm-thick plates, but it did not provide precise results for the thinner plates. Monastyrskiy [40]proposed a modeling tool based on liquid metal deformation due to solidification to model shrinkage porosity formation in a GS 32 Ni-based alloy with low gas content. The model predicted the volume fraction and size of the shrinkage porosity. The nucleation of pores depended on the local stress level in the melt and the pore growth was driven by stress relaxation after pore nucleation. Numerical studies of directional solidification under an imposed temperature gradient and cooling rate were in good agreement with experimental data on porosity formation in Ni-based alloys [18]. Modeling of investment casting of complex-shaped parts has shown to be a more challenging task. Kang et al. [41] applied a model based on the dimensionless Niyama criterion to predict the formation of microporosity in a Ni-based alloys' casting containing

complex shapes with thin walls. The theoretical predictions of microporosity showed reasonable agreement with the experimental results, though they underestimated the porosity content in the complex thin-wall regions. However, the model was not suitable for the shrinkage porosity prediction in the thick parts of the casting, since those sections often formed isolated liquid pools.

Torroba et al. [40] applied an advanced modeling approach to the development of a new generation of Nozzle guide vanes (NGVs) with complex shapes for aero engines. In that work, firstly, a thermal model capable of predicting the thermal history during investment casting of the new generation NGVs is developed. Once the developed thermal model is validated against experimental results, the overall casting process can be analyzed in detail. The second aim of this work was to simulate the development of defects in the as-cast NGVs (such as shrinkage porosity) and the final grain structure. The present manuscript consists of two parts and this (first) part focuses on the development and validation of the thermal model and the porosity prediction tool.

Figure 21 shows the porosity predictions (left) and the experimental data (right) of the transversal section of a solid vane in the as-cast NGV. The optical micrographs corresponding to the trailing edge (zone a), middle part (zone b), and leading-edge (zone c) are also plotted in Figure 21 The analysis of these results shows a good agreement between simulation predictions and experimental results in all zones.

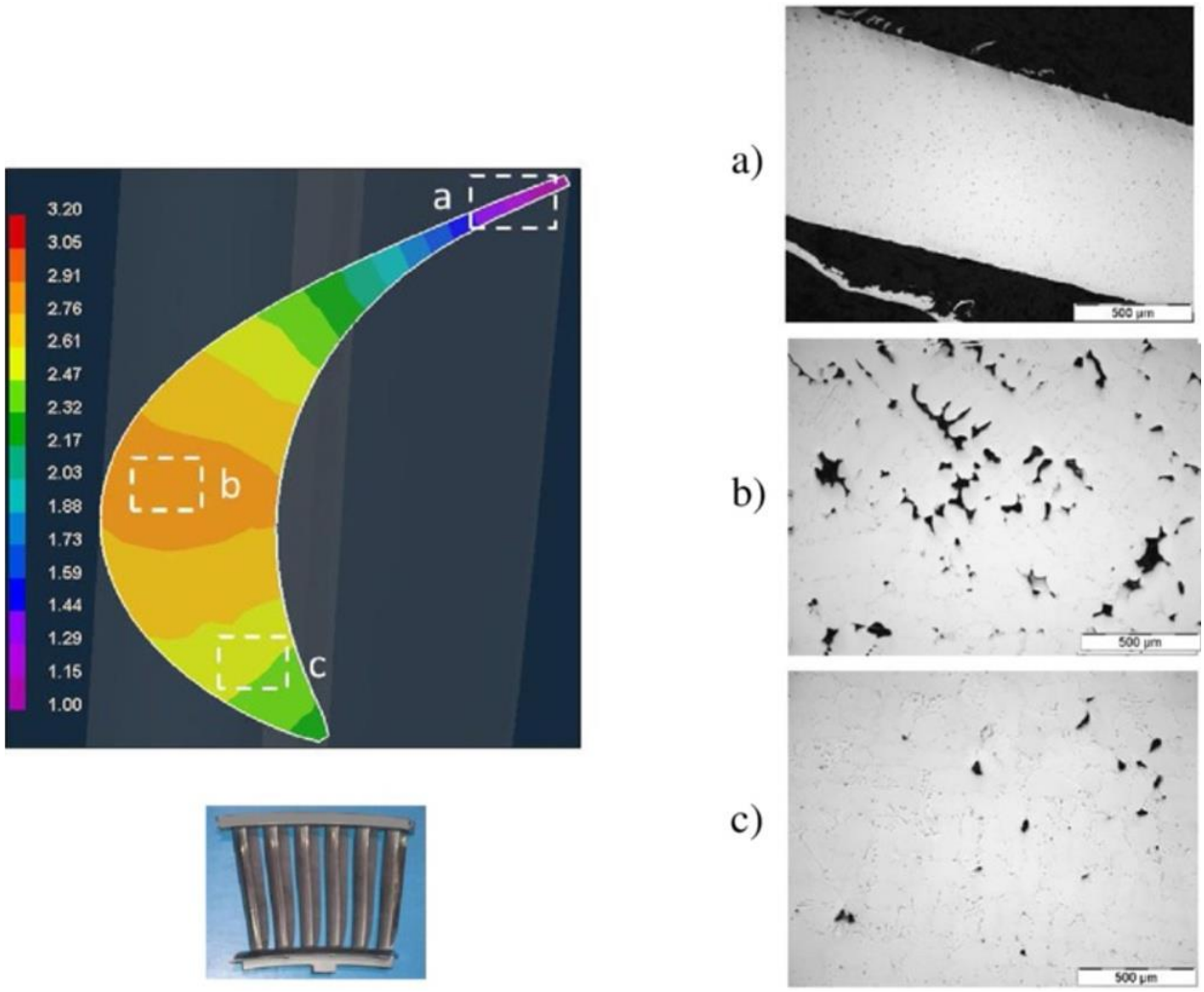

Figure 21. Porosity prediction by the ProCAST model and optical microscopy images of porosity. Porosity prediction by the ProCAST model (left) and optical microscopy images of porosity for the defined areas (right). The location of the analyzed section in the NGV is marked by red circle [40].

5. MATERIAL AND EXPERIMENTAL METHODS

5.1 MATERIALS

In this study four samples were analyzed. Figure 22 shows the uncut geometric of the samples.

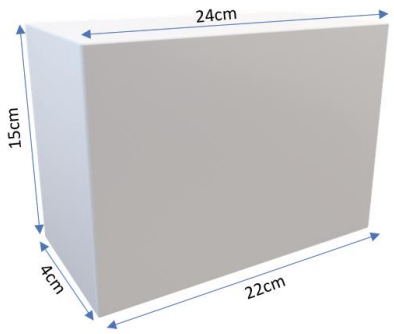

Figure 22. Dimensions of as-cast samples

All samples were in the same shape but with different percentage of the revert. As:

- Sample 1 = 0%

- Sample 2 = 30%

- Sample 3 = 70%

- Sample 4 = 100%

It means that, for example, sample number 2 contained 30% of scrap and sample number 3 has 70 of that. The scrap content of CW6MC, inserted in the melt before the pouring process. Scrap consists of recyclable materials

left over from product manufacturing and consumption; in this case, it is the content of CW6MC. Unlike waste, scrap has monetary value, especially recovered metals, and non-metallic materials are also recovered for recycling. From the previous casting, the scrap material may include runners, feeding systems, and other wastes. So, the scraps are cleaned from sand and release agent only by steel powder and they are not purified with specific methods. Table 8 shows the standard alloy composition.

Table 8 Chemical composition of standard CW6MC [12]

CW6MC chemical composition (wt%, typical values)					
Ni	**C**	**Cr**	**Mo**	**Fe**	**Nb**
Bal.	**<0,06**	**20 - 23**	**8-10**	**<5**	**3,14 - 4,15**

Two different forms of the study were applied to the samples, the first one was as-cast form and the next one was in solution annealed form. For solution annealing, the Furnace Carbolite HRF7/22 was used. The heat treatment was done following standard ASTM A494/A494M. Samples were taken at 1200°C for enough time and then water quenched [19]

Samples nomenclature is defined in Table 9.

Table 9. Samples nomenclature

Amount of scrap	**0%**	**30%**	**70%**	**100%**
Sample name	**Sample 0%**	**Sample 30%**	**Sample 70%**	**Sample 100%**

In industry, in the case of high-cost material like nickel-based alloys, using scrap is an option to reduce the cost and also production impact. However, the use of revert inside casting may cause the reduction of final product mechanical properties. Thus, the four different ingots were analyzed to understand what is the maximum allowable percentage of scrap that can be used. Test specimens are produced by simple sand casting and the microstructure, mechanical properties, and casting defects of the four ingots were analyzed to find the maximum allowable percentage of recycled material. Test specimens were produced from different castings. In each sample, four different parts which were distributed in the whole part of the samples were cut and analyzed. As shown in figure 23 the green parts were cut and studied.

Figure 23. Focused and analyzed parts of the samples

5.2 SAMPLES PREPARATION

To be able to examine material and come to a satisfactory conclusion about its quality, grinding & polishing of a sample is an important initial step in metallography i.e. material graph. This scratch-free step suitable for macro and/or microscopic observation must have a representative, sharp-edged and level surface of the material to be examined, which allows clear recognition of its structure. Therefore, no scratches, unwanted fractures, foreign bodies, or deformations must appear in the preparation of the material. Preparation normally takes place in three main steps:

- cut-off

- polishing

-etching

5.2.1 Cutting

Step number one involves cutting off a section to be tested/examined as a sample of the material using a cut-off machine and the corresponding clamping tools which have been designed to clamp at strategic positions. If the specimen is large enough, it can be mounted and then ground and/or polished with a holder without further preparation. As nickel-based alloys are very dense materials, so cutting machine was used to obtain the small sample dimension. The cutting operation was performed manually by the machine Mod C250S (see figure 24).

Figure 24. Schematic of machine Mod C250S

These machines are reliable machines for sample preparation. Some advantages of this machine are:

- The large shatter-proof viewing window is in high-density polycarbonate for a perfect view inside the cutting chamber.

- Facilitated by the fluorescent lamp illuminating the area

- An electromagnetic braking system rapidly stops the wheel rotation

- Sets the motor in the mechanical pause at the end of the cutting procedure

5.2.3 Polishing

To make the crystal structure visible, the sample surface must be initially ground even, and then polished. The grinding & polishing process takes place using a unit with the same name; either per hand, for example with pre-grinding on the pre-grinding unit, or conversely automatically – which

is more normal for today's metallography laboratories. In contrast to manual grinding & polishing, in the case of automatic grinding, the sample is fixed in a sample holder and pressed onto the grinding medium (grinding paper, grinding wheel, etc.) with a grinding & polishing head. The polishing medium sits on top of a working wheel. A series of grinding steps follows whereby each new step makes use of the even finer grinding medium, to proceed step-by-step towards the grade of polished surface desired. The sample has to be rotated through 90° after each grinding step, to cancel out the grooves leftover from contact with the previous grinding medium. During the whole process, a lubricating & cooling fluid ensures that the sample is cooled and waste material washed away. The sample should be cleaned regularly with water and alcohol between the single steps, to ensure that waste material (sludge) and coarse grinding particles from the previous step are not carried over to the following step.

The following polishing phase uses various polishing cloths. The last scratches leftover from the previous grinding is polished away by removing a last final layer. This step-in metallography is best served with a diamond suspension in poly or mono-crystalline form as a final polishing medium. In particular, where many samples are polished one after one another, the use of an automatic grinder & polisher (such as in the case of system labor or even the system automate) is of advantage.

In this study, the procedure was based on the use of different grits. Grits are used in the following order: P120, P180, P320, P600, P800, P1200, P2500. Then, the use of two rotating pads with various diamond suspensions is performed. The first pad is used with a suspension of 6 µm

and the second pad with a suspension of 1 µm. The pads for steel are used due to the absence of specific rotating pads for nickel-based alloys (see figure 25).

Figure 25. Schematic of polishing mashing

5.2.4 Chemical Etching

After completion of the last polishing step, first predictions about the purity of the material can be ascertained through the different reflections. To make the crystal structure visible for being contrasted, the sample has to undergo a further preparation step either manually per immersion into an etching liquid or through the deployment of an electrolytic etching unit such as the model “Kristall“. The particular etching fluid for the particular sample has the effect of changing the reflection behavior of the integral crystalline component so that an optical difference is possible. Following etching, the sample is washed in alcohol and then rapidly & thoroughly dried under a flow of warm air.

In the present study, for CW6MC alloy, two types of chemical etching were performed:

- macro etching
- micro etching

Macroetching

95% hydrochloric acid (HCl) and 5% hydrogen peroxide (H_2O_2) solution was used to show grains macrostructure. The procedure was carried out following the standard E340 – 00 [42]. The time of application vary from 40 to 45 seconds depending on sample. Solution application was performed immersing the samples in a glass lens containing reagents. Macro etching was performed only on as-cast samples and not on solution-annealed ones.

Microetching

20% nitric acid (HNO_3) and 60% hydrochloric acid (HCl) solution was used to show samples microstructure. The procedure was carried out following the standard E407 – 07 [42]. Time of application ranges from 40 to 45 seconds depending on sample. Micro etching was performed both on as-cast samples and solution annealed ones.

5.3 CHARACTERIZATION OF SAMPLES

To find out the characteristics of the samples, different equipment was used, such as:

- Optical microscope

- Scanning electron microscope
- Optical emission spectrometer

Each device was used for the specific purpose of analyzing the macrostructure and microstructure. In addition, in the first step, for macrostructure analysis, after etching the un-cut samples, the size of the macrostructure was analyzed by Digimizer software.

5.3.2 Optical Microscope

Metallography is the study of the microstructure of all types of metallic alloys. It can be more precisely defined as the scientific discipline of observing and determining the chemical and atomic structure and spatial distribution of the grains, constituents, inclusions, or phases in metallic alloys. By extension, these same principles can be applied to the characterization of any material. Different techniques are used to reveal the microstructural features of metals. Most investigations are carried out with incident light microscopy in brightfield mode, but other less common contrasting techniques, like darkfield or differential interference.

In this study, Physical discontinuities like porosity, cracking, etc., and electrochemical surface modifications like oxidation, corrosion, etc. were focused. In the case of counting the cracks on ingot surfaces, the cracks with lengths equal to or higher than 200µm have been evaluated as dangerous and have been considered in the analysis (see figure 26). As the pictures are black and white, the distinction between oxides and porosity couldn't be possible due to their similar color. So, the concept of defect has been

extended as the sum of porosity and oxides. Another important parameter in the solidification process is the secondary dendrite arm spacing (sDAS). sDAS value is directly correlated with the mechanical properties of the alloy because it reflects the thermal conditions during solidification. It is well established that sDAS tends to decrease increasing the cooling rate. Images of micro-etched samples were used to evaluate sDAS in different samples with different percentages of scrap. Digimizer software, an image-processing program, was used to evaluate these lengths. The images were transformed into binary images (black and white) and the lengths were measured.

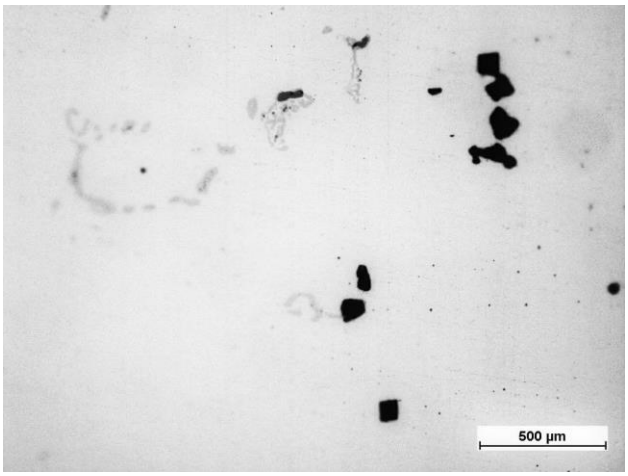

Figure 26. A picture to Porosity and oxides analysis

In the present study, the Leica MEF4 A/M inverter material microscope was used. It is equipped with different lenses from 25x to 500x and for the acquired images, Nikon Eclipse LV150NL was employed. The optical microscope was used to obtain images of etched samples and only polished samples. All the acquired images were captured with the software Nikon NIS Elements D.

5.3.1 Optical Emission Spectrometer (OES)

Optical Emission Spectroscopy, or OES, is a well-trusted and widely used analytical technique used to determine the elemental composition of a broad range of metals. The type of samples which can be tested using OES include samples from the melt in primary and secondary metal production, and in the metals processing industries, tubes, bolts, rods, wires, plates, and many more. OES analysis is based on the ablation of sample material by high-frequency electrical sparks applied between a metallic sample and an electrode. The ablated material is excited in the argon plasma generated by the sparks and a corresponding light in the UV-visible range is emitted. The emitted wavelengths are characteristic of each element and their intensity is proportional to the element concentration. The light emitted is directed towards the optical system. The main component of the system, the diffraction grating, separates the polychromatic light into its monochromatic constituents by dispersion over a certain wavelength range. The photons of the wavelengths of interest are usually collected by a detector and transformed into electrical signals. The analysis provides faster results with higher accuracy.[43]

5.3.3 Scanning Electron Microscope (SEM)

In conventional scanning electron microscopy (SEM) systems, the surface of a solid sample was excited with a highly-focused energetic beam of electrons which induces X-ray fluorescence from the elements within the sample. Samples must be run under high vacuum conditions and must be conductive or coated with a conducting material such as gold for proper

analysis. X-ray microanalysis of uncoated non-conductive samples in the conventional SEM was hampered by specimen charging which can reduce the energy of the electron beam and make quantitative analysis impossible.

Accelerated electrons in an SEM carry significant amounts of kinetic energy, and this energy is dissipated as a variety of signals produced by electron-sample interactions when the incident electrons are decelerated in the solid sample. These signals include secondary electrons (that produce SEM images). Secondary electrons are most valuable for showing morphology and topography on samples and backscattered electrons are most valuable for illustrating contrasts in composition in multiphase samples (i.e. for rapid phase discrimination).

SEMs always have at least one detector (usually a secondary electron detector), and most have additional detectors. The specific capabilities of a particular instrument are critically dependent on which detectors it accommodates. In the present research, Observations of microstructures at higher magnification (up to 20000X) were performed with Zeiss SMT EVO 50 scanning electron microscope [44].

5.4 HARDNESS

The hardness of material is an ability to resist surface deformation. Hardness is an important factor to the seal ring, such as a significant impact on wear. There are three general types of hardness test, including Brinell hardness test, Rockwell hardness test and Vickers hardness test. The first step of brinell hardness test is to exert a certain load. Then the indenter made by quenching steel ball or sintered carbide ball would be pressed into the surface of the materials and maintain a certain time before unloading. Finally, the hardness can be calculated by the indentation diameter. The formula is:

$$HB = \frac{P}{A} = \frac{2P}{\pi D(D - \sqrt{D^2 - d^2})}$$

Here, P is the load; A is the area of indentation; D is the diameter of steel ball; d is the indentation diameter. The hardness of the specimen determined by Brinell hardness testing machine with 29.400 N load and 10mm diameter steel ball indenter. The detention time for the hardness measurement was 30 seconds . The tests were carried out at five different locations taken from each specimen. Each hardness result was obtained from an average of at least five repetitions on the same sample. Brinell hardness test is suitable to measure the metallic materials with Brinell hardness less than 450HB, especially for test material with large difference in hardness, such as iron casting [45].

6. RESULTS AND DISCUSSION

In this chapter, the result of the analysis on CW6MC samples will be discussed. The list of analysis is:

Macrostructure

Chemical Composition Analysis

Microstructure

Casting Defects

Phase Analysis

6.1 MACROSTRUCTURE

The first step of analyzing was studying the macrostructure of the samples. As mentioned in the previous chapter, to show grains macrostructure, the solution was 95% hydrochloric acid (HCl) and 5% hydrogen peroxide (H2O2). In large ingots and similar products, the solidification structure is ruled by thermal exchange conditions and by segregation phenomena. It typically depends on the distance from the surface. By analysis of a transversal section, two main regions are recognized (see figure 27).

- Columnar dendritic region
- Equiaxed central region

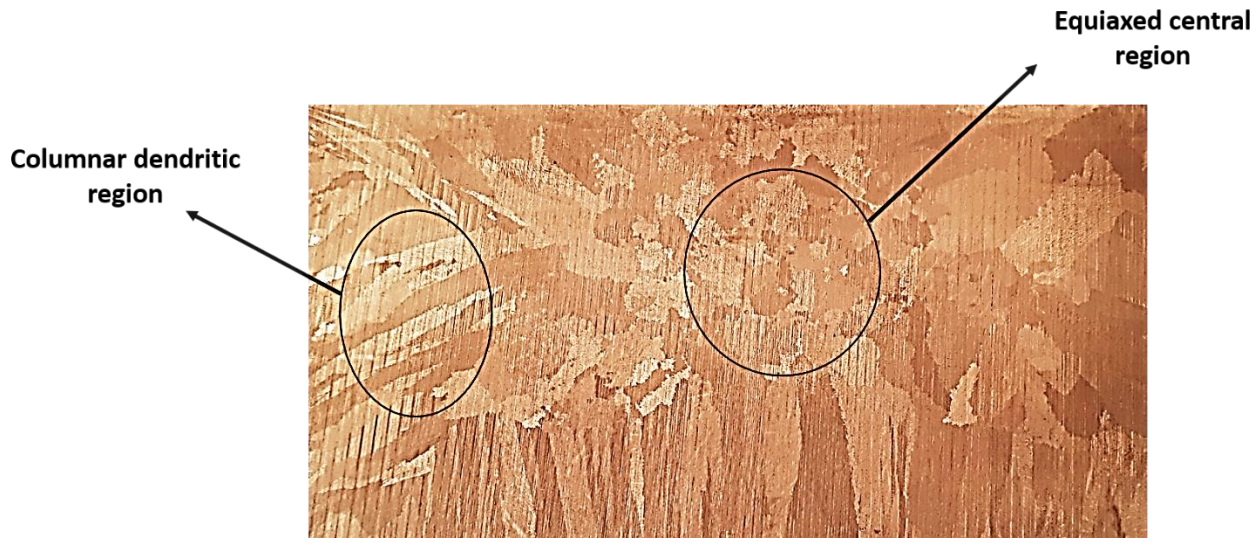

Figure 27. Columnar dendritic and Equiaxed central region zones in sample 0%

As figure 28 shows, the grain size and shape of the samples are different, there are a lot of parameters that affect grain size, such as:

- Casting parameters (temperature and velocity)
- Mold dimension and geometry
- Cooling parameter (sand, alluminium cooler,...)
- Chemical composition

These parameters prove that the shape and size of the grains are influenced by various conditions.

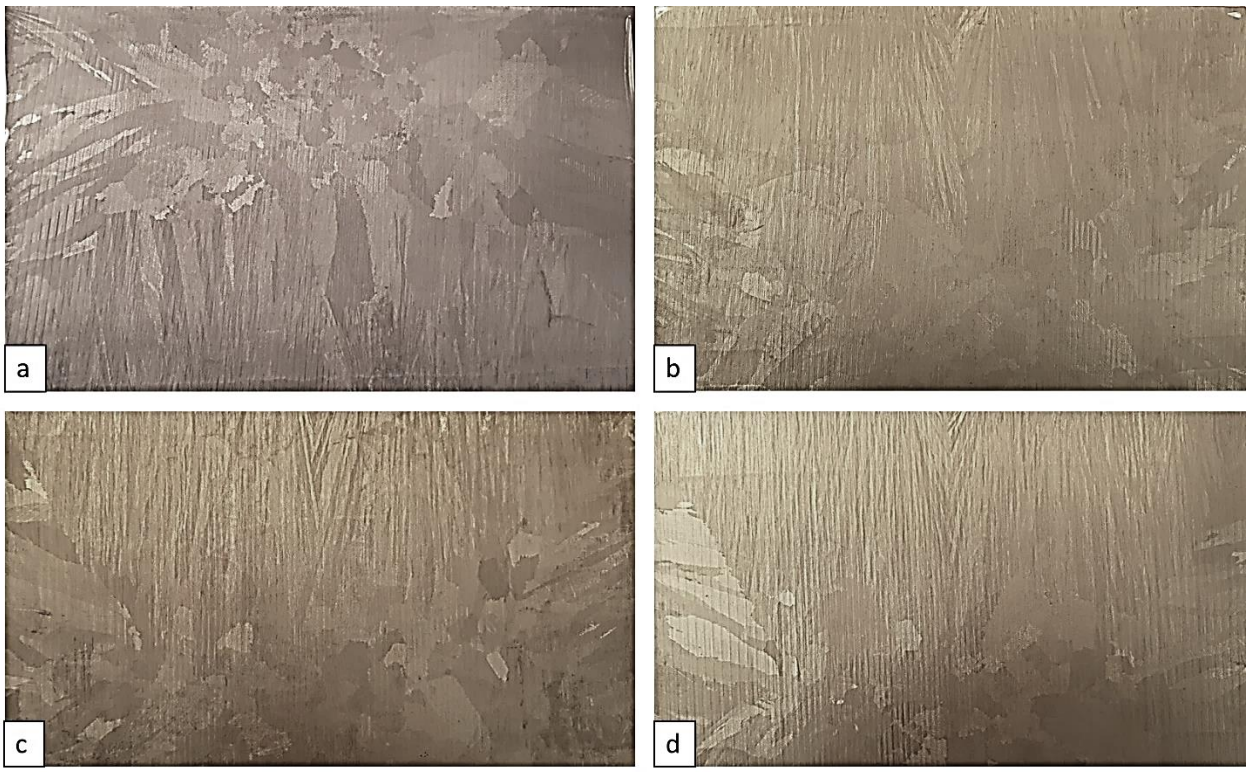

Figure 28. Four samples macrostructure; (a) Sample 0%; (b) Sample 30%; (c) Sample 70%; (d) Sample 100%;

As mentioned above, in all samples two main macrostructures that columnar and equiaxed structure were determined.

6.1.1 Columnar Structure

Columnar grains are long, thin, coarse grains created when a metal solidifies rather slowly in the presence of a steep temperature gradient. There is competitively growth between columnar structures and oriented grain respect of the thermal flow grew to stop the others. The main reason for the construction of these structures is the undercooling and the thermal extraction direction.

Figure 29 Shows the columnar structure in four samples. All four samples mainly present a columnar grain structure oriented in heat extraction direction.

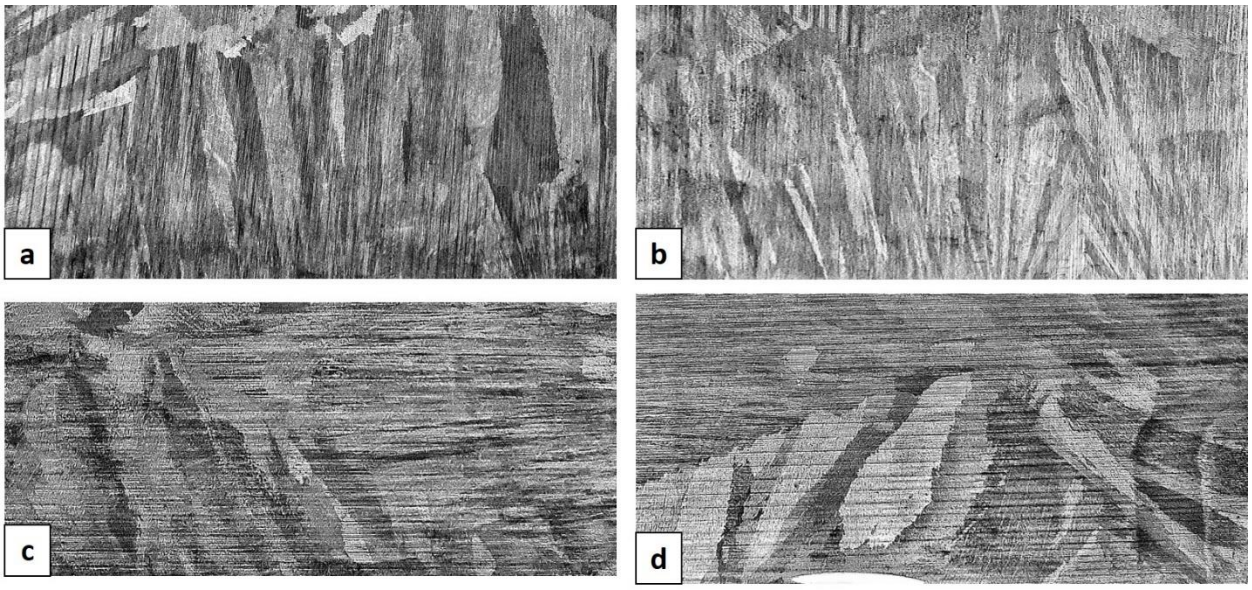

Figure 29. columnar grain structure of four samples; (a) Sample 0%; (b) Sample 30%; (c) Sample 70%; (d) Sample 100%

In all samples, the columnar grain structure was oriented based on heat extraction direction. Grains dimension will be fundamental in the analysis of surface hot cracks because it influences significantly this phenomenon. The main structure in all samples is equal and the only difference is in grain size (see figure 30). There is not a clear trend for difference, it's just fluctuation and they are mainly due to the process. Graphs 1 and 2 show the difference between grains' high and width.

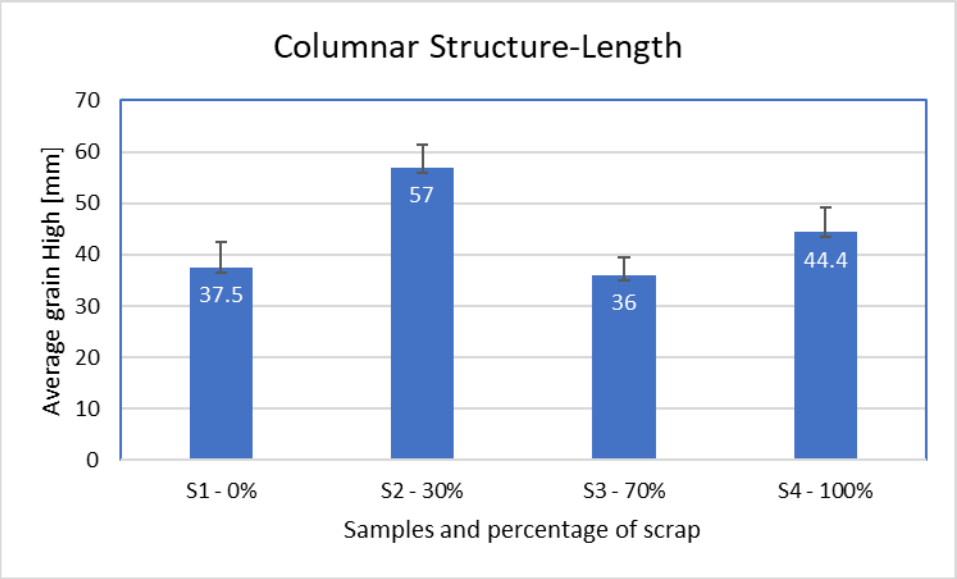

Graph 1. columnar grains' length in samples

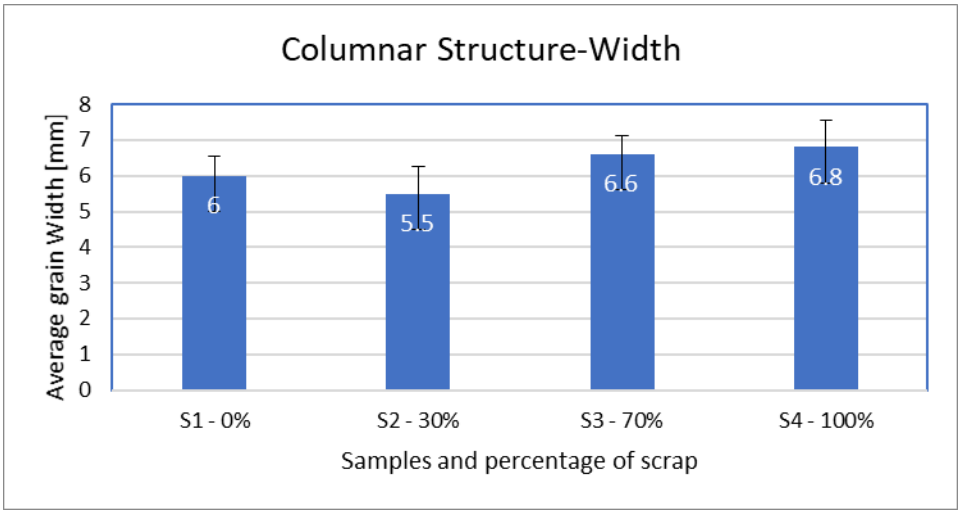

Graph 2. Columnar grains' Width in samples

Based on Graphs 1 and 2, sample 2 has the longest columnar structure and sample 3 the lowest one. On the other hand, sample 2 has the lowest width between the samples. Moreover, Graph 2 shows that sample 100% exhibits

a higher average grain width. Moreover, there is an influence of the revert on the width, by increasing the revert the width seems to increase.

6.1.2 Equiaxed Structure

Equiaxed crystals are crystals that have axes of approximately the same length and in some cases be an indication for recrystallization. The equiaxed formation is based on equal extraction of thermal in every direction. Equiaxed grains start to form the fragments in front of the columnar zone. Initially, the equiaxed grains are small and move along with the liquid. At around 40-50 seconds, the grains start sedimenting. The columnar front is blocked first at the bottom and then further up in the ingot. Figure 30 shows the overall view of the equiaxed structure part in samples.

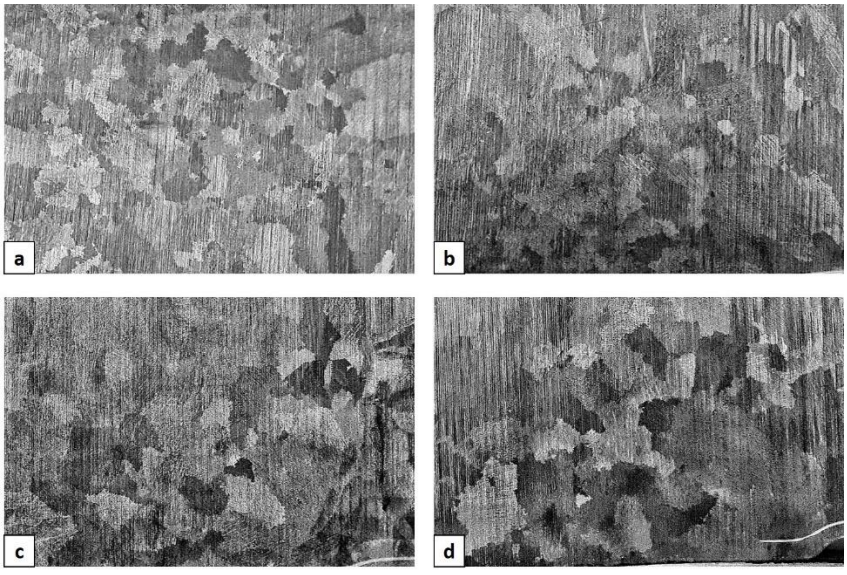

Figure 30. Equiaxed grain structure of four samples; (a) Sample 0%; (b) Sample 30%; (c) Sample 70%; (d) Sample 100%;

Based on Figure 31, the diameter of samples is different, due to finding out better the difference, the average size of the determine. Dimensional comparison shows that the grin size has more or less has a direct relation with the percentage of scrap, which means that with increasing the scrap the diameter of the equiaxed structure increase. Graph3 shows, samples 3 and 4 have higher diameter sizes than the others.

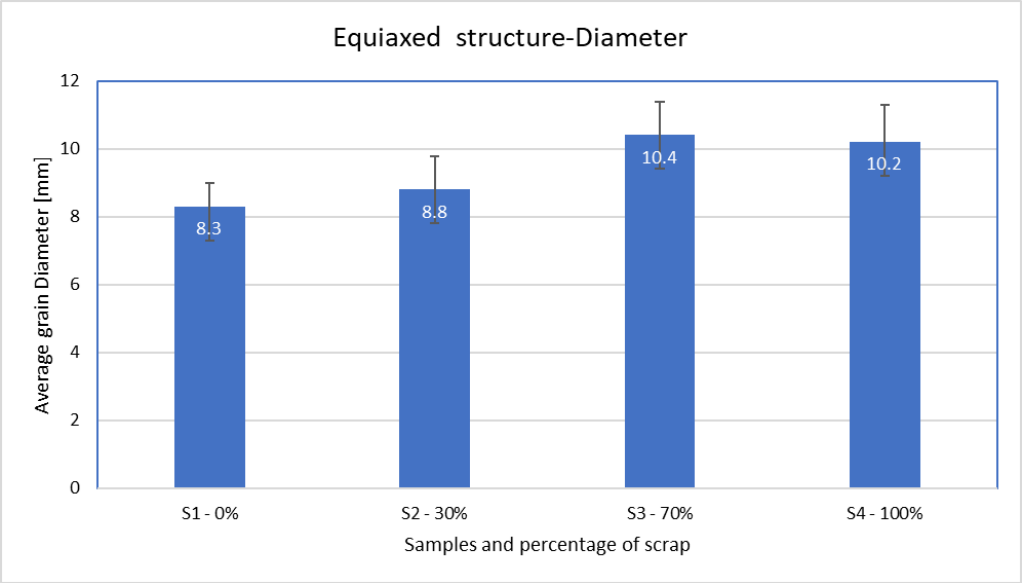

Graph 3. Equiaxed grains' diameter in samples

The equiaxed grain material exhibited the highest strength but the lowest plasticity. Depending on the grain size, the smaller the grain size, the higher the strength, but the lower the elongation. In other words, sample 1 with the smaller grain size, has less proportion of deformation but higher strength. Moreover, the critical shear stress is strongly dependent on the grain size, and the larger the grain size, the higher the critical shear stress, as sample 3 and 4 has the highest grain size, has the lower critical shear stress [46]. Moreover, based on graph 3 it seems that there is a trend, by

increasing the revert, the grain size increase. On the other side, there is no evident explanation for this trend, and there is no idea on the real casting parameter, maybe the S3 and S4 were cast at higher temperatures.

6.2 CHEMICAL COMPOSITION

Accurate analysis of the chemical composition of a material will provide invaluable information, assisting chemical problem solving, supporting R&D, and ensuring the quality of a chemical formulation or product. Chemical composition analysis can require the application of a combination of analytical methods in order to achieve a full picture of the chemical structures and concentrations of the components in a sample. To aid product development, the concentration of specific components, such as an active ingredient that imparts a unique function to the product, should be determined to understand the product's performance or quality. In the present study, chemical compositions of the solid ingots were performed. For comparing the chemical compositions, six main elements (carbon, nitrogen, silicon, manganese, iron, and nickel) were focused.

Graph 4 shows the behavior of Carbon contents varying the amount of scrap. Considering the percentage of C versus the amount of revert, the C content is increasing from sample 0% to sample 100%.

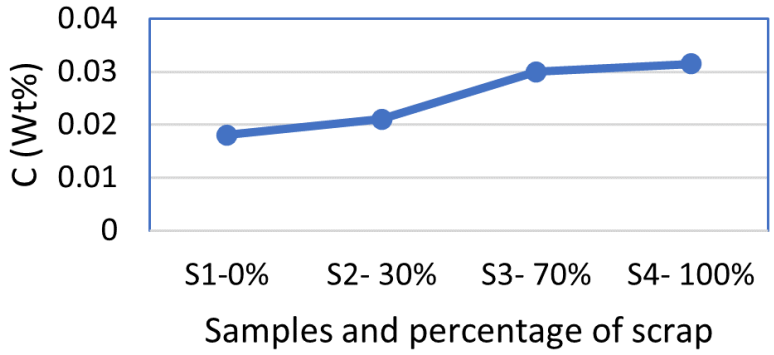

Graph 4. The weight percentage of carbon in samples

The amount of C is one of the main parameters in carbide formation, so if carbide formation is distributed homogeneously, it can be considered harmful phases. Moreover, Considering C and Si, their trends versus the amount of revert exhibit an increase passing from sample 0% to sample 100% (Si increases because of sand entrapment). The amount of C is one of the main parameters in carbide formation, so homogeneously distributed carbides can be considered harmful phases. Moreover, like other materials, with increasing the amount of Carbon, ductility, forgeability, machinability and weldability will decrease. The increase of C content can be related to cover powders used in melt protection or the ball for sand-blasting (from casting send, organic matter). The change of C amount is slight and this small increase in C, can increase solidification temperature range and changes the alloy hot cracking behavior. [47]

Graph 5 illustrates the behavior of Nitrogen content in ingots varying the amount of scrap. It is well known that the amount of N acts very similar to Carbon in the CW6MC alloy. Obviously, Nitrogen forms Nitrides, not

Carbides. Even a slight increase in N content can increase the hardness but on the other hand, significantly decrease the mechanical properties. Graph 5 appears that the amount of N increases with the increase in the percentage of scrap from sample 1 to sample 4.

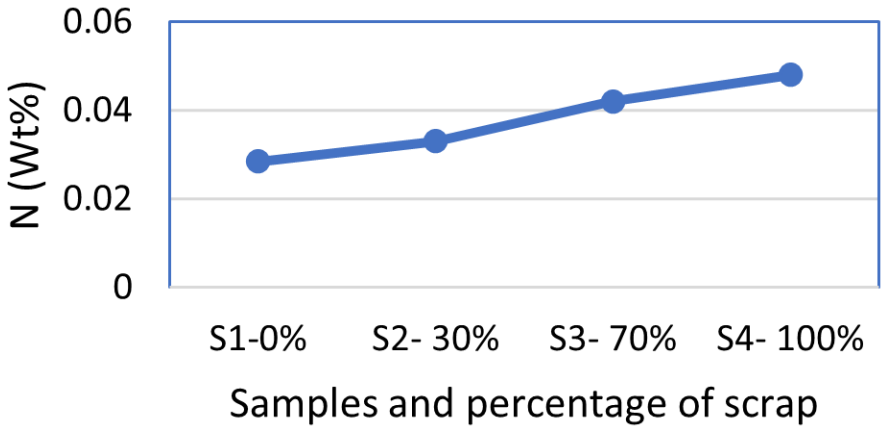

Graph 5. The weight percentage of Nitrogen in samples

Final component properties effected by extra percentages of N that are entrapped from several casting. In the case of recycled ingots, a part of N is just entrapped in the pre-melted scrap, and the addition of further virgin melts incorporates again more air and can remain after solidification [30].

Considering Si, silicon helps to remove bubbles of oxygen from the molten nickel-based alloys. It is the element that is most commonly used to produce semi- and fully killed alloys, and normally appears in amounts less than 1 percent. The behavior of Si depending on scrap content is illustrated in Graph 6.

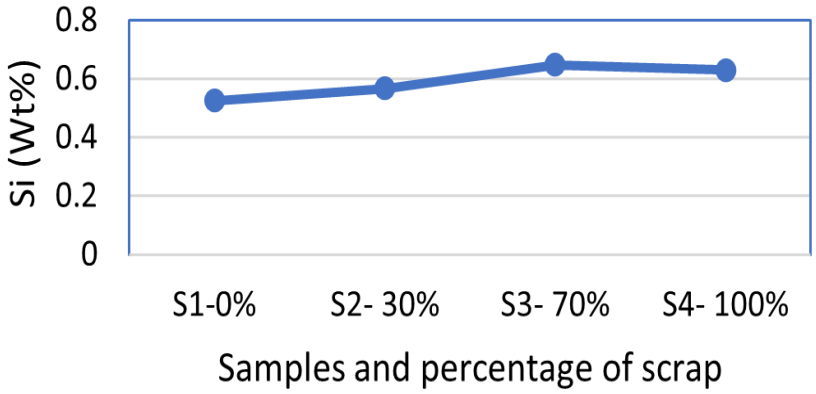

Graph 6. The weight percentage of Silicon in samples

Based on graph 6, Si amount is higher in sample 70% and sample 0% presents a lower amount of Si. The increase in Si with scrap percentage could be due to silica sand used for the casting process that is reinserted with revert addition. Scrap can show residual sand on the surface that is not removed by the cleaning process. [48]

Concerning Mn content, graph 7 shows the trend of Mn versus the amount of scrap. Mn tends to decrease until 70% of scrap, and then it shows a slight increase in sample 100%. In virgin alloy, Mn remains inside the solidified product because it is from oxides. These oxides can flow and be entrapped both in the ingot. The reason for increasing Mn from sample 3 to sample 4 can be justified considering that operators add this element to reach the required standard composition. By increasing Mn, the hardenability and tensile strength increase but ductility decrease.

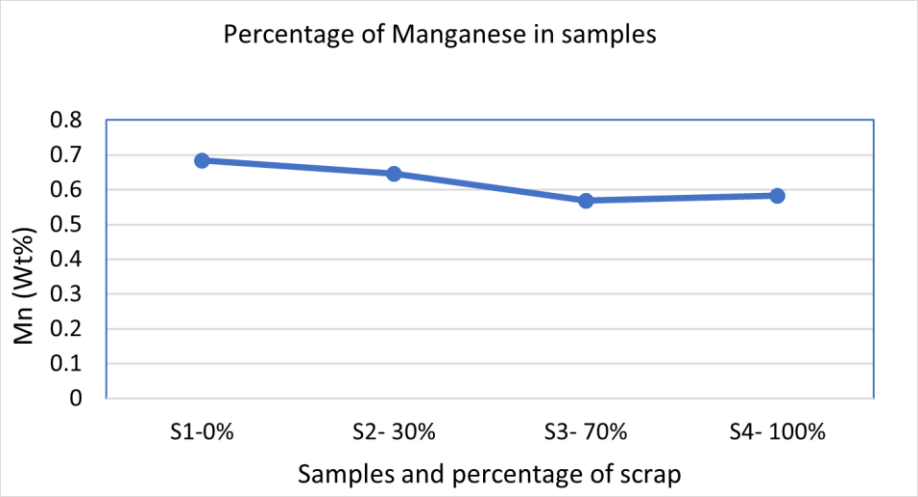

Graph 7. The weight percentage of Manganese in samples

The Mn decreasing trend can be explained considering that this element shows high reactivity and tend easily to be oxidized [31]. Another detrimental element is shown in Graph 8. It is well known that increasing the amount of revert, the Fe content increases. In this case, samples 70% and 100% are the ones with higher Fe content. Fe promotes laves phase formation and its increase could be responsible for the reduction of mechanical properties [8]. In passing from sample 2 to sample 3, an important change in Fe content is shown. Since scraps are not purified before the re-melts, they are only cleaned with steel powder and then they are immediately reinserted in the furnace, residual Fe can be inserted in the melt. Thus, Fe content is expected to be higher increasing the amount of recycling.

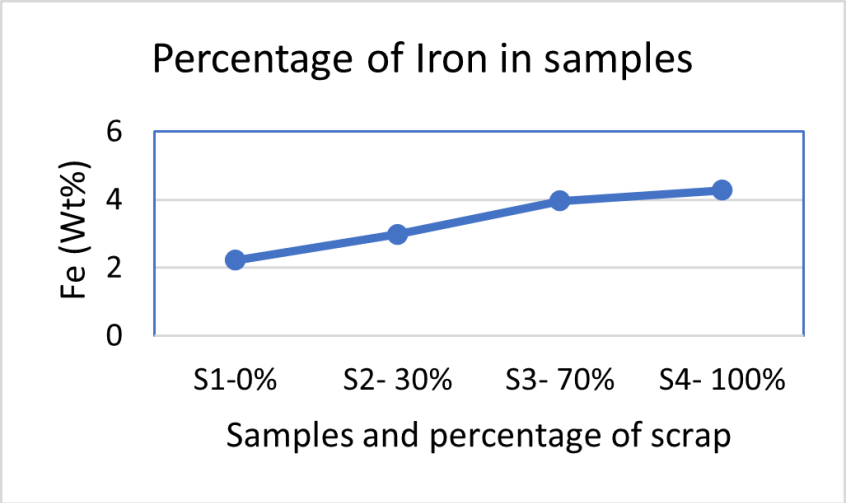

Graph 8. The weight percentage of Iron in samples

The last but not the least element is Nickel. Graph 9 illustrates the behavior of Ni content in ingots varying the amount of scrap. It is well known that the amount of Ni is the main parameter to be considered for CW6MC mechanical properties as CW6MC is a nickel-base alloy. As expected, by increasing the amount of scrap, from 0% to 100%, the amount of Ni decrease.

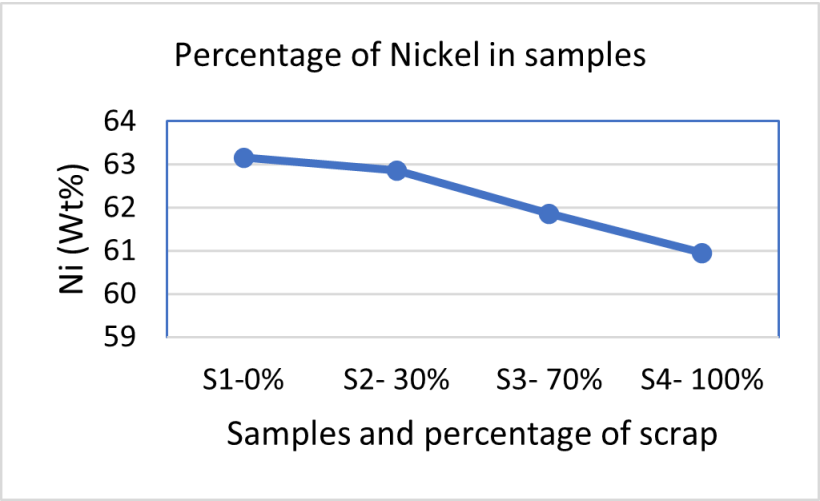

Graph 9. The weight percentage of Nickel in samples

Table 10 illustrates the weight percentage of other elements in the chemical analysis of solid ingots. P and S come from elements addition in melts. These elements are considered the main detrimental elements in most alloys so they should not promote loss in properties. Table 10 show that they decrease in ingot with increasing the amount of revert [49].

Cr amount presents a slight decrease passing from sample 0% to 70% but then it increases again at 100% of scrap. However, the ingots with 30% and 70% of scrap exhibit a lower Cr content concerning the other two samples. An increase in the amount of Cr in ingot with 100% of scrap can be done by the operator to reach the required standard composition.

Considering Mo, it shows a great effect in solution strengthening and corrosion resistance, but it can also be responsible for detrimental Laves phases formation. The behavior Mo depending on scrap content is illustrated in Table 10 The increase in Mo amount in samples 3 and 4 can be justified by considering that the addition of Mo was done before this casting. Sample 2 is expected to be the one with lower localized corrosion resistance for its lower amount of Mo [31].

Nb content decreases with increasing the amount of scrap. As Mn is highly reactive, so it has been continuously oxidized during remelt operations.

The last two elements are Al and Ti, the amount of these two elements does not vary significantly increasing the revert. The amount of Al slight decrease in sample 4 because not more deoxidizer is needed.But the amount of Ti isn't changed with increasing the scrap [29].

Table 10. Weight percentage of some elements in samples

Element	***S1-0%***	***S2- 30%***	***S3- 70%***	***S4- 100%***
P	**0.0043**	**0.0041**	**0.00435**	**0.0042**
S	**0.0175**	**0.016**	**0.014**	**0.011**
Cr	**20.74**	**20.735**	**20.525**	**20.83**
Mo	**8.678**	**8.3445**	**8.589**	**8.8715**
Nb	**3.4015**	**3.3035**	**3.256**	**3.175**
Al	**0.0032**	**0.002**	**0.002**	**0.002**
Ti	**0.001**	**0.001**	**0.001**	**0.001**

6.3 DEFECTS ANALYSIS

Defects corresponding to the number of pores in a material. It sometimes refers to the percentage of pores compared to casting and can also be defined with cross-sections as the ratio of the sum of the cross-sectional areas of pores to the cross-sectional track area. Defect analysis is very important because it is directly related to the mechanical properties, like the yield stress, which is proportional to the inclusion number density in the samples. Defects are also the preferential sites for the initiation and propagation of cracks. Those cracks are responsible for a decrease in mechanical properties, which is not suitable for structural applications, where structures need to bear high charges or to resist a high number of

cycles. For each sample, the percentage of area occupied by defects was calculated. Two kinds of defects were studied oxides and porosity. Based on the clear distinction between them, it cannot be possible to study them separately, so for each sample, defect analysis means the summation of porosity and oxides. Figure 31 illustrates oxides and porosity that were considered in the analysis.

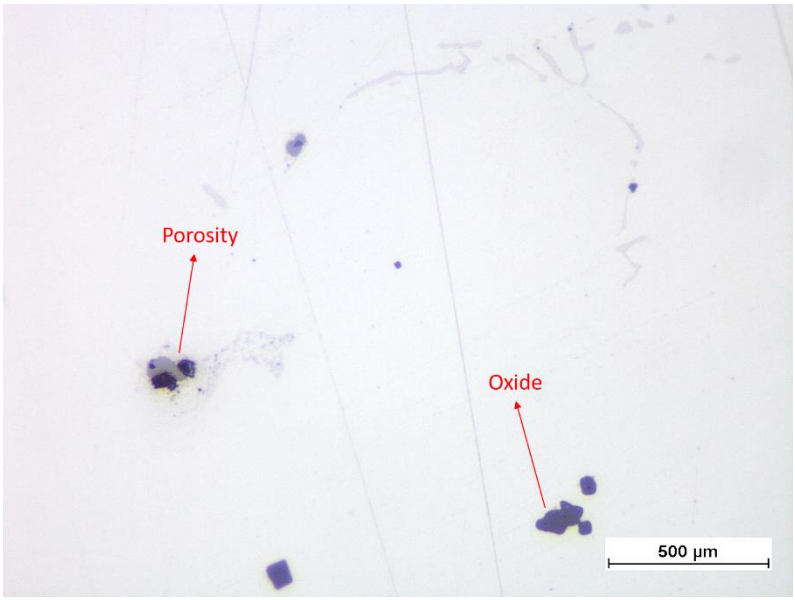

Figure 31. 500X magnification of analyzed oxides and porosity.

Graph 10 illustrates the percentage of the area of the defect in each sample. As expected, increasing the amount of recycled material, the area of defects increases. From sample 1 to sample 4, by increasing the percentage of revert, surface oxides just present in the added scrap are incorporated in the alloy. As the casting process is not based on slag, oxides cannot be removed from the melt. There is a big difference in removing processes between normal steel alloys and nickel-based alloys. In the CW6MC case is

different, slag formation is only related to surface oxide (mainly chromium oxide) that spontaneously form on the bath surface. Anyway, this slag is not the controlled one of steel production and cannot attract impurities. Thus, once formed, the oxide cannot be easily removed in this specific melt.

In steel, casting slag is intentionally added to attract impurities that then can be easily removed. In the case of steel production, stirring is used to promote the oxide flow toward surface slag. Even chemical affinity between slag and impurities promotes contaminants removal. Thus, impurities in steel melts are easily removed. To sum up, in CW6MC, more scrap is present, more defects are introduced and even the possibility to form porosity is enhanced[50].

Another source of porosity can be shrinkage or gas content. Shrinkage porosity originates from the volume contraction during cooling. In general, feeders suitably placed can help reduce shrinkage porosity. In the present study, shrinkage porosity can increase if the change in composition between the four samples increases the solidification temperature range and the amount of residual liquid. Revert additions increase solute content. Thus, more elements can segregate in interdendritic regions and volumetric shrinkage is more probable due to undercooling increase. Gas porosity originates from the fact that gas solubility inside the metal decreases during the solidification process. According to N increase passing from sample 0% to sample 100%, it is probable that gas porosity is prone to form adding revert [8]. These reasons lead us to conclude that, the total area of defects has a direct relationship with the percentage of scrap. This trend is clearly shown in graph 10.

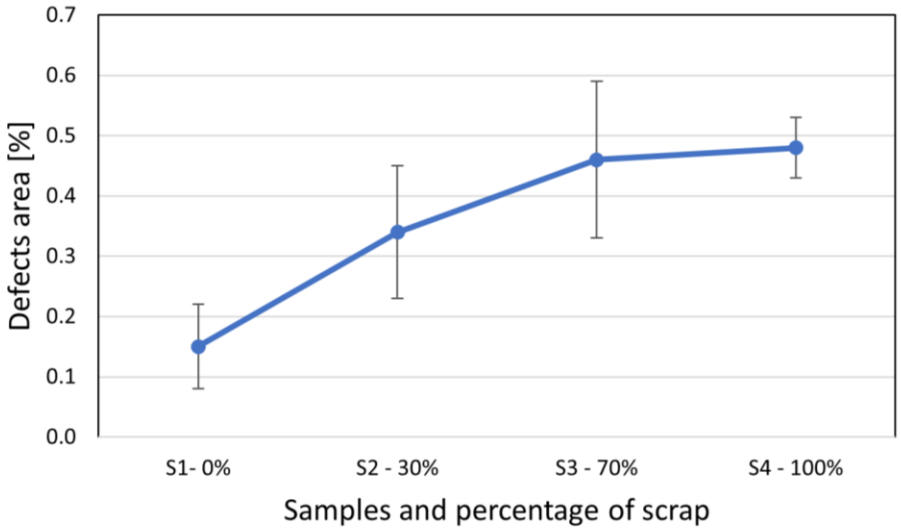

Graph 10. Defects' area percentage in different samples

In graphs 11 to 14, the distribution of defects area in each sample is illustrated. To compare the results in a better way, the number of defects was fixed(in each sample 16 defects were analyzed). Based on graph11, in sample 1, as expected, defects mostly were distributed in the range of 0 to 0.2 percentage of the total area, the biggest defect percentage was 0.5.

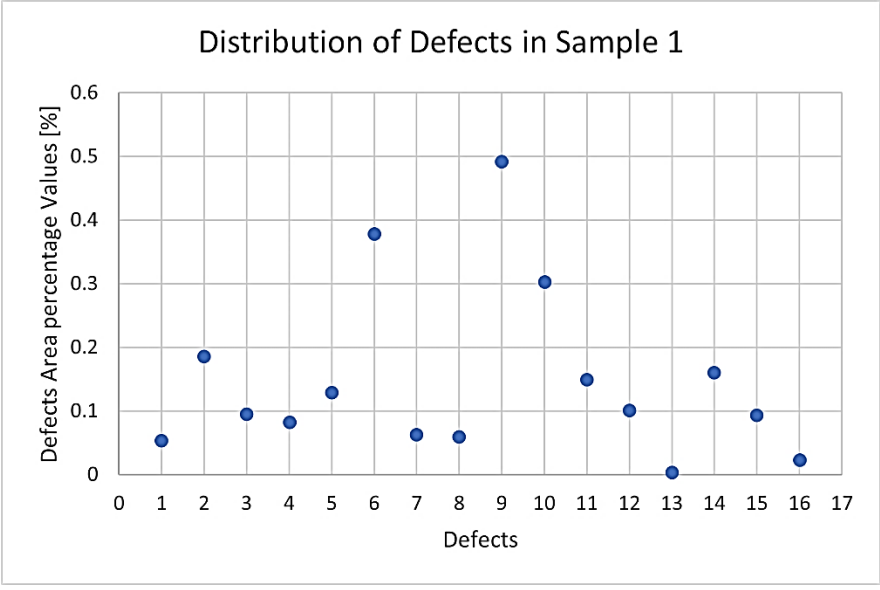

Graph 11. Distribution of defects area on sample 1 in 16 experiment

Graph 12 shows the defects distribution in sample 2, it shows a slight growth of defects area percentage. In this case, 2 large defects presented with 0.6%, and others are distributed between 0.05% and 0.5%.

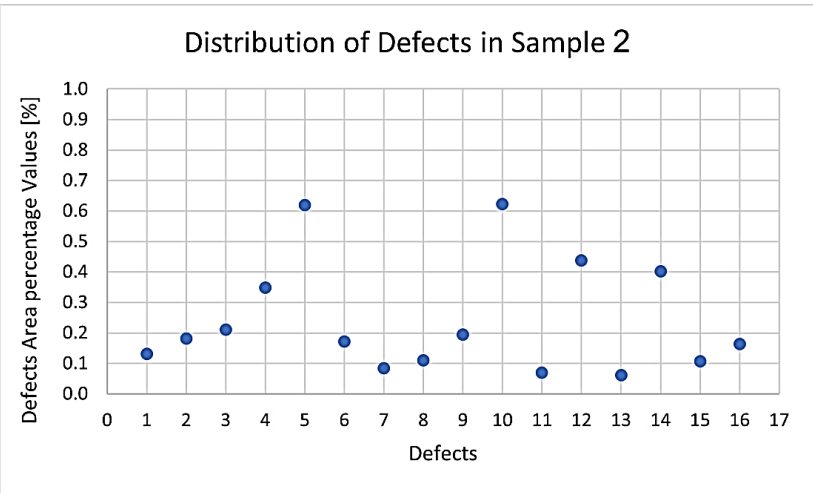

Graph 12. Distribution of defects area on sample 2 in 16 experiment

Same as 2 previous samples, graph 13 and 14 shows the percentage of defect area in last two samples. Obviously, with increasing the scrap percentage, defects' area increases, in sample 4 the biggest area is 1.2%, and in sample 3 is 0.85%. To sum up, Increasing reverts, the presence of defects increases. Thus, it is expected that mechanical properties decrease in samples 70% and sample 100% because of their higher oxides and porosity amount [2].

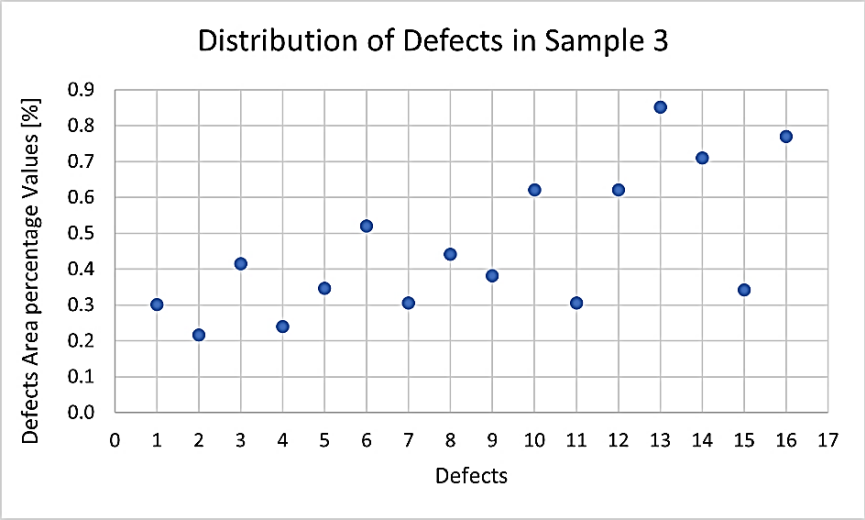

Graph 13. Distribution of defects area on samples 3 in 16 experiment

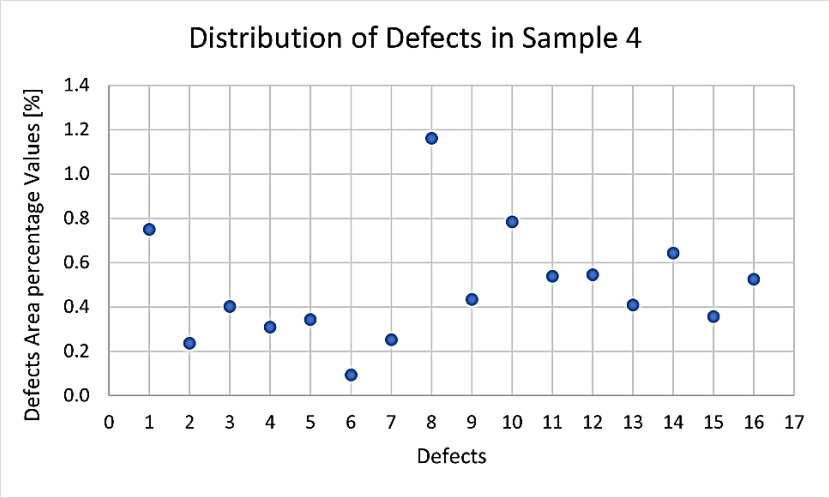

Graph 14. Distribution of defects area on sample 1 in 16 experiment

6.4 SOLIDIFICATION STRUCTURE

By optimizing the solidification process, the performance of the Ni-based superalloys can be further improved. The solidification process is complex due to the multicomponent system with up to 11 alloying elements. To

control the solidification process, a thorough investigation of the solidification behavior of the system is essential to combine theoretical and practical approaches. For the present study, microstructural analysis shows dendrites typical of solidification. Figure 32 illustrates the dendritic structure presents in each sample.

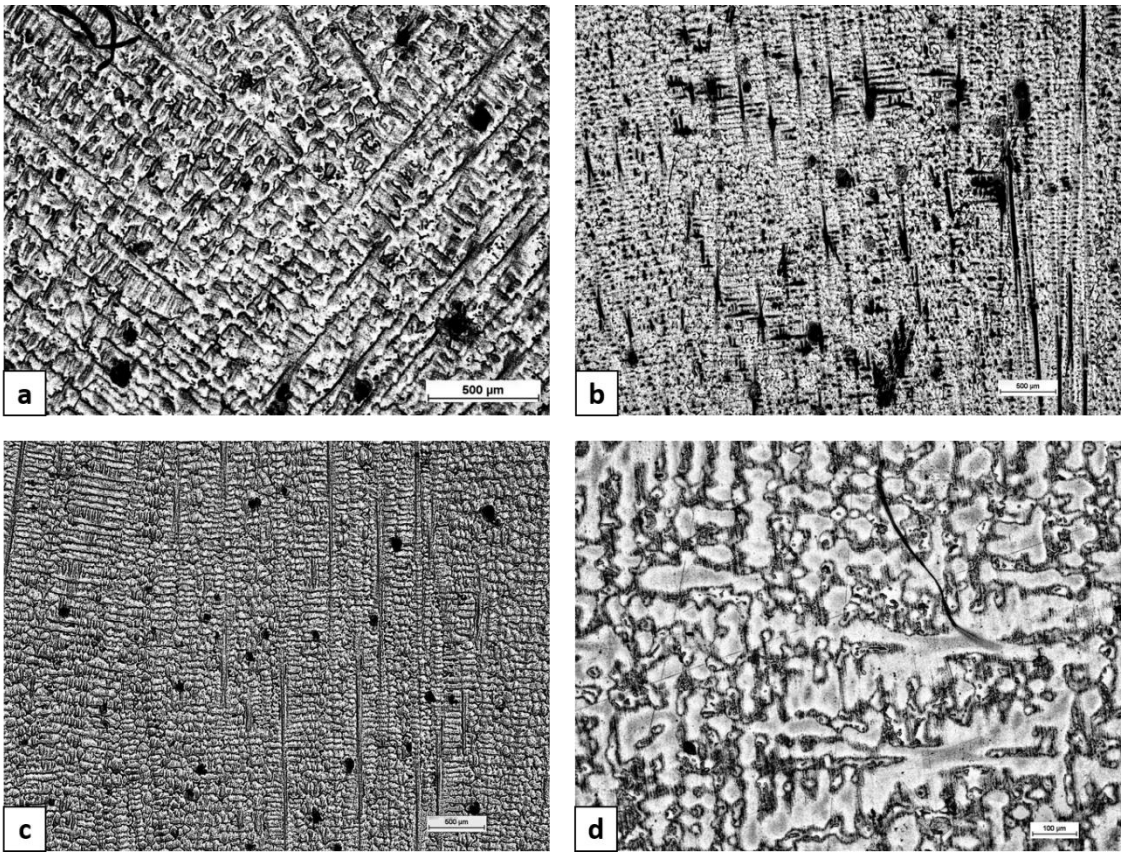

Figure 32. 25X magnification of primary and secondary dendritic arms in samples (a) Sample 0%; (b) Sample 30%; (c) Sample 70%; (d) Sample 100%;

As shown in figure 32, primary and secondary dendritic arms are presented. Secondary Dendrite Arm Spacing (sDAS) is one of the most important microstructural features in dendritic solidification of alloys during the casting process. sDAS has a significant influence on the

mechanical behavior of the cast components. A lower value of sDAS is desired in order to achieve better fatigue strength of the cast components which can be controlled by governing several casting parameters. For directional solidification, sDAS is dependent on various casting parameters i.e. chemical composition of the alloy, cooling rate and liquid melt treatment. During industrial casting of an alloy with predefined chemical composition, cooling rate during the mushy zone becomes the dominant parameter for controlling sDAS. Based on figure 32, in four samples, regarding dendritic arm spacing, no essential differences between samples seem to be present. As mentioned above, the most important zones are the dark ones. In these regions, elements segregate outside γ dendrites core and they form secondary phases[50].

6.5 PHASE ANALYSIS

6.5.1 General Structure and Composition

In order to find the main secondary phases present in segregation regions, Microstructure analysis was performed in two different situations, as-cast samples and annealed ones. No need to say CW6MC is a nickel base alloy, the fcc matrix is γ and rich in nickel. Regarding the microstructural characterization, metallographic analyzes were performed by SEM and the results indicated the presence of three main types of secondary phases, which are, Laves, carbide and oxide. The chemical mapping by EDS in some of these phases, indicated an enrichment of Mo as well as the presence of Nb at higher concentrations (see figure 33). With reference to the elements Ni and Cr, a depletion region in the secondary phase has been observed. Based on the chemical composition and morphology, such particles were characterized as Laves phase rich in Nb.

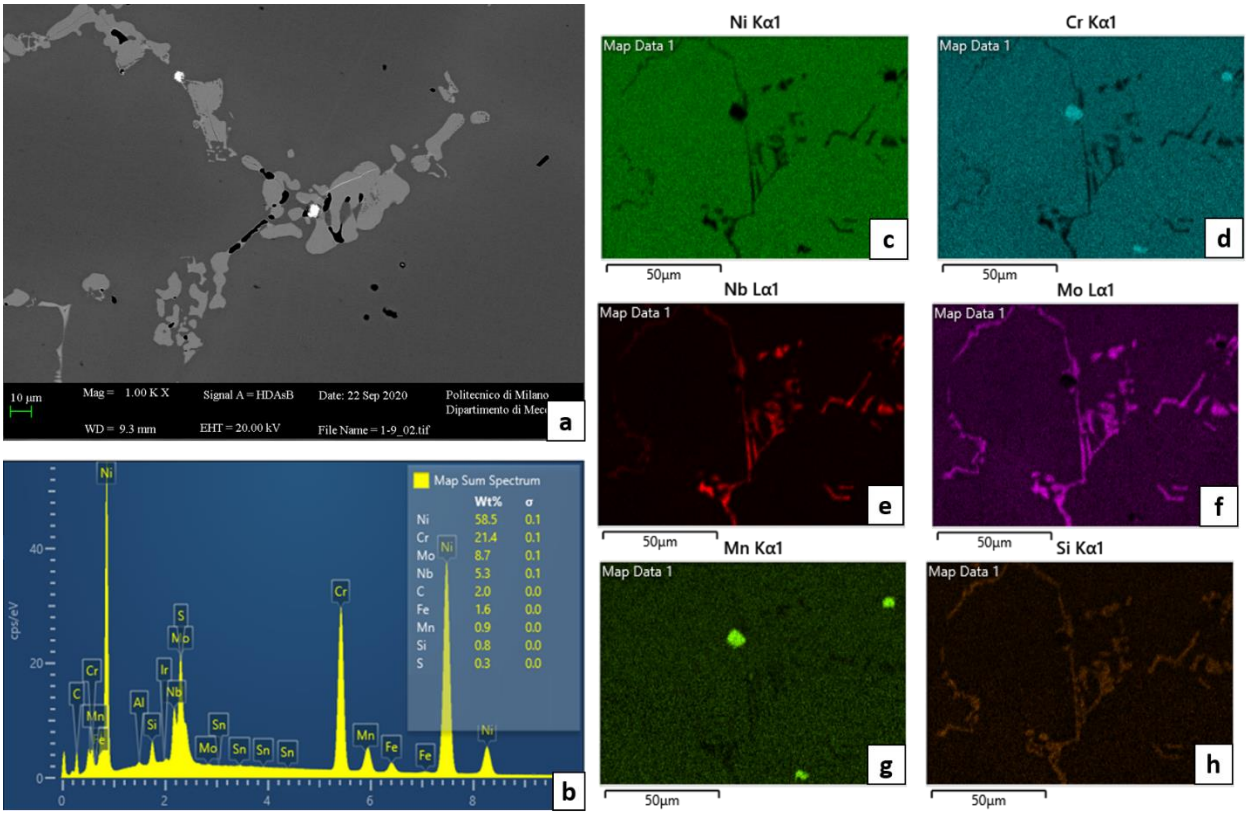

Figure 33. (a) Scanning electron microscopy micrograph obtained in scanning electron operation mode showing the γ matrix and the secondary phases, (b) sum of composition elements for the phases; The elemental chemical maps obtained by energy-dispersive X-ray spectroscopy: (c) Ni; (d) Cr;(e) Nb; (f) Mo; (g) Mn; (h) Si;

Based on the above introduction, three main secondary phases that are shown in the SEM's pictures will be discussed.

6.5.2 Laves and Eutectic-like Phases

Laves phases are present in the eutectic Laves-matrix structures and in form of elongated shape particles. Their typical formula is $(Cr,Fe,Ni)_2(Si,Ti,Nb,Mo)$ and they are rich in Nb which gives them the typical light grey colour visible in SEM images. Laves phases are present in the eutectic laves-matrix structure with three or more elements and the

distribution of the elements is important. Eutectic-like phases typically were in spheroidal shape and dark grey color. In this phase, manganese sulfur (MnS) was found frequently. Figure 34 illustrates the main constituents of this phase. In this case, in the focused region, there are 25% of Mn and 24.6% of S. Graph 15 shows all the components of this phase.

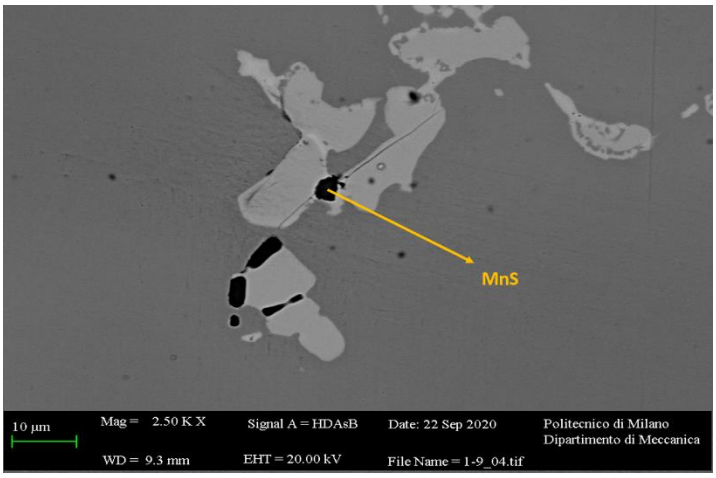

Figure 34. MnS phases in 2500X magnification in sample 1 (0% scrap) microstructure.

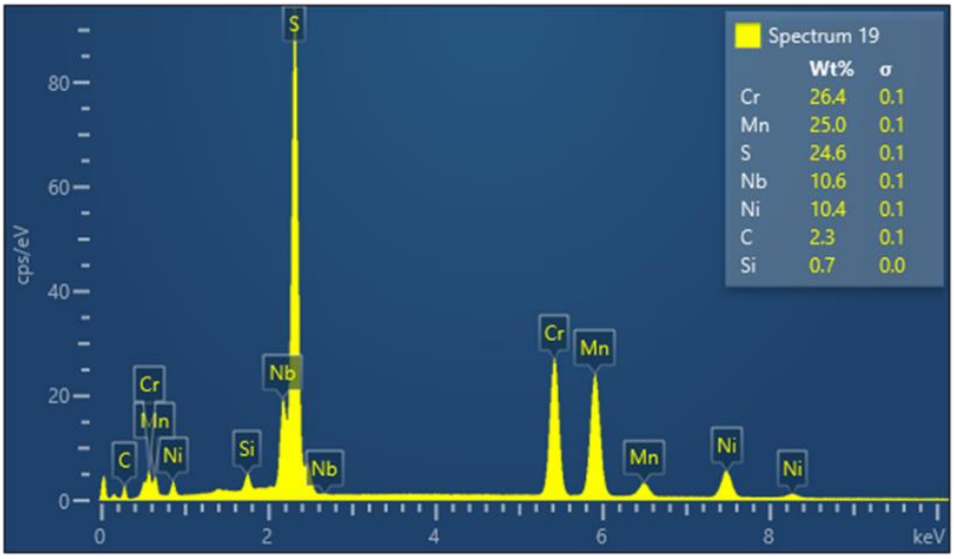

Graph 15. Spectrum of the area of eutectic-like phase from the X-ray data collected during X-ray Smart Map acquisition.

6.5.3 Eutectic-like Structure in As-cast Samples

A eutectic-like structure is a homogeneous, solid mixture of two or more. The mixture either melts or solidifies at a lower temperature than the melting point of any of the individual substances. A eutectic-like structure only forms when there is a specific ratio between the components. The word comes from the Greek words "eu," meaning "good" or "well" and "tectic" meaning "melting." In our case, Eutectic-like structures were found in all SEM pictures of all samples. This structure presents two main phases, γ matrix, and lamellar Laves phase. Eutectic-like structures can be associated with porosity because they are the last phases that form during solidification. Thus, residual liquid can be present near these phases and it could be affected by shrinkage [51]. But it cannot be true in all cases because in some laves phases there is no porosity seen. In the no porosity parts, probably because of eutectics nucleate the structures exhibit globular particles of manganese sulfur. Figures 35 and 36 illustrate a eutectic structure associated with and without porosity.

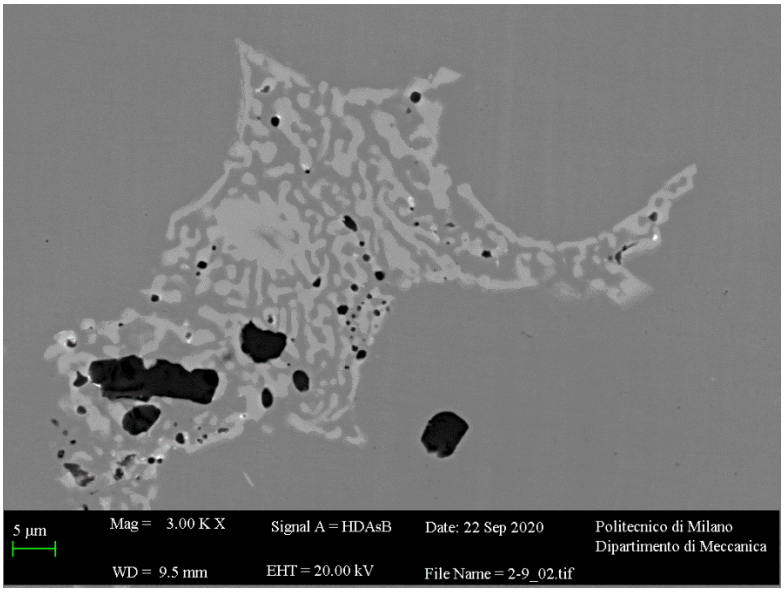

Figure 35. Porosity and black particles of MnS at 3000X magnification of eutectic-like structure in sample 2 (with 30% scrap)

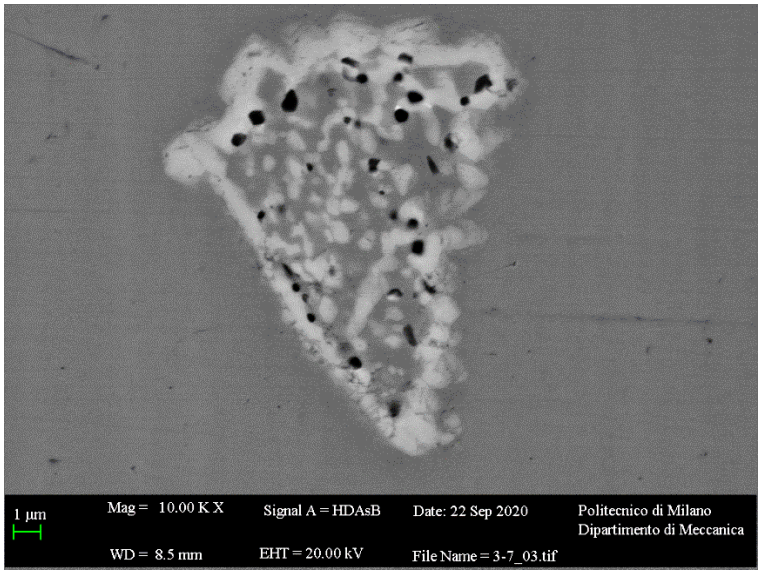

Figure 36. Microstructure of eutectic-like structures at 10000X magnification of CW6MC in sample 3 (with 70% scrap)

6.5.4 Eutectic-like structure after heat treatment

The Eutectic-like structure is modified by heat treatment. In any case, laves phases are weak in tension. Eutectic embrittlement is caused by their inclusion in eutectic-like formations. Moreover, since grain boundaries and inter-dendritic regions are the last to solidify, they grow preferentially there. As a result, they embrittle the whole alloy, resulting in poor grain boundaries.

According to figure 37, after heat treatment, the shape of the laves phase change from the lamellar structure in the as-cast sample to the globular one. In the case of heat treatment, shifting the morphology in laves phase may be the explanation for improved tensile properties. Because stress intensification is seen in lamellar structure but this phenomenon is not seen in globular phases.

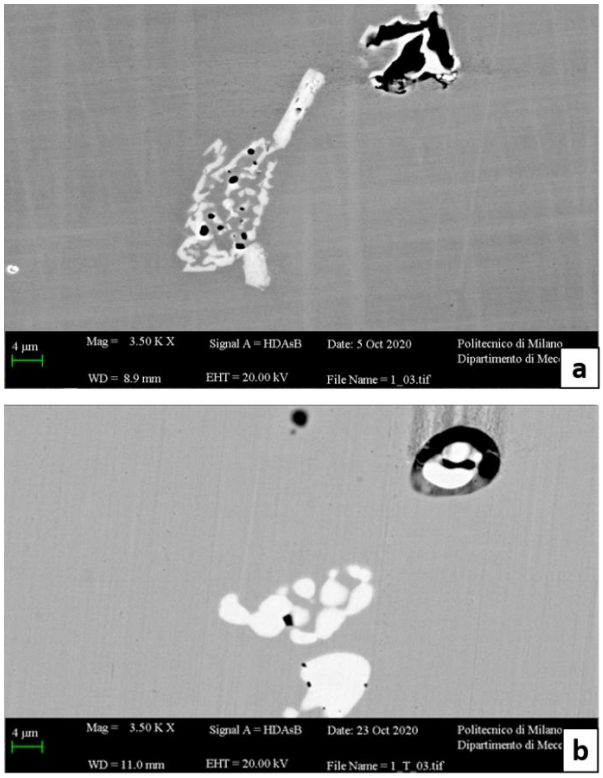

Figure 37. 3500X magnification of eutectic-like structure in (a) as-cast and(b) heat treatment samples

6.5.5 Carbides Structure

The next important secondary phase is carbides which is present in light grey color in SEM images. The morphologies of this phase are globular and Chinese script (elongated shape). Also, carbides are present in intragranular zones and the construction is mainly NbC. As shown in figure 33, 34.8% of the light gray zone is contained by Nb. Graph 16 shows the more detailed information about the carbide phase composition which is shown in Figure 38.

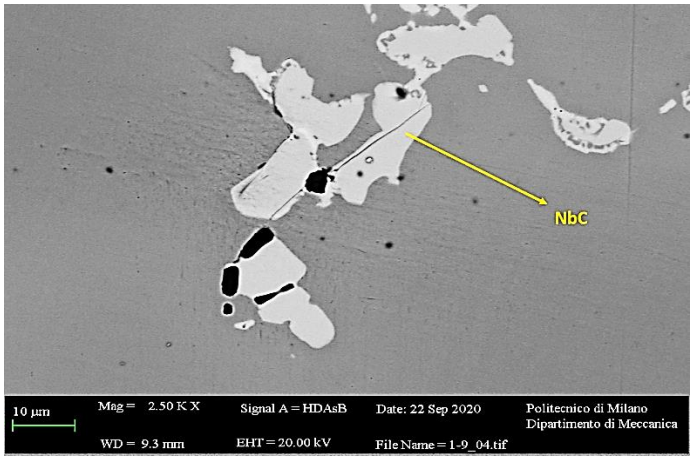

Figure 38. NbC phases in 2500X magnification in sample 1 (0% scrap) microstructure.

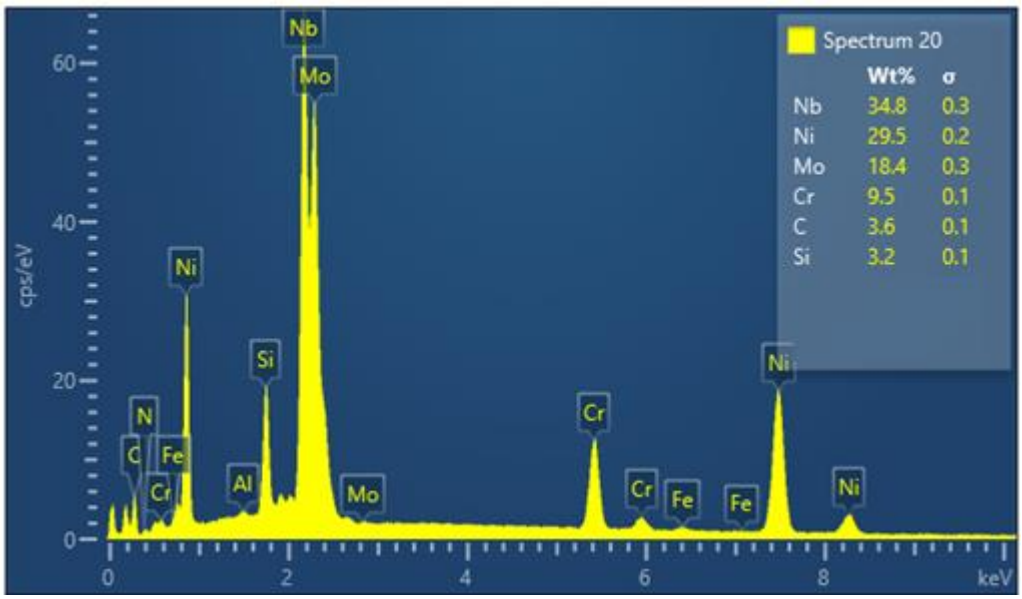

Graph 16. Spectrum of the area of carbide phase from the X-ray data collected during X-ray Smart Map acquisition

6.5.6 Carbide Phase in As-cast Samples

Figure 39 illustrates the carbides phase in the four samples. The first main difference is the area percentage of the carbide phase in the samples. Graph 17 shows the percentage of this phase in all samples. As expected, samples 3 and 4 have more carbide phases in comparison with the other two and the reason should be a high percentage of scrap.

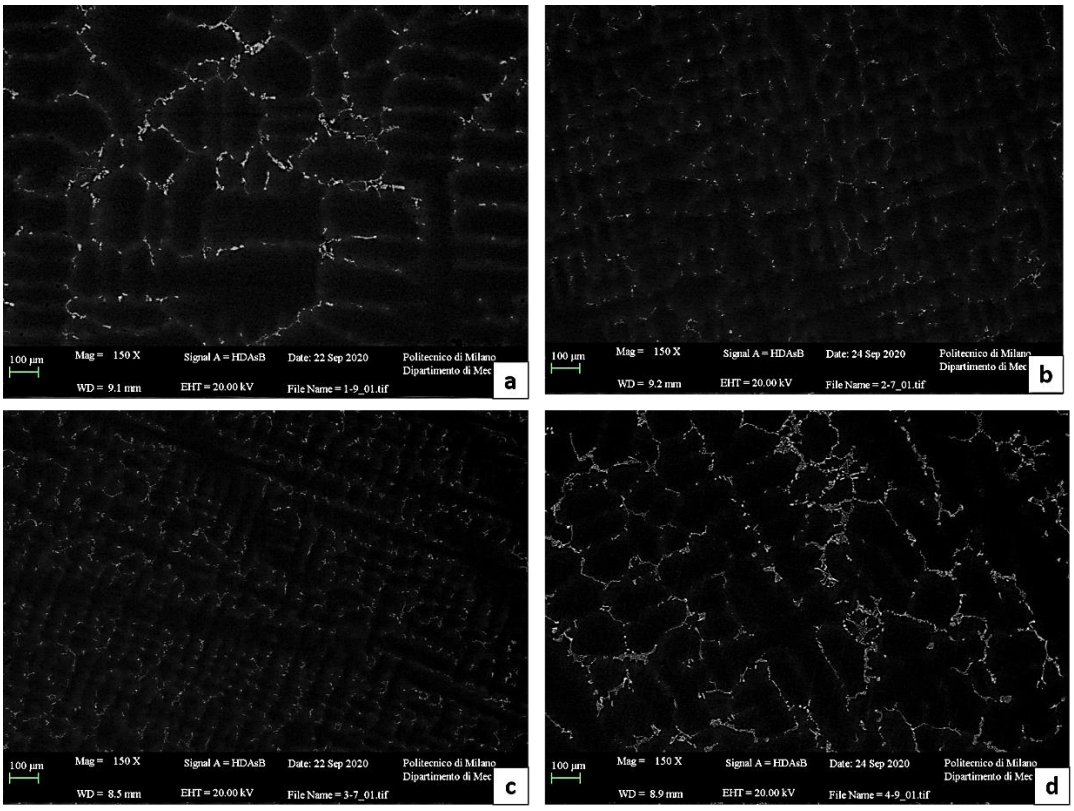

Figure 39. 150X magnification of alloy microstructure. Carbides of white color are visible in Chinese script and globular morphology. (a) Sample 0%; (b) Sample 30%; (c) Sample 70%; (d) Sample 100%;

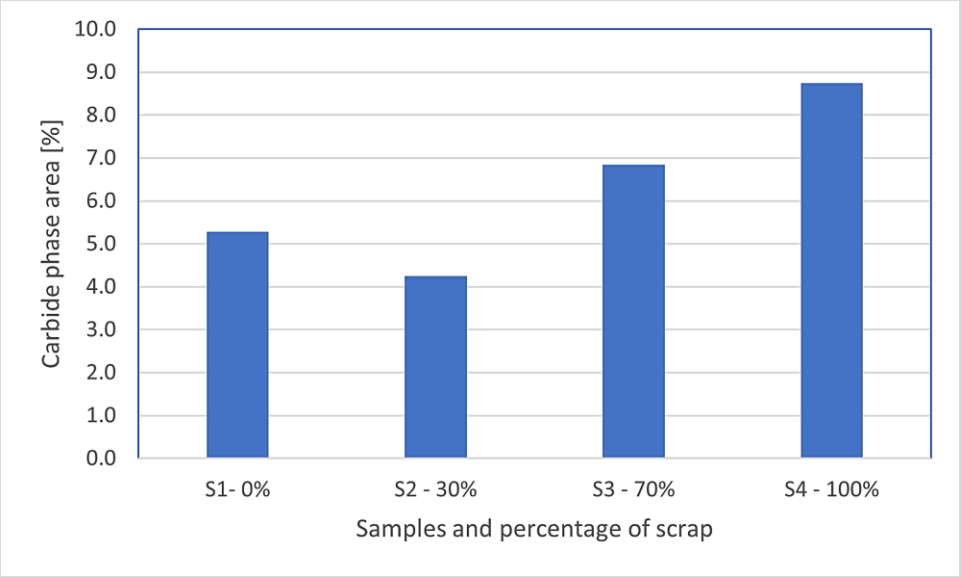

Graph 17. Area percentage of carbide phase in samples

Based on figure 340, another difference in samples is morphology, samples 0% and 100% show big and clear carbide structure network inside the γ matrix, the difference is, in the sample 100%, it's distributed very continuously along the surface. On the other hand, in samples 30% and 70%, the structure is small and less continuous. The coarser structure of carbides in sample 100% could be due to the higher presence of nitrides that act as coarser agents for carbides particles [52].

The last but not the least analyzes of carbide structure is related to the particle concentration in high magnification pictures. This detrimental effect given by carbides is illustrated in Figure 40. The figure shows that in samples 70% and 100% some of the small carbide particles are concentrated in some regions. This distribution is found just in samples 70% and 100%. This carbides behavior can be considered harmful for alloy properties because carbides are not well distributed. [21]

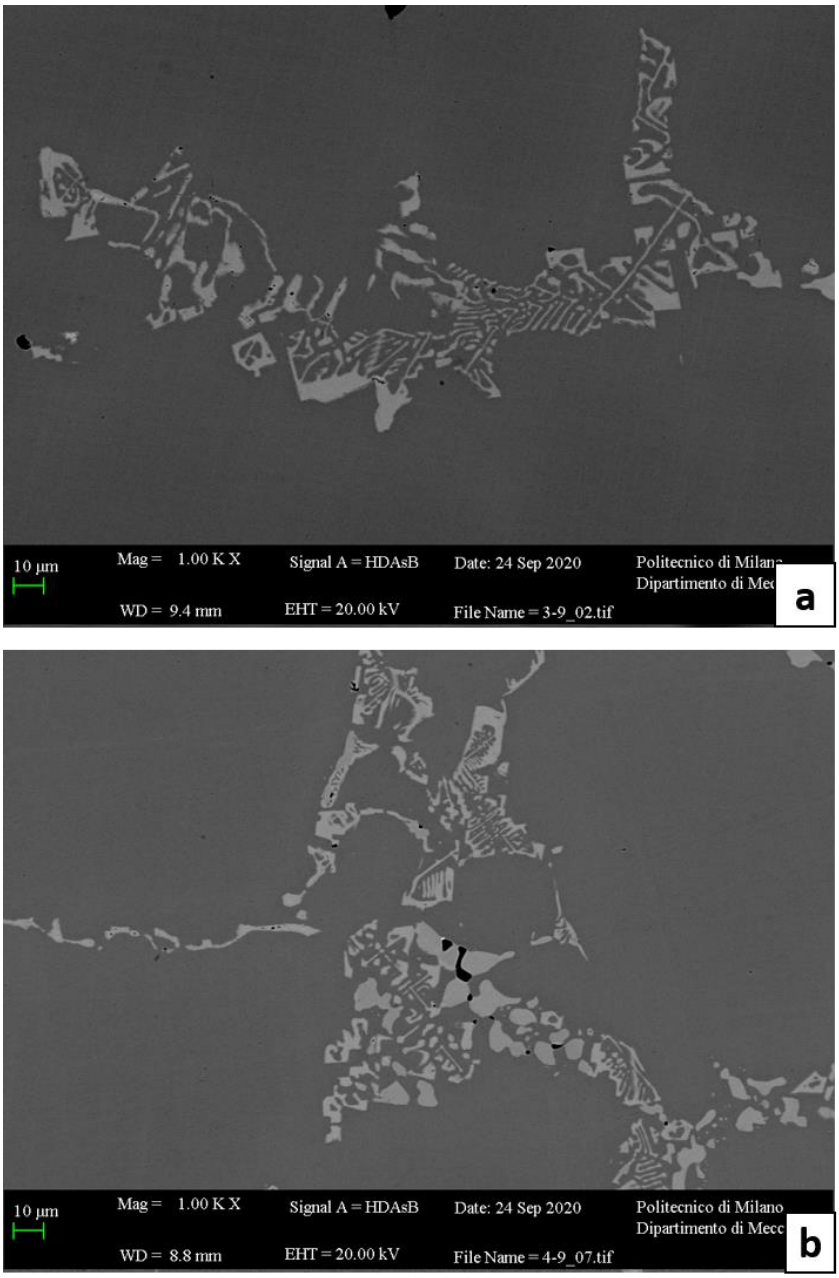

Figure 40. Magnification 1000X of carbides trail in samples 70% and 100%.

6.5.7 Carbide Phase After Heat Treatment

Comparing to the as-cast sample, after heat treatment the networks of carbides are not continuously spread all around the surface. According to figure 41, in all samples even in the case of sample 100%, the problem is

reduced and the carbides continuous network is not seen like the as cast ones. Therefore, it is expect that the mechanical and tensile properties should be higher in case of heated samples rather than the as-cast ones.

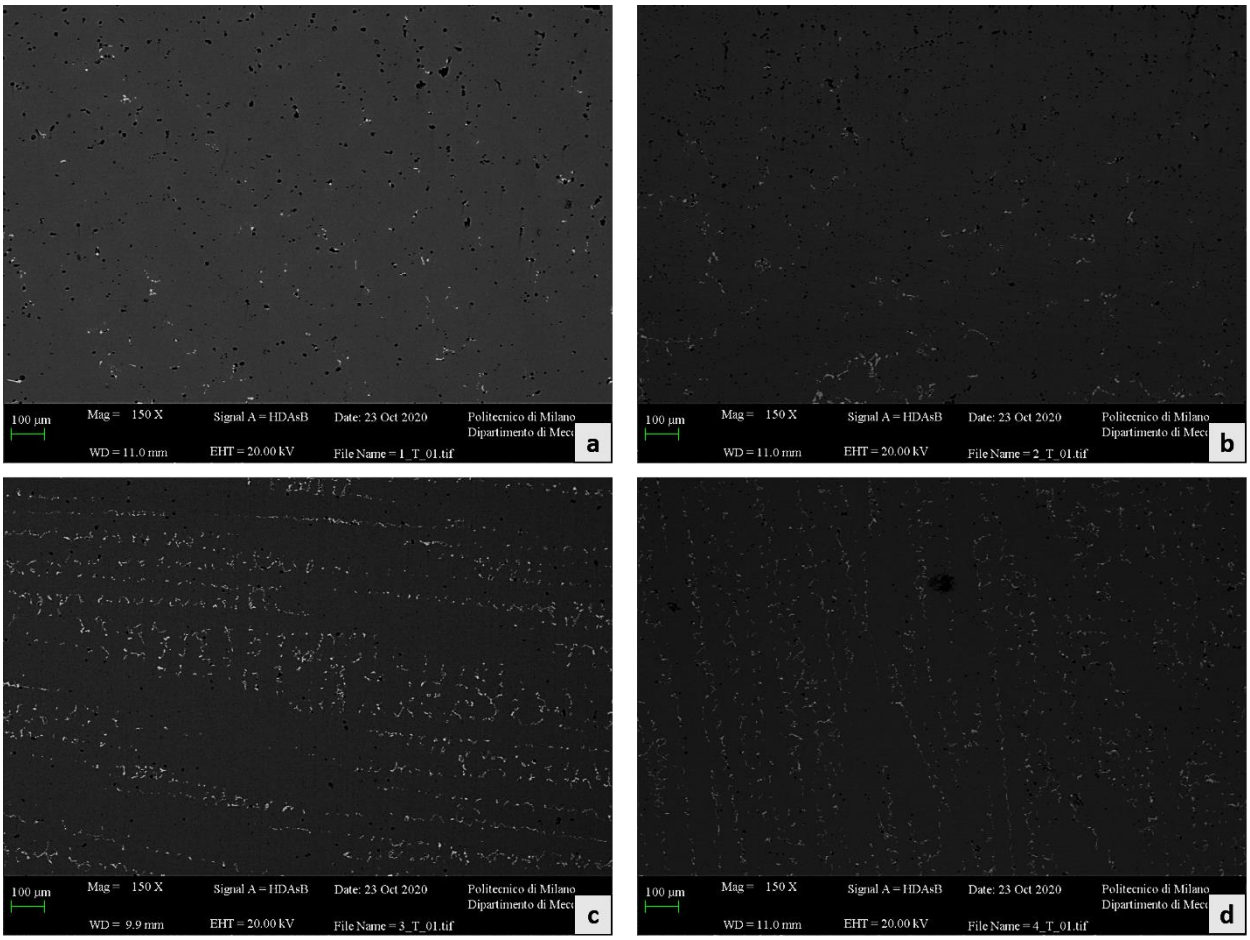

Figure 41. 150X magnification of alloy microstructure after heat treatment. Carbides of white color are visible in Chinese script and globular morphology (a) Sample 0%; (b) Sample 30%; (c) Sample 70%; (d) Sample 100%;

According to figure 42 thermal treatment causes carbides to be partly re-adsorbed, resulting in their rounding. However, the carbide phase cannot eliminate but they remain in smaller and round shapes in solution thanks to rapid cooling[31].

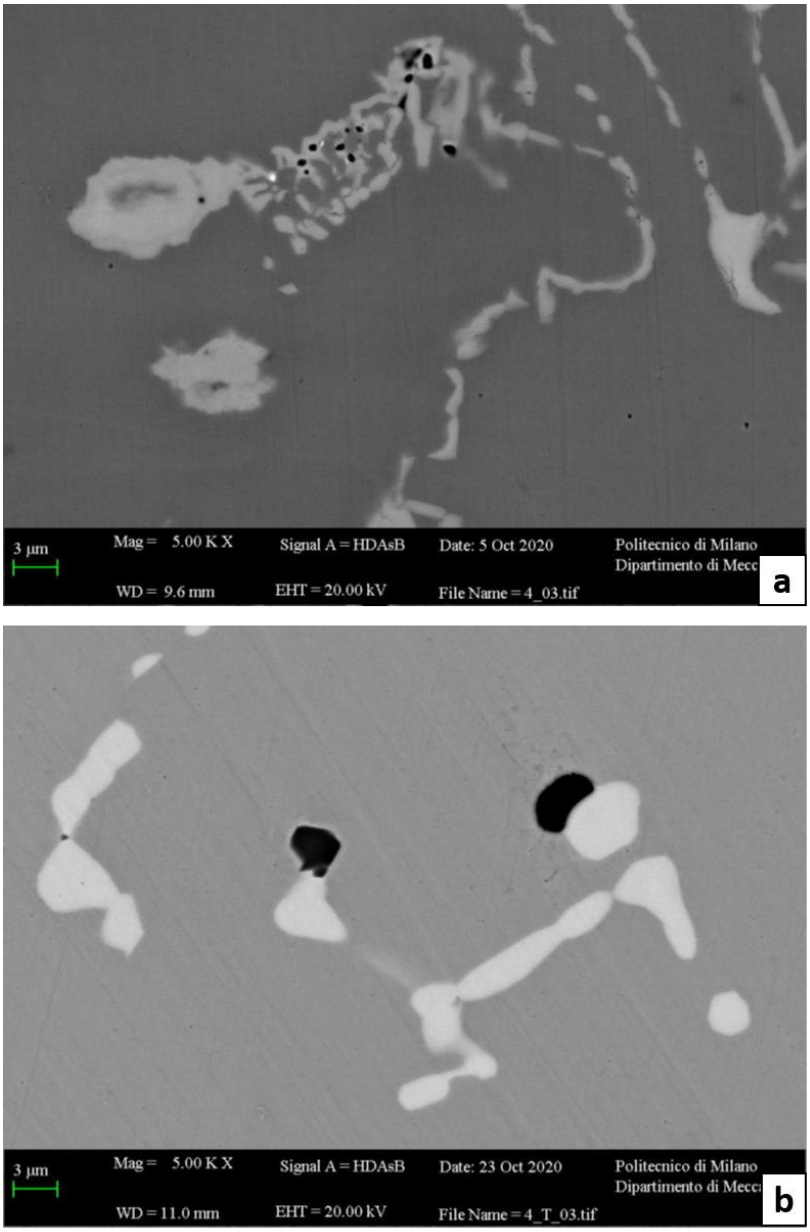

Figure 42. 3500X magnification of Carbide phase structure in (a) as-cast and(b) heat treatment samples

6.5.8 Oxides Phase

One of the main secondary phases is oxides, which are normally recognized by their squared shape and black color. The chemical structure of this phase is mixed with Cr and Mn. Also, in de-oxidized parts, some percentages of Al and Ti can be found. For example, based on figure 43, the oxides zone contained 50% Cr, 25% Mn, and 0.5% Al and Ti. It's well-known that oxides can be considered as defects because they are brittle and a high amount of them, especially if they are not uniformly dispersed, can be detrimental for alloy properties. Besides, a higher content of Cr oxides means that there is the loss of Cr in the matrix and so it is not available for the corrosion-resistant passive film formation [3]. In graph 18, the weight percentage of each element in carbide and oxide phases which are shown in figure 43, illustrated. Graph 18 shows more detailed information about the carbide phase composition which is shown in Figure 43.

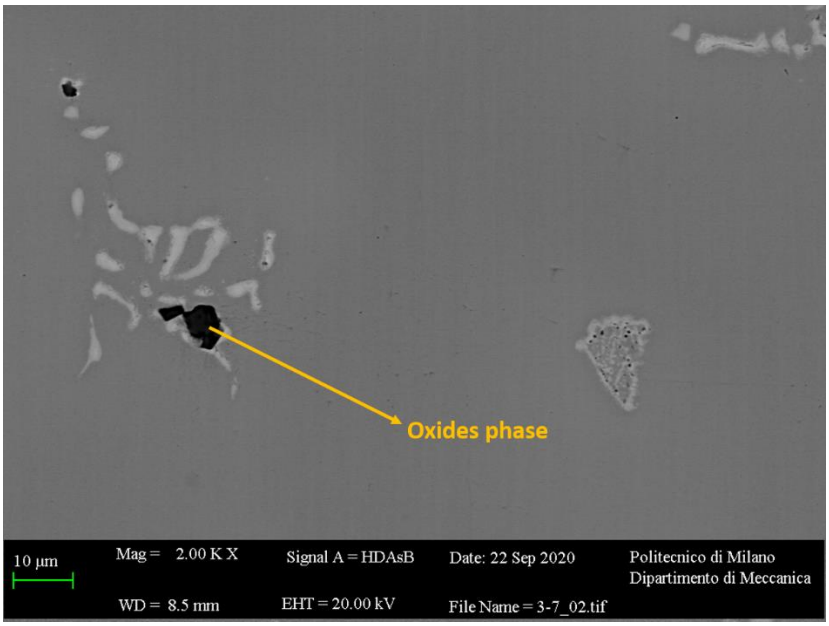

Figure 43. Oxide phases in 2000X magnification in sample 3 (70% scrap) microstructure.

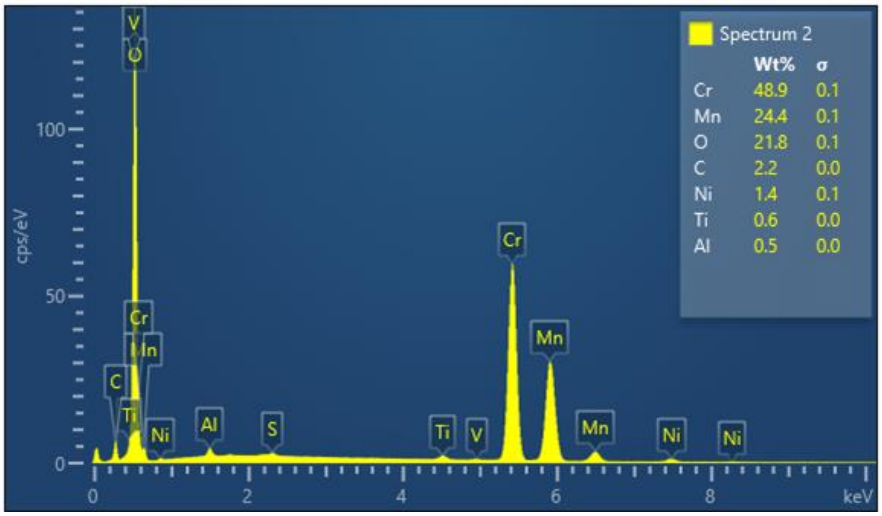

Graph 18. Spectrum of the area of oxide phase from the X-ray data collected during X-ray Smart Map acquisition

6.5.9 Oxide Phase As-cast Samples

No need to say that in all the four samples oxide phase exhibit. But it is not distributed homogeneously and ingot zones near to feeder seem to be richer in oxides, this is valid for all the samples. Based on basic information about the oxide phase, Mn and Cr are playing the main role in this phase. As shown in the previous chapter in the micro-structure part, the trend of Cr and Mn has changed in a small scall during increasing the scrap, so in the general side of view, the oxide area percentage phase should change in this order. Figure 44 illustrates the oxide phase in samples, in this figure, to show the better contrast, the oxide part keeps in black and the matrix is shown in white. The percentage area analysis shows that with increasing the percentage of scrap, a bit change in the area of oxide phase can be seen. Graph 19 Shows the comparing area percentage in four samples microstructure, it seems that samples 70% and 100% exhibit a bit more concentrated oxides compared to the other cases.

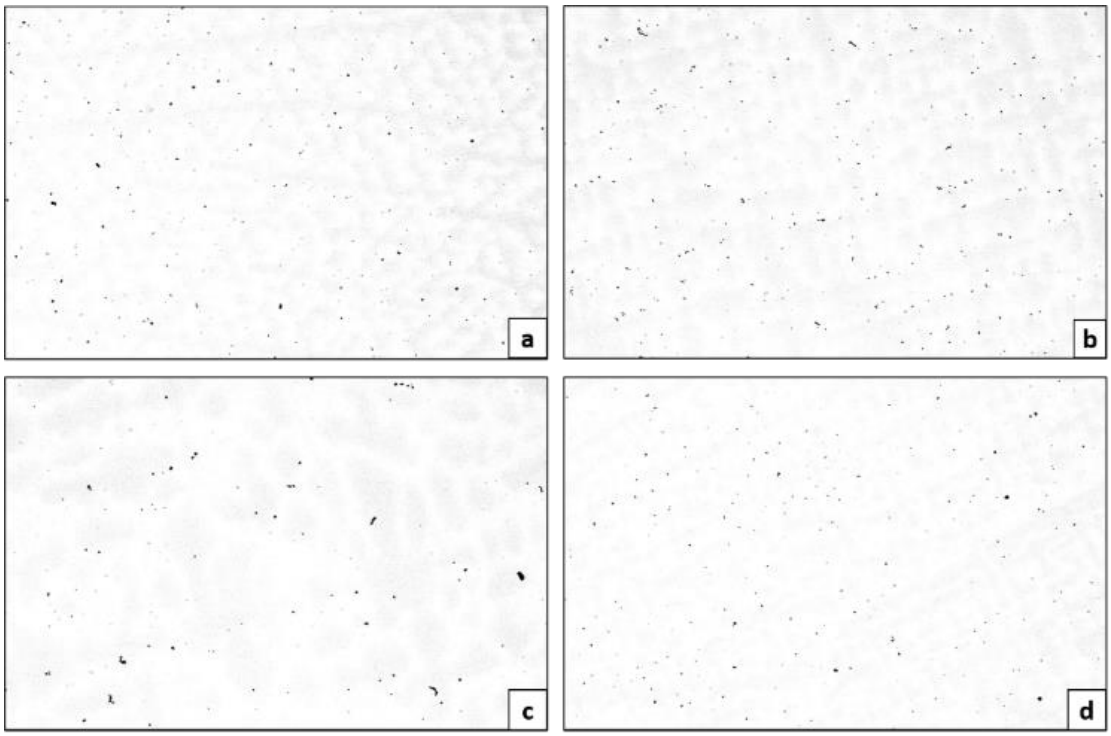

Figure 44. 150X magnification of alloy microstructure. Oxide phase are visible in black color. (a) Sample 0%; (b) Sample 30%; (c) Sample 70%; (d) Sample 100%;

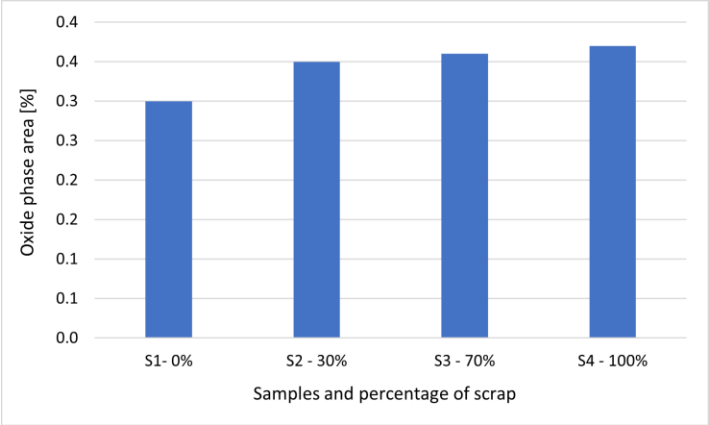

Graph 19. Area percentage of oxide phase in samples

6.5.10 Oxides Phase After Heat Treatment

As nitrides, oxides cannot be dissolved by solution annealing treatment. This is due to their melting temperature that is lower than the casting temperature. Thus, their amount is not expected to decrease in solution-annealed samples [52].

6.6. Hardness Test

The hardness of the specimen was determined by the Brinell hardness testing machine with a 29.400 N load and 10mm diameter steel ball indenter. The detention time for the hardness measurement was 30 seconds. The tests were carried out at five different locations taken from each specimen. Each hardness result was obtained from an average of at least five repetitions on the same sample. Graph 20 illustrates the Brinnel hardness in samples.

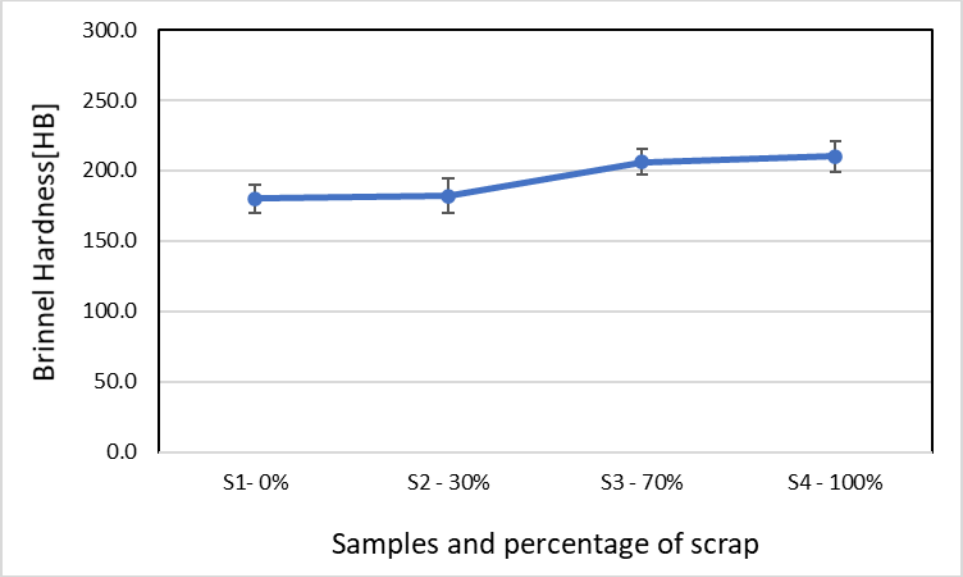

Graph 20. Brinnel hardness values in samples

The first consideration that it is possible to do is that the scrap percentage leads to the hardness trend. As expected, sample 1 shows a lower hardness value (180 HB) and the highest value (210 HB) is belongs to sample 4. On Graph 20, the role of scrap is more clear in the difference of hardness value in samples 30% and 70%. In these samples, the value is jumping from 182 HB to 206 HB. As mentioned in the previous part, the amount of the

secondary phase is increasing from sample 1 to 4, so HB increases with the increase of the secondary phase, as this phase is harder than the primary phase. Moreover, it's not aspected to have differences in yielding (while HB is quite the same) but differences in deformation by increasing the amount of revert. Because scrap increases the defects and secondary phases making void during deformation and anticipate the fracture.

7. CONCLUSION

This study investigates the revert addition effect on nickel-based alloy CW6MC properties. Results interpretation can be summarized in the following conclusions:

- Ingot grains present columnar dendritic and equiaxed structures. This is due to the position occupied by ingot in the mold that modifies heat extraction. There was not an exact trend based on columnar length between the samples and sample 2 has the longest grains but grains' width increase from sample 1 to 4 with increasing the scrap, and sample 4 has the biggest width. About the equiaxed structure, samples 3 and 4 have the largest size and the reason maybe they were cast at higher temperatures.

- Internal defects are considered oxides and internal porosity: they increase in amount passing from sample 0% to sample 100%. The increase in scrap content means more surface oxides that are entrapped from revert material. Even chemical composition changes with revert addition and this affects also porosity formation.

- For chemical composition analysis, six main elements (C, N, Si, Mn, Fe, and Ni) were focused on. Based on the analysis, the amount of Nitrogen, Carbon, Silicon, and Iron increase passing from sample 0% to sample 100% but on the other hand, Manganese and Nickel decrease with increasing the amount of the scrap.

- Inter-dendritic regions are rich in secondary phases. The main constituents are Laves and Eutectic-like phases, carbides structure, and oxides phase. NbC, Laves, and eutectic-like structures form a more continuous network in samples 70% and 100%. Furthermore, micrometric/nanometric carbonitrides and nitrides are expected to be present in these two samples because of their higher N content. This affects tensile properties. To reduce the amount of the secondary phase, it is appropriate to remain on the minimum quantities of alloying element (Fe, Nb, Si) and modify the solubilization thermal treatment to increase the treatment time and temperature helps in absorbing a large amount of precipitate and avoid a further formation.

- The Brinnel hardness of the samples increases from sample 1 to 4 like the amount of the secondary phase, so HB increases with the increase of the secondary phase, as this phase is harder than the primary phase.

To sum up, the amount of scrap that can be used may exceed the value identified by this study. No need to say it depends on different parameters like area of usage, the plant, the equipment, and the operating procedure. For example, the injection of inert gas from the furnace bottom helps to remove oxides by floating and filter during pouring and casting can reduce also the inclusions content; the protection during pouring and casting, by

gas or nozzle, prevents the incorporation of atmosphere with the consequent decrease of gas porosity and brittle nitrides compounds.

The revert principle is important in modern industry because it reduces environmental effects, saves energy, and reduces pollution while also saving money. It can be concluded that the effect of revert addition has a negative influence on the final properties. The revert amount that is possible to charge can be increased by a dedicated improvement of the casting technology and process of the foundry.

Bibliography

[1] B. Geddes, H. Leon, and X. Huang, “Superalloys: Alloying and Performance, ASM international,” 2010. .

[2] “ASM Specialty Handbook: Nickel, Cobalt, and Their Alloys - ASM International.” .

[3] “ASM Handbook Volume 13B, Corrosion: Materials - ASM International.” .

[4] M. J. Cieslak, “THE WELDING AND SOLIDIFICATION METALLURGY OF ALLOY 625,” 1991.

[5] “INCONEL 625 | Alloy 625 | Corrotherm International.” .

[6] R. L. Ortolan, “P Rocessamento Do S Inal M Ioelétrico Para,” 2002.

[7] M. Rombouts, G. Maes, M. Mertens, and W. Hendrix, “Laser metal deposition of Inconel 625: Microstructure and mechanical properties,” *J. Laser Appl.*, vol. 24, no. 5, p. 052007, Nov. 2012.

[8] J. N. Dupont, “Solidification of an alloy 625 Weld Overlay,” *Metall. Mater. Trans. A Phys. Metall. Mater. Sci.*, vol. 27, no. 11, pp. 3612–3620, 1996.

[9] S. Barella *et al.*, “Solidification microstructure of centrifugally cast Inconel 625,” *China Foundry*, vol. 14, no. 4, pp. 304–312, 2017.

[10] “BS EN ISO 13533:2002 - Petroleum and natural gas industries. Drilling and production equipment. Drill-through equipment.” .

[11] G. A. Young and N. Lewis, “The Stress Corrosion Crack Growth Rate of Alloy 600 Heat Affected Zones Exposed to High Purity Water,” Niskayuna, NY (United States), Apr. 2003.

[12] IAEA, “Stress Corrosion Cracking in Light Water Reactors: Good Practices and Lessons Learned,” *IAEA Nucl. Energy Ser. No. NP-T-3.13*, p. 115, 2011.

[13] G. A. Young, T. E. Capobianco, M. A. Penik, B. W. Morris, and J. J. McGee, “The mechanism of ductility dip cracking in nickel-chromium alloys,” *Weld. J. (Miami, Fla)*, vol. 87, no. 2, pp. 31–43, 2008.

[14] C. C. Nee, W. Kim, and R. Weil, “Pulsed Electrodeposition of Ni-Mo Alloys,” *J. Electrochem. Soc.*, vol. 135, no. 5, pp. 1100–1103, May 1988.

[15] E. Chassaing, K. Vu Quang, and R. Wiart, “Mechanism of nickel-molybdenum alloy electrodeposition in citrate electrolytes,” *J. Appl. Electrochem.*, vol. 19, no. 6, pp. 839–844, 1989.

[16] E. Y. Arquitectura *et al.*, “No Covariance structure analysis Title for health-related indicators in the elderly at home with a focus on subjective health,” *Acta Univ. Agric. Silvic. Mendelianae Brun.*, vol. 53, no. 9, pp. 1689–1699, 2015.

[17] Y. Sun and A. Y. Ganin, “The Synergistic Effects of Alloying on the Performance and Stability of Co3Mo and Co7Mo6 for the Electrocatalytic Hydrogen Evolution Reaction,” *Hydrogen*, vol. 1, no. 1, pp. 11–21, Oct. 2020.

[18] L. Romanin, P. Ferro, A. Fabrizi, and F. Berto, “A metallurgical and thermal analysis of Inconel 625 electron-beam welded joints,” *Frat. ed Integrita Strutt.*, vol. 13, no. 50, pp. 251–263, Aug. 2019.

[19] “ASTM A494 / A494M - 00 Standard Specification for Castings, Nickel and Nickel Alloy.” .

[20] X. L. Guo, J. B. Yu, X. F. Li, Y. Hou, and Z. M. Ren, “Effect of nitrogen content on the microstructure and mechanical properties of a cast nickel-base superalloy,” *Ironmak. Steelmak.*, vol. 45, no. 3, pp. 215–223, Mar. 2018.

[21] E. O. Ezugwu, Z. M. Wang, and A. R. Machado, “The machinability of nickel-based alloys: A review,” *J. Mater. Process. Technol.*, vol. 86, no. 1–3, pp. 1–16, 1998.

[22] S. G. K. Manikandan, D. Sivakumar, and M. Kamaraj, “Influence of weld cooling rate,” *Weld. Inconel 718 Superalloy*, pp. 53–186, 2019.

[23] “A study on the microstructure, mechanical properties and corrosion resistance of centrifugally cast heavy wall thickness low carbon 46Ni-35Cr-9Mo alloy - ProQuest.” .

[24] H. Alves and U. Heubner, “Aqueous corrosion of nickel and its alloys,” in *Shreir’s Corrosion*, Elsevier, 2010, pp. 1879–1915.

[25] D. M. Stefanescu, “Length-scale in solidification analysis,” in *Science and Engineering of Casting Solidification, Second Edition*, Springer US, 2008, pp. 1–4.

[26] R. R. Srivastava, M. S. Kim, J. C. Lee, M. K. Jha, and B. S. Kim, "Resource recycling of superalloys and hydrometallurgical challenges," *J. Mater. Sci.*, vol. 49, no. 14, pp. 4671–4686, 2014.

[27] A. Greenfield and T. E. Graedel, "The omnivorous diet of modern technology," *Resour. Conserv. Recycl.*, vol. 74, pp. 1–7, May 2013.

[28] T. E. Graedel *et al.*, "Methodology of metal criticality determination," *Environ. Sci. Technol.*, vol. 46, no. 2, pp. 1063–1070, Jan. 2012.

[29] C. Fuwang, H. Xuebing, Z. Yun, L. Yulin, and H. Zhuangqi, "Nitrogen in revert superalloys," *Mater. High Temp.*, vol. 14, no. 4, pp. 421–424, 1997.

[30] Y. H. Yang, J. J. Yu, X. F. Sun, T. Jin, H. R. Guan, and Z. Q. Hu, "Effect of revert addition on microstructure and mechanical properties of M951 Ni-base superalloy," *Mater. Sci. Eng. A*, vol. 532, pp. 6–12, Jan. 2012.

[31] "Superalloys: A Technical Guide, 2nd Edition - ASM International." .

[32] H. Asteman and D. Jakobi, "A New Cast Alloy with High Strength and Excellent Corrosion Resistance – An Alternative to the Conventional Ni-base Alloys." OnePetro, 15-Mar-2015.

[33] G. Lai, "High Temperature Corrosion and Materials Applications," *undefined*, 2007.

[34] W. Wang, H. W. Stoll, and J. G. Conley, "Sand Casting Processes," 2010, pp. 1–10.

[35] “Complete Casting Handbook - 2nd Edition.” .

[36] J. Campbell, “Melting, Remelting, and Casting for Clean Steel,” *steel Res. Int.*, vol. 88, no. 1, p. 1600093, Jan. 2017.

[37] R. Noselli, “Casting defects mechanical impact on turbine blades fatigue life-Engine feedback analysis,” 2017.

[38] D. M. Stefanescu, “Computer simulation of shrinkage related defects in metal castings - A review,” *International Journal of Cast Metals Research*, vol. 18, no. 3. pp. 129–143, 2005.

[39] A. N. Jinoop, S. K. Subbu, and R. A. Kumar, “Mechanical and microstructural characterisation on direct metal laser sintered Inconel 718,” *Int. J. Addit. Subtractive Mater. Manuf.*, vol. 2, no. 1, p. 1, 2018.

[40] A. J. Torroba *et al.*, “Investment casting of nozzle guide vanes from nickel-based superalloys: part I – thermal calibration and porosity prediction,” *Integr. Mater. Manuf. Innov.*, vol. 3, no. 1, pp. 344–368, 2014.

[41] M. Kang, H. Gao, J. Wang, L. Ling, and B. Sun, “Prediction of microporosity in complex thin-wall castings with the dimensionless niyama criterion,” *Materials (Basel).*, vol. 6, no. 5, pp. 1789–1802, 2013.

[42] “ASTM, ‘Standard Method for Macro-Etching Metals and Alloys- 1, 2,’ Prakt. Metallogr. Metallogr., vol. 7, no. 4-5–6, 1970. - Google

Search.” [Online]. Available: https://www.google.com/search?q=ASTM%2C+“Standard+Method+for+Macro-Etching+Metals+and+Alloys-+1%2C+2%2C”+Prakt.+Metallogr.+Metallogr.%2C+vol.+7%2C+no.+4-5–6%2C+1970.&rlz=1C1BNSD_enIT939IT939&oq=ASTM%2C+“Standard+Method+for+Macro-Etching+Metals+and+Alloys-+1%2C+2%2C”+Prakt.+Metallogr.+Metallogr.%2C+vol.+7%2C+no.+4-5–6%2C+1970.&aqs=chrome..69i57.316j0j7&sourceid=chrome&ie=UTF-8. [Accessed: 01-Mar-2021].

[43] W. T. Y. Mohamed, “Improved LIBS limit of detection of Be, Mg, Si, Mn, Fe and Cu in aluminum alloy samples using a portable Echelle spectrometer with ICCD camera,” *Opt. Laser Technol.*, vol. 40, no. 1, pp. 30–38, Feb. 2008.

[44] J. I. Goldstein *et al.*, “Electron Beam—Specimen Interactions: Interaction Volume,” in *Scanning Electron Microscopy and X-Ray Microanalysis*, Springer New York, 2018, pp. 1–14.

[45] W. Wang, X. Pang, C. Zheng, and A. A. Volinsky, “Failure analysis of high nickel alloy steel seal ring used in turbomachinery,” *Eng. Fail. Anal.*, vol. 80, pp. 49–56, 2017.

[46] I. Bunaziv, V. Olden, and O. M. Akselsen, “Metallurgical aspects in the welding of clad pipelines-A global outlook,” *Appl. Sci.*, vol. 9, no. 15, 2019.

[47] M. J. Cieslak, T. J. Headley, T. Kollie, and A. D. Romig, "Melting and solidification study of Alloy 625," *Metall. Trans. A, Phys. Metall. Mater. Sci.*, vol. 19 A, no. 9, pp. 2319–2331, 1988.

[48] C. P. Alvarães *et al.*, "Microstructural Characterization of Inconel 625 Nickel-Based Alloy Weld Cladding Obtained by Electroslag Welding Process," *J. Mater. Eng. Perform.*, vol. 29, no. 5, pp. 3004–3015, 2020.

[49] "Foundry technology (eBook, 2001) [WorldCat.org]." .

[50] W. Mu, N. Dogan, and K. S. Coley, "In Situ Observations of Agglomeration of Non-metallic Inclusions at Steel/Ar and Steel/Slag Interfaces by High-Temperature Confocal Laser Scanning Microscope: A Review," *JOM*, vol. 70, no. 7. Minerals, Metals and Materials Society, pp. 1199–1209, 01-Jul-2018.

[51] J. Tinoco and H. Fredriksson, "Solidification of a modified inconel 625 alloy under different cooling rates," *High Temp. Mater. Process.*, vol. 23, no. 1, pp. 13–24, Feb. 2004.

[52] J. B. Singh, A. Verma, B. Paul, and J. K. Chakravartty, "Failure of Alloy 625 tube stub ends - Effect of primary nitrides," *Eng. Fail. Anal.*, vol. 32, pp. 236–247, Sep. 2013.